THE NEURAL BASIS OF COGNITIVE CONTROL OF MOVEMENT INHIBITION

by

Zhe Xu

A dissertation submitted to the Johns Hopkins University in conformity with the requirements for the degree of Doctor of Philosophy

Baltimore, Maryland
May 4th, 2016

Abstract

A crucial component of executive control of behavior is the ability to voluntarily inhibit an action when it has become inappropriate or dangerous in a given situation. A driver cruising through several green lights on a street for a while would have to respond quickly and correctly by stopping his/her car when a red traffic light turns on. Effective inhibitory control is also context-dependent. In the same example, red is only associated with a stop signal in a driving situation. Numerous studies have suggested that the right ventrolateral prefrontal cortex (rVLPFC) is responsible for executive control of movement inhibition, but several questions remain to be answered, how does the rVLPFC dynamically and flexibly exert its control over movement inhibition to accommodate a changing environment? And how does the information flow from rVLPFC to the rest of the brain during stop control? The current thesis research aims to examine these questions using human psychophysical and functional magnetic resonance neuroimaging (fMRI) methods in conjunction with eye tracking and advanced statistical pattern classification and machine learning techniques.

We first identified two sub-regions within rVLPFC that showed differential activations during a context-dependent stop signal task (SST) in Experiment 1. Activation in the dorsal part of the rVLPFC was associated with detecting and encoding the meaning of the signals that were behaviorally relevant, whereas the activation in the ventral part of the rVLPFC was associated with the requirement to withhold an eye movement, regardless of the stop outcome. Furthermore, we found that the frontal eye field (FEF), an ocuolomotor area controlling for eye movement in the frontal cortex, encoded information regarding movements but not the meaning of the signals or the contexts.

We next explored the behavioral variability on Stop and Continue trials in selective stopping, a by-product of the context-dependent SST in Experiment 2, by asking whether the Continue signal-induced delay in motor response is the same form of response inhibition that was induced by the Stop signal. We found evidence in favor of a two-stage stopping process. Specifically, we found that participants slowed down their reaction time in Continue trials despite the instruction to ignore the Continue signal when preparing for a speeded go response. There was no detectable difference in the time it took to respond to a Stop signal compared with responding to a Continue signal (first stage of stopping). However, merely delaying the planned response did not change behavior in the subsequent trial. Either successful stop trials, or negative feedback in failed stop trials (second stage of stopping), resulted in greater engagement of inhibitory processes in the subsequent trial. Although there was no direct measure of brain activity during the selective stopping experiment, we speculate that the dorsal part of the rVLPFC may be the neural basis of pausing in order to focus attention on the relevant stimulus and make a decision about the course of action (first stage), and then if the signal requires stopping, ventral part of rVLPFC and FEF may be recruited to complete stopping.

In Experiment 3, we further validated human fMRI findings by recording single neuron activity in one macaque monkey and comparing the results from rVLPFC (area 45) versus FEF while the monkey performed a context-based SST. We found that FEF neurons encode for movement-related activities, but not the meaning of the signal. On the other hand, neurons in area 45, a primate homologue of human rVLFPC, encoded context information by either selectively increasing their firing rate to a particular context or by increasing their firing rate at the time of context switching.

Finally, we examined the functional connectivity of ventral and dorsal parts of rVLPFC with FEF and the rest of the brain with additional analyses using the data collected in Experiment 1. We found that dorsal and ventral rVLPFC modulated stop-related activity for the rest of the brain differentially, with the former influencing an attention-related network and the latter influencing a motor-related network. Our results indicated that functional separation exists in the rVLPFC during executive control of movement inhibition, such that subregions within this area form distinct distributed networks with the rest of the brain to collaboratively instantiate cognitive control.

From a reverse engineering perspective, understanding the biological and computational processes required for the brain to control for complicated situations such as context-dependent movement inhibition will support advancement of artificial intelligence (e.g. the development of self-driving cars). On the other hand, understanding the contribution of rVLPFC to inhibitory control is also highly significant from a clinical point of view, because it might lead to improvements in assessing or even treating disorders such as attention deficit and hyperactivity disorder (ADHD), Parkinson's disease, and obsessive–compulsive disorder (OCD).

Advisors:
Steven Yantis, PhD
Susan Courtney, PhD
Veit Stuphorn, PhD

Readers:
Jason Fischer, PhD
John Desmond, PhD
Shreesh Mysore, PhD
Soojin Park, PhD

This dissertation is dedicated to my advisor,
Steven George Yantis

Acknowledgements

I had a lot of fun in graduate school. Type I and Type II funs. Type I fun is fun in its true sense, and Type II fun is delayed gratification-- like solo backpacking with a 55 pounds backpack in 50/mph gusty wind in Patagonia, Chile, or pursuing a doctoral degree. The journey had its ups and downs, but when I look back, I am proud of what I have achieved, and forever grateful to the people who have helped, supported, and encouraged me during the past five years in my pursuit of the doctoral degree.

I would like to thank my advisors: Dr. Steven Yantis, Dr. Susan Courtney, and Dr. Veit Stuphorn. Veit helped me start the line of research that ultimately evolved into this thesis work in my early years in graduate school, and the completion of my doctorate work would not have been possible without Susan's kind and welcoming acceptance of me into her laboratory following Steve's passing at the end of my third year. Aside from providing guidance for my research projects, she has also been very understanding and supportive for the most important decisions I made in graduate school.

I would also like to thank my committee members, Dr. Shreesh Mysore, Dr. John Desmond, Dr. Jason Fischer, Dr. Soojin Park, and other faculty members from the Department of Psychological and Brian Sciences: Dr. Marina Bedny, Dr. Lisa Feigenson, Dr. Howard Egeth, and Dr. Jonathan Flombaum for giving numerous feedbacks on my research projects and course work performance, and pointing me to the right direction when I was lost.

I wanted to thank my wonderful lab mates and colleagues: to Dr. Anthony Sali, Dr. Brian Anderson, Dr. Erik Emeric, and Dr. Jeffery Mayse for teaching me the very technical side of research, and for their camaraderie. To Dr. Zheng Ma, for sharing the

most precious moments throughout graduate school. She and I arrived at Hopkins at the same time, and I have the deepest respect for her from seeing her overcome hardship in graduate school and the way she treats people around her in life.

I would like to thank Michelle DiBartolo, Michelle Chiu, Dori Blank, and the staff members from the Kennedy Krieger Institute: Terri Brawner, Kathleen Kahl, Ivana Kusevie, and Joseph Gillen for helping collect behavioral and imaging data that were presented in this thesis work. I would also like to thank Julie Bullock, Laura Dalrymple, Rebecca Swisdak, Jim Garmon from PBS and Charles Meyers, Debby Kelley, Eric Potter, Leslie Bravo and Ofelia Garalde from the Mind and Brain Institute for their administrative and technical assistance, without which the current thesis work could not have been completed.

I am grateful for having been friends and colleagues with these individuals both from my department and from Hopkins community: To Jesse Warford, my amazing housemate and IT support for the past five years. I could not have asked for a better housemate to live with, and 2936 Huntingdon is my home away from home. To Dr. Alyssa Toda, my trusted confidant, emotional companion, and intellectual equal, for all the adventures we have gone on together in graduate school and in life. To Dr. Nicolas Arbez, Dr. Wu-Jung Lee, Dr. Yi-Shin Sheu, Dr. Dennis Sasikumar, Jenny Wang and Feitong Yang for their unconditional friendship support.

For my parents:谢谢爸爸妈妈这么多年来给我的无微不至的爱，关怀，和支持。 没能陪你们度过的在国外读书的 11 年是我的遗憾。希望接下来的很多很多年我能让你们少一些牵挂，多一分安心， 也祝你们身体健康开心。

Dr. Steven Yantis represented everything a student could ask for in a mentor: a pioneer in the field, a patient listener, a caring academic father, and a proud advocate of his students' work. He made me feel doing scientific research is fun, and on top of everything, he taught me the art of working with people at work and in life. I cannot describe the hole his passing has left on me, but I know I want to be a researcher, a co-worker, and a colleague just like him in my future career.

Table of Contents

List of Tables

List of Figures

Chapter 1: Introduction

1.1 Background and significance

Cognitive control, the ability to coordinate thoughts and actions to accomplish one's internal goals, is one of the most remarkable features of human beings. There are many forms of control: the control of one's thoughts, attention, and emotion, as well as the control of initiating, inhibiting, and switching an action. The form of cognitive control that this thesis research focuses on is the control of movement inhibition.

A crucial component of cognitive control of behavior is the ability to voluntarily inhibit an action when that action has become inappropriate or dangerous in a given situation. For example, a cyclist is biking across a street when he has the right of way and, suddenly, a careless driver from his left side turns right. The cyclist has to immediately hit the break and stop pedaling to avoid getting hit by the car. This real life example involves a series of actions of inhibitory control, and the consequence due to a failure of inhibition can be detrimental. Effective inhibitory control not only requires actual stopping of dangerous or inappropriate behaviors, but also requires the detection and recognition of the appropriate contexts, which specific needs and forms of stopping are associated with. For example, if a cell phone rings during a meeting, an appropriate response under this situation would be to choose not to answer the call and silence the phone; however, if the cell phone rings again after the meeting, one would choose to answer the phone without feeling embarrassed for interrupting the meeting. In this real life example, the need to exert inhibitory control is selectively associated with a particular context that defines which action is more socially appropriate.

Studying the neural basis of inhibitory control is in itself an intriguing scientific endeavor, but it also has a significant clinical implication. Deficient action inhibition has been characterized in a number of disorders, including ADHD, Parkinson's disease, schizophrenia, OCD, and chronic substance abuse (e.g. cocaine, amphetamine, methamphetamine), and is also seen as a useful behavioral marker of genetic risk factors (Eagle et al., 2008). Clinical research has consistently shown that the time it takes to inhibit an action is significantly longer in methamphetamine addicts, cocaine addicts, and people who abuse alcohol, as well as in ADHD, OCD, and eating disorders than normal control participants. In ADHD, in particular, meta-analysis shows that inhibitory deficits, as indicated by the prolonged reaction time to inhibit an action in executive function tasks, are associated with a large effect size (Aron, A, 2011; Chambers et al., 2009; Lipszyc et al., 2010).

Despite the important role of inhibitory control in people's daily lives and its clinical implications, much of its underlying neural mechanisms remains unknown. How does the brain exert its control over thoughts and movements? How does it dynamically and flexibly adjust its control over behavior to accommodate a changing environment? The current thesis research aims to examine these questions using tools that are already available to the behavioral and cognitive neuroscience, such as human psychophysics and function magnetic resonance imaging (fMRI), and to advance of our knowledge in the area of cognitive control of movement inhibition.

1.2 Literature review

1.2.1 The stop signal task and the horse race model

Whereas excitation is often obvious in its effects, inhibition is much subtler and generally viewed only in the context of excitation. For most of its history cognitive inhibition has only been assessed in the context of its effects on response generation. The overwhelming majority of tasks assessing cognitive inhibition require participants to suppress irrelevant information (often information that was previously relevant), and infer the effect of inhibition by the reaction time (RT) cost for making a response. For example, inhibition in the Stroop task (Stroop, 1935), in which participants must report the typeface color of a word while suppressing the innate tendency to read the word itself, is often assessed by quantifying changes in RT as a function of the degree of conflict between the color of the typeface and the word itself. However, while changes in RT are strongly indicative of the presence of cognitive inhibition, they provide relatively little information about the features of specific mechanisms for suppressing irrelevant information or inappropriate behaviors.

The development of the stop signal task (SST) was a major turning point in the study of cognitive control of movement inhibition because it allows for the estimation of a characteristic of the inhibitory process itself (Lappin and Eriksen, 1966; Logan and Cowan, 1984; Logan et al., 1984). In the SST, participants are required to make a rapid behavioral response following a go signal and cancel the preparation of this response following an infrequent stop signal (Lappin and Eriksen, 1966; Logan et al., 1984). The ability of participants to stop on a given trial is a function of the delay between the go and stop signals onset (stop signal delay, SSD), with stopping being more difficult at longer delays. Additionally, accuracy also depends on the speed of response preparation, with

stopping being more difficult when participants' overall performance are faster (Logan and Cowan, 1984).

The empirical relationship between selective stopping (i.e., canceling only the action(s) being prepared), SSD, and the speed of response preparation led to the development of a simple model to describe inhibition in the context of the SST. In this model, called the Horse Race model, two hypothetical processes race to control behavioral outcome, each initiated following presentation of its accompanying stimulus: a generative go process and an antagonistic stop process (Logan and Cowan, 1984). These two processes accumulate arbitrary activity from a baseline to an activation threshold, at which point the winning process determines the behavioral outcome. If the go process reaches threshold first, the response is made, whereas if the stop process reaches threshold first, preparation of the response is arrested (Logan and Cowan, 1984). Because this model assumes both that the rate of accumulation for each process is constant on a given trial and that the duration of the stop process is constant and invariant (or has such low variability as to be functionally constant within measurement error; Band et al., 2003), the only factors that determine whether stopping will be successful is the delay between when the stop and go processes are initiated, set by the SSD, and stochastic variability in the rate of accumulation of the go process, measured via the variability in the empirical go RT distribution.

Importantly, in this race model, any response generated on a trial in which the stop signal was presented (i.e. failed to stop) happens because the go process won the race. Therefore, any response observed on a (failed) stop trial is a response drawn from the fast portion of the go trial RT distribution and is unaffected by the presence of the

stop process. Using this knowledge and the two aforementioned known parameters (SSD and go trial RT variability), it is possible to estimate the latency of the stop process (stop signal reaction time, SSRT) by comparing the observed sampling distribution of go RTs on trials in which the stop signal was presented to the full go RT distribution on trials in which the stop signal was not presented (Logan and Cowan, 1984; Logan et al., 1984). While there are many methods for estimating SSRT, they all rely on one simple principle: any response that would be generated with an RT longer than SSRT will be captured by the stop process, canceled, and not observed in the go RT sampling distribution (Logan and Cowan, 1984; Logan et al., 1984). Therefore, by finding the slowest RT observed (assuming infinite data points; empirical methods for estimating SSRT must account for noisy data), we can derive SSRT (Mayse et al., 2014).

Large volumes of studies have applied SST and the Horse Race Model to investigate the neural circuits that substantiate motor inhibition. In primates and humans, oculomotor saccades are often used as primary task responses in the SST because the neural circuits for generating saccades are well understood and provide an easy framework for understanding inhibition. Neurons in the supplementary eye field (SEF) and superior colliculus (SC) compete to either shift or maintain gaze: so-called fixation neurons are active when monkeys maintain gaze on a target, and so-called movement neurons accumulate activity to a threshold prior to eye movements (Brown et al., 2008; Everling et al., 1998; Hanes et al., 1998; Hanes and Schall, 1996; Paré and Hanes, 2003; Sparks, 1978). When stopping is required, the activity of fixation neurons increases and the accumulation of movement neurons is arrested prior to SSRT (Boucher et al., 2007a). This relatively simple circuit provides a rich framework for constraining the possible

mechanisms of stopping: first, any neuron that controls movement initiation must differentially modulate its firing rate when stopping is and is not required, and second, this modulation must precede SSRT in order to successfully control for stopping. Similar circuits for stopping skeletal movements are less well understood, but emerging theories suggest the involvement of large populations of neurons in the motor cortex (M1)(Stuphorn, 2014). Regardless, the same constraints apply to controlling skeletal movements as applying to controlling eye movements, even if the neural circuits underlying movement initiation are different.

The Horse Race Model provides a theoretical ground of understanding the interaction between go and stop processes, and the studies using simple SSTs provide substantial knowledge into understanding the neural basis of motor inhibition. However, inhibitory control of goal-directed behavior is often more complicated than what the race model and simple SST can capture because it requires one to attend to contextually relevant sensory information, map the sensory information to specific goals (i.e. inhibition), plan and execute appropriate actions accordingly. The process demands an adaptive system, which is flexible and capable of updating action plans, organizing and optimizing processing pathways to meet the sophisticated demands in the environment.

1.2.2 A frontal-basal-ganglia model of response control

A frontal-basal-ganglia model of response control proposes that three "pathways" are involved in controlling movement initiation (direct pathway) and inhibition (indirect and hyperdirect pathways) (Figure 1).

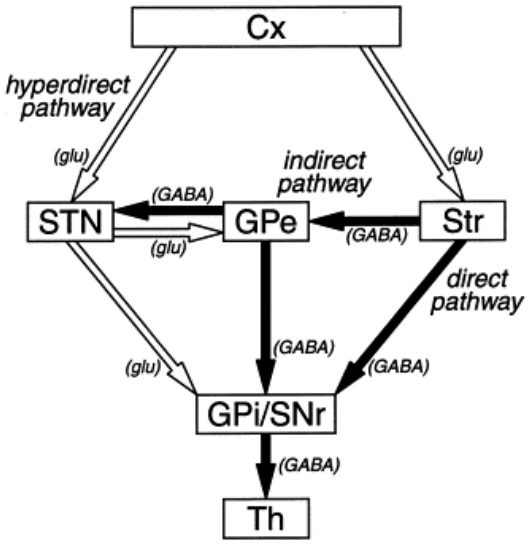

Figure 1. Schematic diagram of the three pathways (Nambu et al., 2002). Cx, cerebral cortex. STN, subthalamic nucleus. GPe, external segment of the globus pallidus. GPi, internal segment of the globus pallidus. Th, thalamus. Str, striatum. SNr, substantia nigra pars reticulata. Open and filled arrows represent excitatory glutamatergic (glu) and inhibitory GABAergic (GABA) projections, respectively.

When a voluntary movement is about to be initiated by cortical mechanisms, a corollary signal is transmitted from the motor cortex to the striatum (Str) within the basal ganglia (BG) through "direct" excitatory glutamatergic projections. Activated striatum then inhibits the activity of substantia nigra pars reticulata (SNr) and internal segment of the globus pallidus (GPi) through inhibitory GABAergic projections, which in turn releases the inhibition (i.e. disinhibition) of thalamus, whose output causes the generation of a movement (go process). To inhibit a movement, striatum, after being excited by motor cortex, inhibits the external segment of the globus pallidus (GPe) through inhibitory GABAergic projections, which in turn disinhibits the activities of GPi/SNr. As a result, GPi/SNr inhibitory neurons are activated and further inhibit the activity of thalamus, resulting in movement inhibition (stop process). This inhibitory effect through the "indirect" pathway acts slower than the excitatory effect through the "direct" pathway,

which as a result would predict that once the go process is initiated, the process is almost impossible to be stopped by the slower stop process. In order to exert rapid stop control, excitatory signal from the cerebral cortex is transmitted through subthalamic nucleus (STN) to the GPi/SNr, whose output inhibits the activity of thalamus, resulting in movement inhibition. This cortical-STN-pallidal "hyperdirect" pathway exerts powerful excitatory effects on the output nuclei of the basal ganglia, bypassing the striatum, and is faster in signal conduction from the cortex than both "direct" and "indirect" pathways (Chambers and Bellgrove, 2009, Nambu et al., 2000 and Nambu et al., 2002). Together, the frontal-basal-ganglia model of response control hypothesizes that cortico-basal-ganglia "direct", "indirect", and "hyperdirect" pathways form the neural circuitry that underlies selective movement initiation and inhibition, and understanding how the motor-related cortical areas modulate the activity of the output nuclei of the basal ganglia is an important issue for understanding the mechanisms of response control.

1.2.3 Prefrontal cortex as a hierarchical control system

Comparative studies in both humans and primates have concluded that the prefrontal cortex (PFC) is a crucial neural substrate of cognitive control (Assad et al., 1998; Fuster, 2001; Passingham and Steven, 2012). Anatomically, the PFC is connected with the brainstem, the thalamus, the basal ganglia, and the limbic system (Fuster, 2001); thus, PFC is able to bias information selection and transformation through serial/ parallel feedback pathways onto other structures throughout the brain. Functionally, sustained PFC neural activity is robust to interference; PFC associative areas integrate multimodal sensory stimuli that carry behaviorally relevant information; and the PFC neural plasticity is adaptive to the demands of new tasks (Miller and Cohen, 2001). Findings from lesion

studies further corroborate that PFC is crucial for cognitive control. Humans with PFC damage show stereotyped deficits in the Wisconsin Card Sorting Task (WCST), which is a test of the ability of participants to flexibly alter their responses to the same stimuli based on certain abstract rules. These patients are able to acquire the initial mapping between the sensory stimuli and the abstract rule without much difficulty but are unable to adapt their behavior when the rule changes (Milner, 1963). Monkeys with PFC lesions are impaired in an analog of this task (Dias et al., 1996b, 1997).

Studies in humans with focal cortical damage have demonstrated a consistent relationship between damage to the PFC, especially the right ventrolateral prefrontal cortex (rVLPFC), [1]and elevated SSRT (Aron et al., 2003; Rieger et al., 2003). These studies are corroborated by functional imaging data demonstrating elevated BOLD signal in the rVLPFC when stopping was required comparing to when no stopping was required (Aron and Poldrack, 2006; Swann et al., 2009). In addition, functional connectivity studies show increased connectivity between the rVLPFC and the subthalamic nucleus (STN) when stopping is required, and this connectivity is greater in more proficient stoppers (Aron and Poldrack, 2006; Aron et al., 2007) and degraded in aged individuals with impaired cognitive inhibition (Coxon et al., 2012).

Recent theoretical and empirical results suggest that the rostro-caudal and anterior-posterior axes of the frontal lobes may reflect a hierarchical organization of control. Koechlin et al. (2003) first proposed a cascade model of executive and cognitive control

[1] Various studies have used right inferior frontal cortex (rIFC), right inferior frontal gyrus (rIFG), right inferior frontal sulcus (rIFS), and right ventrolateral prefrontal cortex (rVLPFC) to refer to a similar (if not the same) area that is thought to be associated with inhibitory control. In addition, some studies used Talariach coordinates, while others used MNI coordinates, to report the foci/peak of BOLD activation. Furthermore, even groups that used the same coordinate system, the foci/peak of BOLD activations were different

in the lateral prefrontal cortex (LPFC); Badre and D'Esposito (2007) later took this model and further developed and incorporated it into a hierarchical model of PFC organization and function.

Cascade model of cognitive control argues that LPFC is organized as a hierarchy of representations, originating from the lateral premotor cortex, through the caudal LPFC, and ending in rostral LPFC. It is responsible for processing distinct information that is involved in controlling the selection of appropriate stimulus-response associations (Koechlin et al., 2003). The model assumes a cascade of top-down controls in PFC: at the bottom level, lateral premotor area implements sensory control that involves the selection of motor action in response to external sensory stimuli. In other words, lateral premotor cortex is responsible for establishing the initial stimulus-response associations. At the middle level, caudal PFC implements contextual control that involves the selection of stimulus-response associations, which were previously established by the lateral premotor cortex. At the highest level, rostral PFC implements episodic control that involves the selection of *sets* of stimulus-responses associations, which were evoked by the same context, according to events that previously have occurred or to ongoing internal goals (i.e. the "temporal knowledge").

The authors designed a human neuroimaging study to test their model. In their study, participants performed a task that involved selecting a response either on the basis of a sensory input (termed the ''sensory level''), a contextual cue (termed the ''context level''), or an episodic context (termed the ''episodic level''). The cascade model predicts that the increasing demands of sensory, contextual, and episodic controls have additive effects on behavior, which can be measured in the form of reaction time; that is,

the higher the task demands, the longer it will take the participant to perform that task. Furthermore, these increasing task demands also have additive cumulative effects on the local brain activity, as measured by human functional magnetic resonance imaging (fMRI). Specifically, the model predicted that lateral premotor cortex would be active while participants performed the sensory-level task due to the effect of the sensory stimulus; both lateral premotor cortex and caudal LPFC would be active while participants performed the context-level task due to the effect of the sensory stimulus plus the context information; and all three regions, lateral premotor cortex, caudal LPFC and rostral LPFC would be active while participants performed the episodic-level task due to the additive effect from the stimulus, context, and episode. The results confirmed the model's prediction. Participants' reaction time increased with the stimulus, context, and episode factors. In addition, blood oxygen level dependent (BOLD) activity in lateral premotor cortex exhibited an effect of sensory stimulus, caudal LPFC exhibited an effect of context, but not sensory stimulus, and rostral LPFC exhibited an effect of episode, but not sensory stimulus nor context (Koechlin et al., 2003).

Koechlin et al. (2003)'s cascade model showed very strong evidence in favor of a representational hierarchy in the PFC. However, a critique of the cascade model is that although the model differentiates levels of control on the basis of differences between control signals (i.e. episodic, context, and sensory), the operationalization of these differences in the fMRI experiment and how participants generally assign a given control signal to a given level of hierarchy is not always concrete. It seems that while the episodic level of control uses the temporal knowledge (e.g. events that happened in the past, or an internal ongoing goal) as a control signal to guide behavioral responses, both

context and sensory control signals involve the sensory-response association, because a cue that indicates a particular context is inherently a sensory stimulus itself (Badre and D'Esposito, 2007).

Badre and D'Esposito (2007) later took the cascade model of LPFC and further developed and incorporated it into a hierarchical model of PFC organization and function. This model states that the functional gradient along the anterior-posterior axis of the PFC derives from a representational hierarchy, ranked by the abstractness of the representation to be selected, rather than by the control signal. Furthermore, there is a dominance relationship whereby higher, more anterior regions influence processing in lower, more-posterior regions to a greater extent than vice versa (Badre and D'Esposito, 2009). To test this model, the authors designed a human imaging experiment that involves parametrically manipulating the abstractness of rules that guide action selection. Specifically, rules that resolve concrete motor response competition form the lowest level of abstraction; rules that resolve feature competition (i.e., the number of specific textures of an object or the number of specific orientations of an object) form the immediately superordinate level of abstraction; rules that resolve dimension competition (i.e., classes of features such as size, orientation, shape, and texture) form the next immediately superordinate level of abstraction; and the rules that resolve context competition (overlapping mappings between a particular contextual cue and different dimensions) form the highest level of abstraction. The authors predicted that the level of BOLD activation would increase from posterior PFC to the anterior PFC as the abstractness of the rule that is used to guide action selection increased. The results confirmed the hierarchical model's prediction by showing that 1) dorsal premotor cortex is sensitive to

response competition; 2) anterior dorsal premotor cortex is sensitive to feature competition; 3) the inferior frontal sulcus is sensitive to dimension competition; and 4) frontal polar cortex is sensitive to context competition.

Koechlin et al. (2003)'s cascade model and Badre and D'Esposito (2009)'s hierarchical model of executive and cognitive control showed very strong evidence in favor of a representational hierarchy in the PFC. A network consisting of multiple densely connected clusters (i.e. sub-regions within the PFC) is more efficient at information transmission and retention than either randomly connected or highly regular lattice networks (Dosenbach et al., 2008). Furthermore, according to these two models and the anatomical nature of the right ventrolateral prefrontal cortex, this region would be ranked at the higher end of the control hierarchy. Therefore, it is reasonable to speculate that rVLPFC might be responsible for encoding the abstract rules that represent inhibitory demand instead of the motoric stopping per se. On the other hand, it is also possible to speculate that subregions within the rVLPFC control for different aspects of motor inhibition, with more posterior or caudally located rVLPFC subregion(s) representing motoric aspect of inhibitory control, and more anterior or rostrally located rVLPFC subregion(s) representing rules that require response inhibition.

1.2.4 Four hypotheses concerning the role of right ventrolateral prefrontal cortex in behavioral control and movement inhibition

Across numerous studies that examined the function of prefrontal cortex in cognitive control, four alternative hypotheses had been proposed regarding the functional organization of rVLPFC and its role in inhibitory control. These alternatives are: I) rVLPFC is responsible for direct control of movement inhibition, II) rVLPFC is

responsible for reflexively reorienting attention to external stimuli that are behaviorally-relevant, III) rVLPFC is responsible for encoding task-relevant rules, and IV) sub-regions within rVLPFC contribute heterogeneous functions in movement inhibition.

In a human lesion study, Aron et al. (2003) first reported that the ability to inhibit a movement during a SST was most severely disrupted in patients with lesions in ventrolateral prefrontal cortex (rVLPFC), compared to those with lesions in other brain areas such as middle frontal gyrus (MFG) and orbital frontal cortex (ORB). The authors proposed that rVLPFC is critically responsible for inhibitory control of movements. However, with lesion studies, it is hard to directly address the specific functional role of rVLPFC in controlling movement inhibition. Many subsequent studies, using human psychophysics, event-related potentials (ERP) from electroencephalogram (EEG) data, transcranial magnetic stimulation (TMS), and functional magnetic resonance imaging techniques (fMRI), have directly and extensively addressed the role of rVLPFC in movement inhibition (Chikazoe et al., 2009; Sakagami et al., 2001; Sakagami et al., 2006; Swann et al., 2012; Verbruggen et al., 2010). However, the results of these studies varied and at present there is no consensus about the specific functional contribution of rVLPFC in movement inhibition.

A number of studies claimed to have found evidence supporting the hypothesis that rVLPFC directly mediates movement inhibition in human participants. For example, in a TMS study (Verbruggen et al., 2010), participants performed a task that was composed of switching between four types of trials: signal ignore trials, dual-signal trials, Stop signal trials, and additional control trials where the signal was subsequently removed after initial presentation. For all trials, participants were instructed to respond as

quickly as possible to the color of the cue by pressing one of two computer keys. On the Stop signal trials, participants were instructed to withhold the key press. In contrast, in signal ignore trials, participants had to press the keys upon seeing the cue, while in dual-signal trials, participants had to press another, additional key. Three cortical regions, right inferior frontal gyrus (rIFG), which is bordered by precentral sulcus and lateral sulcus, right inferior frontal junction (rIFJ)[2], which resides between the junction of precentral sulcus and inferior frontal sulcus, and pre-SMA were stimulated separately using TMS while participants were performing the task. The authors found that both stop and dual task performances were impaired when either rIFG or rIFJ was disrupted, but not when pre-SMA was disrupted; however the disruption of rIFG did not interact with stimulus onset asynchrony (SOA) for when the visual stimulus was presented while the disruption of rIFJ did, which suggested that rIFJ was more related to the detection of stimulus onset than rIFG. Based on these results, the authors concluded that rIFG is critical for action inhibition whereas rIFJ is critical for the detection and classification of the visual cue instructing the change in behavioral response.

While some studies claimed the role of rVLPFC is to directly control the action of movement inhibition, others found evidence supporting a role of rVLPFC in voluntarily reorienting attention to external events that are behaviorally relevant. The "attention" hypothesis assumes that rVLPFC is part of the ventral lateral prefrontal-parietal circuit that is involved in detecting the abrupt onset of a sensory stimulus which bears behaviorally relevant information of the immediate environment (Corbetta and Shulman,

[2] rIFG and rIFJ are both within the broadly defined rVLPFC. Relatively speaking, rIFG occupies mid-rVLPFC that includes both pars triangularis and pars opercularis, whereas rIFJ occupies posterior and dorsal rVLPFC (Verbruggen et al., 2010; Levy and Wagner, 2011).

2002). According to this view, rVLPFC detects the signal that indicates "stopping" in the environment, and updates the current behavioral goal, while other brain regions, such as pre-SMA and frontal eye field (FEF), are the primary areas for direct motoric inhibition and action updating (Hampshire et al., 2010).

Sharp et al. (2010) used fMRI to directly investigate the function of rVLPFC with human participants performing a modified version of Stop Signal Task (SST). In their design of the SST, in addition to trials with standard stop signal (colored in red), a second type of trials, with "continue" signal (colored in green) was introduced to instruct participants to continue the eye movement they had already planned during initial fixation. The authors found that BOLD signals in rVLPFC did not differentiate "stop" trials from "continue" trials, but pre-SMA activity was specifically more activated during the response inhibition. Therefore, the authors argued that the elevated BOLD signal in rVLPFC is not the result of this region exerting inhibitory control, but rather, it reflects the role of rVLPFC in reorienting attention to behaviorally relevant, external stimuli and in processing of unexpected change of task performance. In contrast, pre-SMA was argued to be specifically associated with successful movement inhibition.

A third, new perspective brings out the role of rVLPFC in contextual behavioral monitoring. Effective inhibitory control not only requires actual stopping of unwanted thoughts or inappropriate behaviors, but also requires detecting and recognizing the appropriate contexts, which are associated with specific needs and forms of stopping. For example, if a cell phone rings during a meeting, an appropriate response under this situation would be to choose not to answer the call and silence the cell phone; however, if the cell phone rings again after the meeting, one would choose to answer the phone

without feeling embarrassed for interrupting the meeting. According to the context-monitoring hypothesis, rVLPFC plays a critical role in monitoring the environment, and inhibitory control of behavior is exerted contingent on the environmental context (Swann et al., 2012; Chatham et al., 2012).

Support for this hypothesis comes from a recent ECoG study of a single patient that was surgically implanted with electrodes subdurally, with both dorsal medial and right lateral coverage (Swann et al., 2012). The participant performed a task that involved both preparing for stopping and stopping outright. In addition to ECoG recordings, brain imaging and macrostimulation of pre-SMA were conducted during separate experimental sessions. The authors found that diffusion tensor imaging (DTI) results revealed strong interconnection between preSMA and rVLPFC. Macrostimulation of pre-SMA induced motor arrest, and subsequently caused a signal increase in rVLPFC. In addition, pre-SMA and rVLPFC were specifically engaged during task performance, with pre-SMA showing task-related response proceeding rVLPFC. Therefore, the authors argued that both pre-SMA and rVLPFC are involved in movement inhibition. They suggested that pre-SMA is more important for preparing for the movement inhibition, while rVLPFC is more important for monitoring the environmental need of abolishing or implementing inhibitory control, rather than inhibition per se.

In another study (Chatham et al., 2012), the authors aimed to dissociate the motoric and cognitive aspects of inhibitory control by instructing participants to performed a "Stop" and "Double-Go" task. During the experiment, participants were required to make a 2-alternative forced choice (2AFC) to indicate the direction of the arrow on 75% of trials. For the remaining 25% of trials, participants either repeated the

previous 2AFC on the same trial (Double Go task, indicated by a white square inside the circle), or stopped the motor response on the same trial (Stop task, indicated by the red square inside the circle). The authors found overlapping neural activity in rVLPFC for both the Stop and Double-Go tasks. Furthermore, the authors used the multivariate pattern analysis (MVPA), to determine whether rVLPFC encodes the same information for the Double Go task and Stop task. They trained classifiers to identify patterns of activation that reliably predicted subject-specific patterns of activation in rVLPFC during the Double Go task, and the same classifiers were able to reliably distinguish patterns of activation across individuals in the Stop task. Although this MVPA did not directly demonstrate that the cognitive processes for the two tasks are the same, it at least showed that the patterns of neural activity in rVLPFC failed to show differential sensitivity to the explicit stopping demand. The authors thus suggested that the functional role of rVLPFC in controlling movement inhibition is not centered on the motor aspects of stopping, but rather on context-monitoring of stopping (Chatham et al., 2012).

While most literatures discussed so far have been focusing on the direct investigation of the right VLPFC, considerable evidence indicates that specific forms of cognitive control are associated with distinct functional sub-regions within the left VLPFC (lVLPFC; Gold et al., 2006; Badre and Wagner, 2007; Poldrack et al., 1999). Poldrack et al. (1999) found that the dorsal lVLPFC (BA 44/45) is more activated during phonological processing of words compared to a perceptual control task, whereas ventral lVLPFC (BA 47/45) is more activated during a semantic decision task compared to a perceptual control task. In another memory study, Badre and Wagner (2007) found double disassociation between left anterior-VLPFC (~BA47) and left mid-VLPFC

(~BA45) during controlled retrieval and post-retrieval selection, respectively. It is, therefore, reasonable to hypothesize that a similar functional heterogeneity exists in right VLPFC and specifically, different sub-regions within rVLPFC may be responsible for motor inhibition, reflexive reorienting of attention, and context monitoring (Levy and Wagner, 2011). Furthermore, these subregions might be organized in the form of a hierarchy, along the anterior-posterior, or rostral-caudal axes within rVLPFC.

This hypothesis is also corroborated by comparative neuroanatomy of human and primate brains (Figure 2). In humans, rVLPFC consists of area 44, the most caudal part of rVLPFC, area 45A/B, the mid-rVLPFC, and area 47/12, the most Rostral and anterior part of rVLPFC.

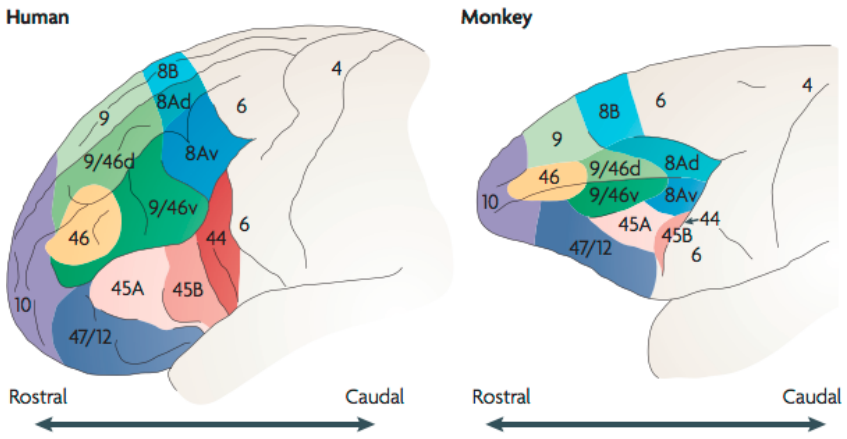

Figure 2. Cytoarchitectonic division of human (left) and monkey (right) right frontal lobe (Badre and D'Esposito, 2009).

Petrides and Pandya (2009) compared the cytoarchitectonic maps of the lateral and orbital surfaces of the human and macaque monkey prefrontal cortex, and found that area 45 A/B was the macaque homologue of human Brodmann area 45, which occupies the triangular part of the VLPFC. In a later study (Gerbella et al., 2010), the authors

applied anterograde and retrograde labeling methods, and mapped out the cortical areas that are connected to area 45 in macaque monkeys. The authors found that area 45A has stronger connections to prefrontal areas such as rostrodorsal 46 and superior temporal polysensory (STP) areas; area 45B has stronger connections to prefrontal oculomotor areas, such as FEF (Area 8) and SEF, and area TE in temporal cortex. Based on these results, the authors argued that areas 45A and 45B are two distinct brain regions with different functional roles; area 45A is involved in communicating and monitoring attention, whereas area 45B is involved in eye movement control. These anatomical results in the monkeys area 45 provided a neural ground to postulate the possible differential functional roles of area 45 as well as the rest of the rVLPFC in humans.

Taken altogether, numerous researchers have used human psychophysics, event-related EEG, TMS, functional brain imaging techniques (fMRI and DTI), and patient ECoG studies to investigate the neural basis of inhibitory control, and have identified the prefrontal region, the right ventrolateral prefrontal cortex in particular, as playing a crucial role in this type of cognitive control of movement inhibition. Nevertheless, the mechanism of rVLPFC in inhibitory control remains controversial. Is it likely that rVLPFC is responsible for encoding the abstract rules that representing inhibitory demand instead of the motoric stopping per se? Is it even more likely that subregions within the rVLPFC control for different aspects of response inhibition, with some rVLPFC subregion(s) representing motoric aspect of inhibitory control, some representing the effect of attentional capture of the stop signal, while the others representing rules that require response inhibition? The current thesis research aims to examine these questions using human psychophysical, univariate functional magnetic

resonance imaging (fMRI), and advanced statistical pattern classification techniques in conjunction with eye tracking.

1.3 Overview of the current studies

In the current thesis I investigated the neural basis and the behavioral characteristics of voluntary control of inhibitory behavior in humans. In particular, I examined the role of right ventrolateral prefrontal cortex, and its possible subregions, in contextual and selective stopping in Chapter 2. I administered a new variant of conventional SST, in which participants were trained to make speeded saccades following a visual target onset, and occasionally they needed to detect a secondary sensory signal that appeared infrequently after the initial target onset. Depending on the meaning of the signal, participants had to *selectively* inhibit the saccade that they had already planned for. In addition, the meaning of the signal could either be "stop saccade" or "continue to make saccade" depending on which context cue that was shown at the beginning of the trial. This task design encompassed all three critical factors that are involved in voluntary motor inhibition: 1) attending to a sensory signal, 2) interpreting the meaning of the signal and 3) associating the signal meaning to appropriate contexts. I found that there were two subcomponents within rVLPFC that are differentially involved in contextual and selective stopping. Specifically, the more dorsal part of the rVLPFC is responsible for detecting sensory stimuli that are behaviorally relevant and is also encoding for the meaning of a sensory signal in the current context, whereas the more ventral part of the rVLPFC is responsible for controlling stopping behavior only, yet it did not differentiate between the stop outcome (successful stopping versus failed stopping). This finding is the first time showing that there exists a ventral-dorsal

separation in rVLPFC in the context of controlling for movement inhibition, and suggests that instead of viewing this region as a single uniform entity, we should reconsider rVLPFC as a more heterogeneous area with subcomponents of differential functionalities for inhibitory control. On the other hand, I also found the patterns of BOLD activation in frontal eye field (FEF) encoded differentially for the stop outcome but not the meaning of a sensory signal, establishing a functional double dissociation between rVLPFC and FEF.

In chapter 3, I further examined the behavioral characteristics of selective stopping by testing whether the process, when activated by the Continue signal, which subsequently delays preparation of a behavioral response, is the same as the process, when activated by the Stop signal, which ultimately cancels the preparation of a behavioral response. If the continue signal does not affect subsequent behavior in the same way that a stop signal does, then this is further evidence for a different function role for the brain area that responds to both continue and stop signals than for the brain area that only responds to stop signals. The continue signal in the contextual, selective SST instructed participants to proceed with the go response they were preparing. Although the continue signal does not carry an imperative to alter the participant's planned response (in contrast to the stop signal), it cannot simply be ignored because participants must first disambiguate the perceptually similar stop and continue signals. Therefore, it can be assumed that the stop and continue signals carry similar attentional and sensory processing demands, but only the stop signal activates neural processes involved in canceling the planned go response, allowing these neural signals to be resolved from those involved in allocation of attention or conflict monitoring. In this study, I used a very similar experimental design as in Experiment 1 in chapter 2, but without the

contextual manipulation. That is, Stop and Continue signals were always associated with a particular color respectively, but were counterbalanced across different participants). I found, in agreement with prior studies, that RTs on Continue trials were bimodally distributed and the overall mean RT was greater than primary task (Go) mean RT (Sharp et al., 2010). This finding suggests that the preparation of a response was delayed on both Stop and Continue trials, perhaps by a common mechanism. These trials differed greatly, however, in the ultimate behavior (initiate or inhibit a saccade), whether positive or negative feedback was received, and subsequent behavioral adjustments. These data suggest that stopping is at least a two-stage process achieved first by a rapid delay of response preparation followed subsequently by either resumption (Continue) or suppression (Stop) of the planned behavioral response. The results also indicate that the first stage of stopping is not sufficient to affect subsequent behavior; either 1) successful completion of both stages results in cancelation of the response and affects subsequent behavior, or 2) negative feedback in failed stop trials results in greater engagement of inhibitory processes in the subsequent trial. Merely delaying the planned behavior due to the onset of a Stop/Continue signal, however, does not change subsequent behavior. To tie the behavioral results in Experiment 2 in chapter 3 with the neural imaging results in Experiment 1 in chapter 2, I speculate that dorsal rVLPFC detects the onset of a sensory signal and encodes the meaning of that signal, whether it is a Continue or Stop signal, and this process would take time, which would result in a brief pausing of the ongoing motor preparation process. Furthermore, in order to completely stop a saccade, the ventral rVLPFC would need to be further engaged. The behavioral results suggest that subsequent behavior may be affected only when the more ventral subregion is engaged.

In chapter 4, Experiment 3, I further validated human fMRI findings by recording single neuron activity in one macaque monkey and comparing the results from rVLPFC (area 45) versus FEF while the monkey performed a context-based SST. We found that FEF neurons encode for movement-related activities, but not the meaning of the signal. On the other hand, neurons in area 45, a primate homologue of human rVLFPC, encoded context information by either selectively increasing their firing rate to a particular context or by increasing their firing rate at the time of context switching. These results confirm the functional dissociation between rVLPFC and FEF found in the fMRI study.

So far, I have considered only the role of regions within the rVLPFC, but voluntary control of movement inhibition requires information flow across brain regions beyond merely the rVLPFC itself, and these regions collectively form a distributed inhibitory control network. In chapter 5, I used psychophysiological interaction (PPI) analysis to ask the question, how do ventral and dorsal parts of rVLPFC and FEF function collectively as part of a frontal control circuit that instantiates context-dependent inhibitory control? The results showed that the dorsal rVLPFC modulated areas of the brain that are known to be part of a previously identified stimulus-driven attention network, specifically during Stop trials. On the other hand, ventral rVLPFC modulated areas of the brain, including FEF, that are known to be part of a network more closely related to motor control and endogenous attention control, specifically during Stop trials, supporting the previous findings in Experiment 1 that dorsal and ventral rVLPFC are two separate subregions within rLVPFC and functionally connected to separate brain regions to serve different purposes during inhibitory control.

Taken altogether, understanding the specific contribution of PFC sub-regions to cognitive control of response inhibition, and how these sub-components might be integrated to form a frontal neural circuit for controlling voluntary behavior will shed light on the understanding of the biological and computational processes it takes for the brain to control for complicated situations such as movement inhibition and on the advancement of artificial intelligence, it also has important relevance toward understanding neuropsychiatric disorders such as ADHD, OCD and Parkinson's disease, which involve dysfunctions of motor inhibition.

Chapter 2: The mechanism of right ventrolateral prefrontal in cognitive control of movement inhibition (Experiment 1)

2.1 Introduction

Human lesion and imaging (fMRI) studies have used standard Stop Signal Task (SST) to demonstrate that the right ventrolateral prefrontal cortex (rVLPFC) is critical for stopping action, but the specific function of rVLPFC activity in stopping is debated. While some argue for a direct role of rVLPFC in response inhibition (Aron et al., 2003), others have argued for a role of this region in either guiding attention to external events relevant to the task goal (Sharp et al., 2010; Corbetta and Shulman, 2002), or in encoding behaviorally relevant task rules (Koechlin and Kouneiher, 2003). It is also likely that sub-regions that are responsible for each of the aforementioned functionalities coexist in the rVLPFC, giving rise to heterogeneous roles of rVLPFC in cognitive control of movement inhibition (Levy and Wagner, 2011).

In a standard SST, participants make a simple movement (e.g. saccade or button press) following an imperative go signal and have to cancel the movement that they have

already been planning for in the face of an infrequent but highly salient stop signal. While SST examines the motor interactions between go and stop responses, it is also a cognitively demanding task that involves both attention and conflict resolution. During the SST, participants have to first orientate their attention to the stop signal itself. The stop signal is a highly salient signal with an unpredictable onset that carries a high behavioral imperative. The abrupt onset of a salient stimulus can result in a delayed response time even when that stimulus is irrelevant, an effect known as "attentional capture" (Yantis and Jonides, 1990, Yantis, 1993), and generally involves activation of brain regions implicated in attentional allocation and control (Serences et al., 2004 and Serences et al., 2005). Furthermore, the anticipation of the possible appearance of the stop signal introduces a high degree of conflict and uncertainty – participants cannot know when the stop signal will be presented and whether they will be able to successfully stop (Ito et al., 2003). Taking these features into account, it can be difficult to separate out specific neural signals related to the cognitive demands involved in performing the SST from the neural signals related to motoric inhibitory control. For instance, either lapses in attention or ineffective stop control or both could result in failed stopping, which makes it difficult to separate the specific neural signals underlying each factor. Failures to properly sort such neural signals could result in the misinterpretation of findings and improper analysis of the factors that underlie inhibitory control. To date, few studies have examined these issues. We thus administered a context-dependent SST that incorporates motor inhibition, attention capture and reorientation, and contextual rule encoding in one comprehensive experimental paradigm, using saccadic eye movements. Specifically, we aim to test four alternative hypotheses regarding the functional

organization of rVLPFC and its role in inhibitory control. Those alternatives are: I) rVLPFC is responsible for direct control of movement inhibition, II) rVLPFC is responsible for reflexively reorienting attention to external stimuli that are behaviorally-relevant, III) rVLPFC is responsible for encoding task-relevant rules, and IV) sub-regions within rVLPFC contribute heterogeneous functions in movement inhibition. Furthermore, to fully address all four alternative hypotheses, we used an approach that included univariate data analysis with general linear model (GLM), and regions of interest (ROI) based multi-variate pattern classification analysis (MVPA). Using the combined univariate and multivariate pattern analysis techniques not only allowed us to ask the question of where the foci that encode inhibition within rVLPFC are, but also how different information is encoded differentially within the same brain region.

2.2 Method

Participants. 21participants[3] (7 M, 14 F, mean age of 22 (range, 18-30 years)) were recruited from the Johns Hopkins community. All were screened for normal or corrected-to-normal visual acuity and color vision. Written, informed consent was obtained from all participants, and all of the experimental procedures were approved by the Institutional Review Boards of the Johns Hopkins University and the Johns Hopkins Medical Institutions. All participants completed either 4 or 5, 1.5-hour behavioral training sessions and one 1.75-hour fMRI scanning session, in exchange for monetary compensation. All participants' last two behavioral training sessions met *a priori* criteria for them to be

[3] Eight participants were excluded from the final fMRI data analysis due to four factors: a) two voluntarily withdrew from the study during behavioral training sessions, b) two experienced difficulty calibrating for eye tracking due to the nature of their eyes, c) two participants' behavioral data during third and fourth behavioral training sessions were unusable, and d) two experienced difficulty calibrating for eye tracking due to technical difficulties in the MRI scanner.

qualified for the fMRI scanning session. The criteria were set such that the average performance accuracy was no less than 40% for Stop trials and 80% for Continue trials. This was to ensure that participants were performing Stop and Continue tasks as instructed.

Apparatus and stimuli. A Mac computer (Apple Inc., Cupertino, California, USA) equipped with MATLAB software (http://www.mathworks.com/) and PsychToolbox-3 extensions (http://psychtoolbox.org/) was used to present the stimuli. During the behavioral training sessions, participants viewed the monitor, an Asus LED HD monitor (60 Hz refresh rate), from a distance of ~56 cm in a dimly lit room. Eye positions were sampled and recorded with an infrared corneal reflection system, EyeLink 1000 (SR Research Ltd, Mississauga, Ontario, Canada) at a sampling rate of 500 Hz that focused on the right eye. During the fMRI scanning sessions, eye positions were sampled and recorded with an infrared corneal reflection system, EyeLink 1000 Plus (SR Research Ltd, Mississauga, Ontario, Canada), located at the back of the bore of the scanner, at a sampling rate of 500 Hz that focused on the right eye. All stimuli were displayed on a back-projected screen located in the bore of the scanner, which participants viewed through a mirror attached to the head coil. For both behavioral training and fMRI scanning sessions, five-point calibrations were performed at the beginning of the session and between each run. Saccadic eye movements were detected online using the EyeLink built-in algorithm in order to give participants performance feedback during the experiment. A valid saccade was further admitted to the behavioral analysis offline if it started from the central fixation window (3° x 3°, visual degrees) and ended in the peripheral target window (3° x 3°).

Stimuli Stimuli and task sequence are illustrated in Figure 3. Stimuli included a shaped context cue, a central fixation point, a target, a colored stop signal, and a colored continue signal. All stimuli were 1° x 1° in visual degree, and were presented against a gray background. The target stimuli were presented at an eccentricity of 10° horizontally from the fixation point, either to the left or to the right.

Procedure Each participant received 3 trial types: Go trials (56%), Stop trials (22%), and Continue trials (22%), presented in a pseudo-randomized order. All trials started when participants acquired central fixation at a context cue. The shape of the context cue (square or triangle) indicated the rule mapping on that trial, and was visible for 500 ms before it was replaced by a central fixation point. After a random delay (2000ms + jitter; jitter varied from 0 to 1500ms, incrementing by 500ms) the fixation point was then extinguished and, simultaneously, a peripheral target appeared. On Go trials, the target appeared alone and a trial was considered correct if participants generated a single saccade to the target (+/- 2.5° offset) within the 500ms maximum response time window and maintained their gaze at the target for an additional 200ms. On Stop and Continue trials, a central stimulus (blue or yellow dot) was presented after a variable delay (stop signal delay, SSD, for Stop trials, and continue signal delay, CSD, for Continue trials) following the target onset. On Stop trials, the trial was correct if participants maintained fixation for 400ms after the stop signal was presented, indicating that they had canceled the preparation of their planned saccades. On Continue trials, the trial was correct if the participants successfully generated a saccade to the target, despite the presentation of a continue signal. Four fixed SSDs were selected empirically based on each individual's performance during the behavioral training sessions such that at the shortest SSD,

participants generally inhibited the movement in >75% of the Stop trials and at the longest delay, participants inhibited the movement in <25% of the Stop trials, and most of the data points were centered around the two SSDs in which the participants inhibited the movement around 50% of the Stop trials. The SSDs ranged between 50 ms to 250 ms. The same delays were used for Continue trials for the same participant and were referred to as continue signal delays (CSDs). In one context, a yellow point cued the participants to cancel the saccade (Stop trials) while a blue point cued the participants to ignore it and make a saccade to the peripheral target (Continue trials). In the other context, the rule was reversed. Three inter-trial intervals (ITIs), 2s, 4s, and 6s, were used and were pseudo-randomly determined resulting in 60%, 30%, and 10% of trials, respectively. The context alternated every 8,10 or 16 trials, randomly and without prior warning. The first trial following the context alternation was termed a "switch" trial. Participants were given auditory feedback at the end of each trial, with a high-pitch tone indicating a correct response and a low-pitch tone indicating an erroneous response (Figure 3).

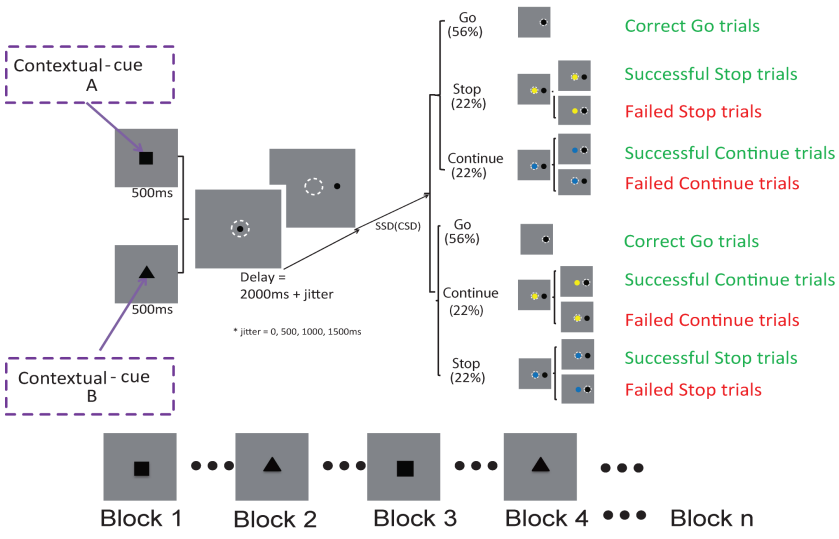

Figure 3. Context-dependent stop signal task. All trials started with a central fixation

spot on the screen for a variable delay period (200-400ms, 50-ms steps). Next, the central fixation spot disappeared and, simultaneously, a visual target appeared signaling participants to saccade to the target as quickly as possible. On Go trials (56% of all trials), the target appeared alone. In Stop trials (22%) and Continue trials (22%), a central stimulus (blue or yellow dot) was presented after a variable delay following the target onset (stop signal delay, SSD; continue signal delay, CSD; 4 fixed SSDs/CSDs ranged from 50ms to 250ms). The context alternated every 8,10 or 16 trials, randomly and without prior warning.

Data Analysis and Estimation of SSRT/CSRT

All data were analyzed using custom-written MATLAB (http://www.mathworks.com) scripts. Reaction times (RTs) were calculated as the time between go signal onset and the initiation of a saccade, and were expressed as mean ± 1 s.e.m. Inhibition functions were constructed by fitting a Weibull function to the relationship between the stop signal delay and the proportion of Failed Stop trials over all Stop trials (i.e. the probability of generating a saccade over all Stop trials).

To estimate SSRT we used the modified integration method. This method has been described in detail previously and this description is summarized here (Mayse et al., 2014). This method is computationally similar to the integration method, in which SSRT is determined by finding the point on the Go RT distribution at which the area-under-the-curve equals the proportion of Failed Stop trials for a given SSD, then aligning this point to the stop signal by subtracting SSD from Go RT. SSRT is then determined by averaging these SSRTs across all SSDs. However, this method relies on having discrete outcomes for each trial. For instance, when stopping is successful, no saccade is generated within the trial window; therefore, the proportion of Successful Stop trials for a given SSD can simply be calculated as

$$1 - \frac{\left(N_{Total\ Stop\ Trials} - N_{Stop\ Trials\ with\ Saccade}\right)}{N_{Total\ Stop\ Trials}}$$

However, such a simple calculation is not possible on Continue trials in which participants make a saccade on nearly all trials. The modified integration method allows for estimation of SSRT and CSRT by comparing the signal distribution (either continue or stop) to a yoked go trial RT distribution (the go RT distribution aligned to the stop signal). The most intuitive explanation of this method comes from describing how it is applied to Stop trials, but the method can be identically applied to Continue trials. Because RTs on Failed Stop trials are simply a subsample of the full go RT distribution, these RTs are statistically indistinguishable from the fast portion of the go RT distribution. Therefore, SSRT should correspond to the earliest time point that the go and stop RT distributions diverge (Mayse et al., 2014; and Figure 4). However, comparing these distributions is difficult because they originate at different points in time (the Go RT distribution has its origin at the onset of the Go signal, and the Failed Stop RT distribution has its origin at the onset of the stop signal). Therefore, the Go RT distribution is "yoked" to the stop signal and compared to the Failed Stop RTs that are aligned to the stop signal onset, collapsed across all SSDs. This method was implemented in the following steps: First, we drew *n* (where *n* is the number of stop or continue trials) random samples without replacement from the number of Go trials in a session. These RTs were aligned to the stop signal by subtracting from this sampling distribution the actual *n* SSDs or CSDs. Separate, yoked Go RT distributions were created for estimation of SSRT and CSRT. Second, this sampling and aligning procedure was repeated 10,000 times to construct a 99.9% (0.05%-99.95%) confidence interval (CI) of the yoked Go RT distribution. Third, we determined the first time point in the sorted Stop or Continue trial RT distribution that fell outside the 99.9% CI (this time point was calculated as the first

time point at which at least 0.15*n* consecutive stop or continue trials were greater than the upper bound of the 99.9% CI to protect against false positives in noisy cumulative RT distributions). This time point is not SSRT or CSRT (which is a point on the Stop or Continue trial RT distribution, not the 99.9% CI) but was used as a conservative cutoff to separate fast and slow continue trials (Mayse et al., 2014). Finally, using this cutoff value, we were able to find the proportion of failed stop or fast continue trials. We then estimated SSRT (CSRT) by finding the latency relative to the Stop (Continue) signal at which the density of the cumulative distribution of Stop-aligned Stop trial (Continue-aligned Continue trial) RTs was equal to the proportion of Failed Stop (Fast Continue) trials. It has been previously demonstrated that SSRTs derived using this method are indistinguishable from SSRTs derived using the integration or median methods (Mayse et al., 2014). Note that because by definition Successful Stop trials were those in which participants did not make a saccade during the trial response window, we assigned a value of 10000ms to RTs on these trials for the purposes of estimating SSRT; this value is arbitrary as long as it is longer than any observed RT and was not used for any other analysis.

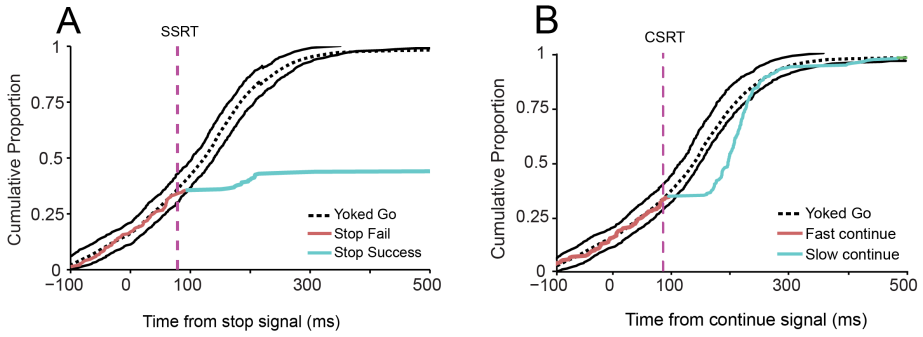

Figure 4. Cumulative distribution functions of reaction times using the new modified integration method. A. Stop trial reaction time distributions relative to Stop signal onset from Stop trials (colored) and yoked (re-aligned) Go trials (mean, dotted black; 99.9% CI, solid black). The intersection of Stop trials and the upper 99.9% CI

bound (solid black) defined an optimal Stop signal reaction time cutoff (magenta vertical dashed line) that best separated Failed Stop (red line) and Successful Stop (blue line) trials. **B.** Continue trial reaction time distributions relative to Continue signal onset from Continue trials (colored) and yoked Go trials (mean, dotted black; 99.9% CI, solid black). The intersection of Continue trials and the upper 99.9% CI bound (solid black) defined an optimal Continue signal reaction time cutoff (magenta vertical dashed line) that best separated Fast Continue (red line) and Slow Continue (blue line) trials.

fMRI Data Acquisition and Analysis

MR images were acquired with a Phillips Intera 3T scanner at the Kirby Center for Functional Brain Imaging at the Kennedy Krieger Institute in Baltimore, MD. For each participant, a high-resolution anatomical scan was acquired with an MPRAGE T1-weighted sequence with an isotropic voxel size of 1 mm isotropic resolution [repetition time (TR) = 8.1 ms; echo time (TE) = 3.7 ms, flip angle = 8°, 150 axial slices, 0 mm gap, SENSE factor = 2]. Whole-brain, T2*-weighted echo-planar images were acquired with a 32-channel SENSE headcoil in 36 transverse, sequential slices [TR = 2000ms, TE = 30 ms; flip angle = 70°, acquisition matric = 76 x76, field of view = 192.00mm x 171.79mm x 107.50mm; slice thickness 2.5 mm, gap = 0.5 mm; SENSE factor = 2], yielding voxels that were 2.5mm isotropic. Each EPI scan began with 4 dummy pulses prior to the context cue onset in order to allow magnetization to reach steady-state. We acquired 234 volumes for each of the 6 experimental runs such that each lasted approximate 7.8 minutes.

Preprocessing of the data was carried out in AFNI (Cox, 1996) with the exception of removing the skull from the anatomical scan, which was carried out using fsl_anat (Jenkinson et al., 2012). We applied AFNI's nonlinear warping (3dQWarp) to morph each participant's anatomical scan into Talairach stereotaxic space (Talairach and Tournous, 1998) according to the Colin 27 template. All functional images were first

corrected for slice time acquisition. Next, we corrected for participant motion and registered each image to the corresponding normalized anatomical scan by applying the parameters from the nonlinear warping. The functional runs were resampled to an isotropic resolution of 2mm during coregistration. Lastly, we performed spatial smoothing with a kernel of 4 mm full width half maximum and normalized the BOLD response in each voxel to the voxel's average MR signal magnitude across the six experimental runs.

Univariate analysis (Voxelwise General Linear Model) for testing the main effect of motor inhibition and/or reflexive reorienting attention to external events

Task-dependent changes in BOLD signal were modeled to test whether elevated BOLD activity in rVLPFC was correlated with motor inhibition and/or with reflexive reorienting attention to external events, using separate regressors representing each possible combination of the two signal colors (blue or yellow) and five trial outcomes (Correct Go, Successful Stop, Failed Stop, Slow Continue, and Fast Continue). Each regressor was time-locked to the target onset. In addition, six head-motion parameters were included in the model as regressors-of-no-interest. All regressors were convolved with the canonical hemodynamic response function (HRF) using a double gamma function. The general linear model (GLM) was estimated for each participant separately using AFNI's 3dDeconvolve function. Contrasts of interest were created for each participant to identify voxels exhibiting greater BOLD responses on: 1) Successful Stop (SS) trials compared with Go trials, 2) Failed Stop (FS) trials compared with Go trials, 3) SS trials compared with FS trials, 4) Stop (SS +FS) trials compared with Go trials, regardless of the outcome of the stopping, 5) Continue (Fast Continue, FC + Slow

Continue, SC) trials compared with Go trials, and 6) Stop trials compared with Continue trials. All contrasts created at the participant-level were entered into a group-level random-effect analysis using a one-sample t test against a contrast value of zero at each voxel. The statistical maps were thresholded using a voxel-level threshold of $p < 0.01$, corrected for multiple comparisons at a cluster-level of $p < 0.05$ (family-wise error correction). All whole-brain group-level results were corrected for multiple comparisons by running 10,000 Monte Carlo simulations in 3dClustSim to determine the probability of obtaining a cluster of significant activity of a certain size given the spatial smoothness of the data.

Defining Regions of Interest for testing motor inhibition

We first attempted to use the Stop > Go contrast in the group-level GLM analysis to identify the right lateral prefrontal region that showed significant activation. Next, we manually created an anatomical "mask" for right inferior frontal gyrus (rIFG) using AFNI built-in N27 brain Atlas. (AFNI atlas uses IFG to designate VLPFC). Regions of interest (ROI) were defined as the overlapping area between the functionally defined lateral prefrontal regions and the anatomical mask of rIFG. We extracted the beta weights of the ROI, averaged across all voxels in the ROI, for each participant for the following five regressors/contrasts: 1) Go trials - baseline, 2) SS - Go trials, 3) FS - Go trials, 4) FC – Go trials, and 5) SC – Go trials. Positive value indicates greater BOLD activity.

Defining Regions of Interest for testing reflexive reorientation of attention to external events

We first attempt to use the Signal (Stop + Continue) > Go contrast in the group-level GLM analysis to identify the lateral prefrontal region that showed significant

activation. Next, we used the same anatomical "mask" for right inferior frontal gyrus (rIFG) that was described above. The region of interest (ROI) was defined as the overlapping area between the functionally defined lateral prefrontal region and the anatomical mask of rIFG. We extracted the beta weights of the ROI, averaged across all voxels in the ROI, for each participant for the following three regressor/contrasts: 1) Go trials alone, 2) Stop - Go trials, and 3) Continue - Go trials. Positive value indicates greater BOLD activity.

Defining FEF

We used frontal eye fields (FEF) as an "area of reference" to assess the validity of the pattern classification method (described in detail in the next section) and to benchmark its result with the results found in rVLPFC, since it is well-established that the activation in FEF is associated with oculomotor control (Schiller et al,. 1981; Goldberg and Bushness, 1981; Hanes et al., 1995; Connolly et al., 2005; Curtis et al., 2005). FEF was initially identified functionally by selecting voxel clusters from both left and right hemisphere that showed significant activation using the Go – baseline >0 contrast from the group-level GLM analysis. Second, among the functionally defined FEF-like regions, only areas that were anterior to the precentral sulcus, and lateral to the superior frontal sulcus were further included in the data analysis (Courtney et al., 1996; Courtney et al., 1998).

Multi-voxel pattern classification analysis (MVPA) for signal-meaning encoding

MVPA (Norman et al., 2006) was performed using a linear support vector machine (LinearCSVMC) from LIBSVM library (Change and Lin, 2011) implemented within the PyMVPA software package (Hanke et al., 2009). Preprocessing was the same as described above in the GLM analysis. To reduce the problem related to BOLD signals overlapping across temporally adjacent events, a univariate GLM analysis was conducted to derive trial-type-specific beta estimates for each run, representing each possible combination of the two colors (blue and yellow) and three trial types (Go, Stop, and Continue trials). In addition, six head-motion parameters were included in the model as regressors-of-no-interest. Trials were modeled as events time-locked to the onset of the target with a double-gamma function and were convolved with a canonical HRF. Error Go and Continue trials were excluded from analyses.

Since a signal has two dimensions of properties, one for color (blue or yellow), and the other for the meaning of the signal (Continue or Stop), and since participants needed to use the shape of the context cue that appeared at the beginning of each trial to establish specific association between the color and the meaning of the signal, and subsequently to use this rule to guide their response upon seeing the subsequent colored signal, context rule was defined as the mapping between the meaning of the signal and the color. For each participant, beta values pertaining to each combination of color and meaning were estimated, within each run, yielding four beta maps per run (i.e. “blue Continue”, “blue Stop”, “yellow Continue”, and “yellow Stop”). Overall, the GLM analysis yielded 24 (4 beta maps/run x 6 runs) beta maps for each participant.

Classifications of signal meaning and color were performed within the rVLPFC ROI that was the same as was defined to test reflexive reorientation of attention to

external events. For each participant, the pattern of beta values within each ROI was extracted from each of the relevant beta maps. A leave-one-run-out procedure was used for cross-validation (CV). A classifier was trained using data from five of the six runs and then tested using the data from the held-out run. Six iterations were performed so that each run was tested once. The mean classification accuracy was determined by averaging the results across six iterations. To test the significance of the classification accuracy at the group level, we first performed the permutation testing for each individual. This was done by randomly shuffling the target feature labels in the training sets (test set was not included) 1000 times to simulate the null distribution for a single participant. We then pooled all 21 participants' classification accuracy values and tested them against the chance performance value of 0.5 (because the signal meaning was either correctly or incorrectly interpreted by the participant's classifier), at the level of $p<0.05$ (two-tailed).

Multi-voxel pattern classification (MVPA) for stop outcome encoding

A different univariate GLM analysis was conducted to derive stop-outcome-specific beta estimates for each run, representing Failed Stop and Successful Stop outcomes. In addition, six head-motion parameters were included in the model as regressors-of-no-interest. Trials were modeled as events time-locked to the onset of the target with a double-gamma function and were convolved with a canonical HRF. For each participant, beta values pertaining to both trial outcomes were estimated within each run, yielding two beta maps per run. Overall, the GLM analysis yielded 12 (2 x 6 runs) beta maps.

2.3 Results

Behavioral results

Performance for the current context-dependent SST was similar to that observed in Sharp et., al (2010). Because the performance was comparable between context A, where the Stop signal was yellow and Continue signal was blue, and context B, where this mapping was reversed, behavioral data were collapsed across both contexts. The probability of making a saccade in Stop trials increased as the Stop signal delay (SSD) increased, but remained relatively stable and high in Continue trials for the Continue signal delay (CSD, Figure 5A). The mean reaction time (RT) in Failed Stop trials was [RT = 262.24 ± 6.52 ms, mean ± standard error of mean (s.e.m.)] faster than in Go trials (RT = 289.25 ± 5.34ms), but was the longest in Continue trials (RT = 321.28 ± 6.93 ms; Figure 5B). Pairwise comparison using two-sample paired t test showed that there was a significant difference between Go RT and Failed Stop RT ($t_{(20)}$ =3.25, p = 0.0017), and between Go RT and Continue RT ($t_{(20)}$ = -3.70, $p < 0.001$).

Stop signal reaction time (SSRT) was estimated using the modified integration method (Mayse, et. al, 2012). This novel method provides an estimate of SSRT by directly comparing RT distributions in Stop trials and Go trials in order to determine the time point at which the Stop signal begins to slow down RTs relative to go trial RTs. Using the same method, we were also able to estimate the Continue signal reaction time (CSRT), which is the time it took participants to respond to the Continue signal and continue to make the saccade that they had planned for. CSRT (111.58 ± 3.43ms) and SSRT (118.72 ± 3.44 ms) were statistically indistinguishable ($t_{(20)}$ = -1.47, $p > 0.05$; Figure 5C).

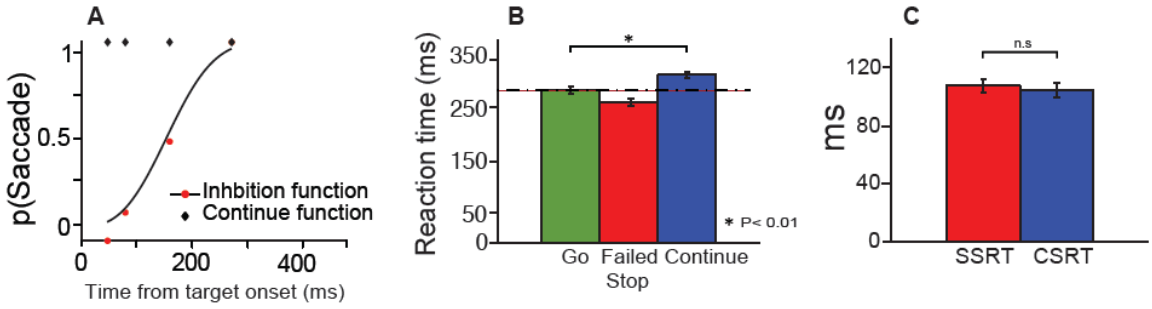

Figure 5 Behavioral results for the context-dependent SST. A) Inhibition function and Continue function for one exemplar behavioral session. The red dots show raw inhibition function, and the black line shows weibull-fitted inhibition function. The black dots show raw Continue function. B) Mean reaction time in Go (green), Failed Stop (red), and Continue (blue) trials. C) Mean Stop signal reaction time (SSRT, red) and Continue signal reaction time (CSRT, blue). Error bars indicate the standard error of the mean.

Neuroimaging results

GLM analysis testing the hypothesis I that rVLPFC is responsible for direct control of movement inhibition. If rVLPFC is responsible for directly controlling movement inhibition, then greater BOLD activity in this area should be observed during successful stopping compared with when an eye movement was generated. In other words, Successful Stop (SS) trials should elicit higher BOLD activation when compared with Go trials. Similarly, SS trials should elicit higher BOLD activation when compared with Failed Stop (FS) trials because in FS trials, an eye movement was erroneously generated. Figure 6 (with raw beta weights shown in Figure 7; Table 1 and Table 2) showed that rVLPFC demonstrated elevated activity for both SS and FS trials when compared with Go trials. This was inconsistent with the hypothesis's prediction. One possible interpretation would be that a second stimulus, i.e. Stop signal, was presented in both SS and FS trials, and the comparable BOLD activation observed in both trials reflected the attentional capture effect from the abrupt onset of the Stop signal (Hypothesis II regarding rVLPFC). If this interpretation were true, then Continue signal

should also elicit increased BOLD activation in Continue trials compared to Go trials, similar to that elicited by Stop trials. We further compared the BOLD activity in Continue trials with Go trials in the same area that previously demonstrated elevated activity for both SS and FS trials, and observed no differential activation (Figures 6 and 7, Table 1 and 2). So far, GLM analysis showed that rVLPFC demonstrated increased BOLD activity for Stop trials, relative to Go trials, and no increased activity for Continue trials. There was no activation magnitude difference, however, between Failed and Successful Stop trials. Therefore, GLM results did not support the hypothesis that this region in rVLPFC is responsible for direct control of movement inhibition.

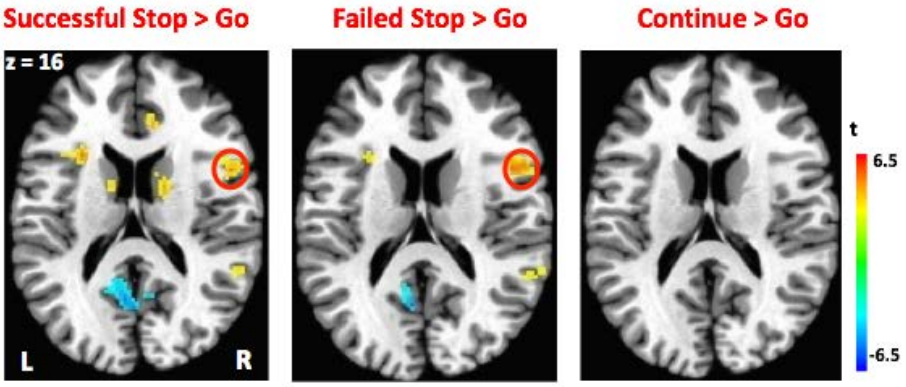

Figure 6. Areas show greater activation (warm color) for Successful Stop and Failed Stop, but not Continue, trials compared with Go trials. Red circle denotes rVLPFC.

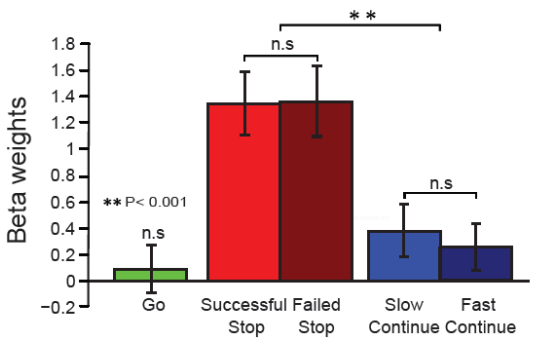

Figure 7. Beta weights for the area within the rVLPFC that showed greater activation for both Successful and Failed stop trials compared to Go trials. This region did not show greater activation for Continue trials compared to Go trials**.** Beta weights for Go trials (green), Successful Stop (red), Failed Stop (dark red), Slow Continue (blue), and Fast Continue (light blue),

Table 1. Regions demonstrating greater activation for Successful Stop compared with Go trials.

Area	Talairach coordinates (mm)			Volume (mm^3)
	x	y	z	
R ventrolateral prefrontal cortex/insula	33	21	6	2,502
R inferior parietal lobule	37	-59	44	1,806
L claustrum	-27	21	10	831
L inferior frontal lobule	-33	-51	38	633
R cingulate gyrus	7	21	34	366
R caudate	11	7	6	268
R superior parietal lobule	15	-65	34	197
L caudate	-11	1	14	184
L precentral gyrus	-41	-1	36	119
R thalamus	13	-11	4	91

Note. Talairach coordinates indicate the peak voxel within each cluster (family-wise error, $p < .05$). R, right; L, left; B, bilateral.

Table 2. Regions demonstrating greater activation for Failed Stop compared with Go trials.

Area	Talairach coordinates (mm)			Volume (mm^3)
	x	y	z	
R ventrolateral prefrontal cortex/insula	41	21	4	2,044
R inferior parietal lobule	33	-55	40	947
L claustrum	-27	21	10	500
L inferior frontal lobule	-33	-51	38	633
L cingulate gyrus	-7	-31	30	425
R superior frontal gyrus	3	17	50	314
L inferior frontal lobule	-33	-53	38	265
R middle temporal gyrus	55	-41	4	92
R precentral gyrus	15	-65	32	88

Note. Talairach coordinates indicate the peak voxel within each cluster (family-wise error, $p < .05$). R, right; L, left.

GLM analysis testing the hypothesis II that rVLPFC is responsible for reflexively reorienting attention to external stimuli that are behaviorally relevant. If rVLPFC is responsible for detecting external sensory stimuli that are behaviorally relevant, then greater BOLD activity in this area should be observed during both Stop and Continue trials, where a second signal appeared after the target onset, compared to Go trials, where no signal was presented after the target onset. Furthermore, the Stop signal and Continue signal should elicit comparable magnitude of BOLD activation because they share identical sensory properties. Figure 8 (Table 3 and 4) shows that rVLPFC demonstrated elevated activity for Stop trials compared with Go trials, as well as elevated activity for Continue trials compared with Go trials. Furthermore, there was no activation magnitude difference between Stop and Continue trials (Figures 8 and 9, Table 3 and 4). This was consistent with the prediction of the hypothesis II. Nevertheless, the part of rVLPFC that showed elevated activity for both Stop and Continue trials in Hypothesis II was centered around the dorsal part within rVLPFC, different from the part of rVLPFC that showed

elevated activity uniquely to Stop trials in Hypothesis I, which was located more to the ventral part (Figure 10).

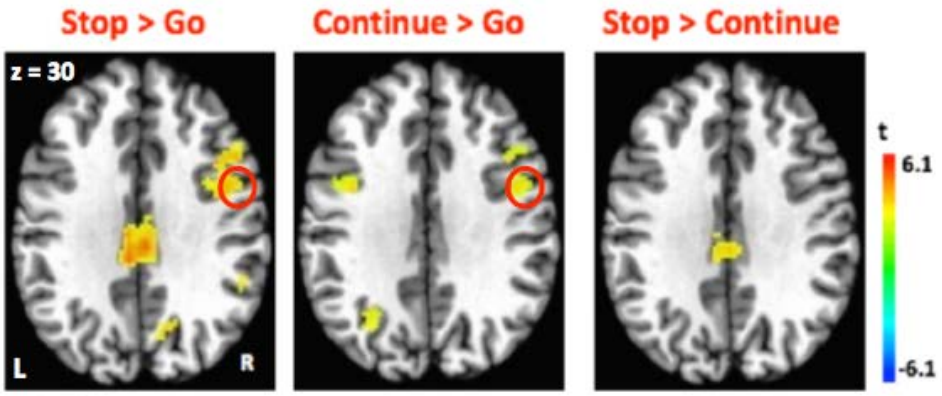

Figure 8. Areas show greater activation (warm color) for Stop and Continue trials compared with Go trials. Red circle denotes the regions within the rVLPFC.

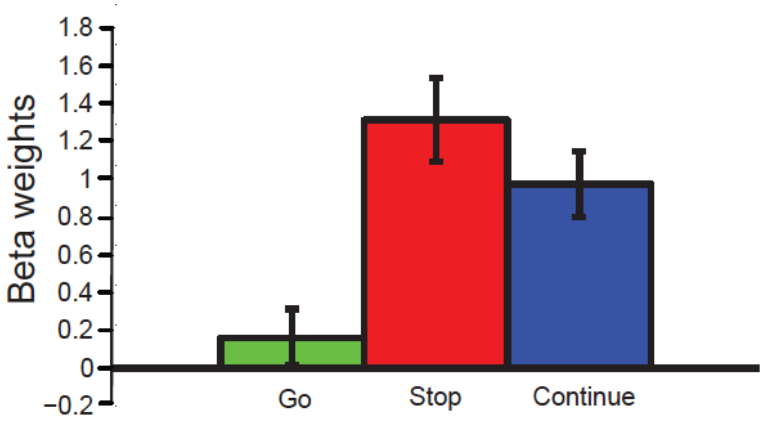

Figure 9. **Beta weights for the area within the rVLPFC that showed greater activation for both Stop and Continue trials compared with Go trials.** The mean voxel activation for Stop and Continue trials were statistically indifferent. Beta weights for Go trials (green), Stop trials (red), and Continue trials (blue).

Table 3. Regions demonstrating greater activation for Stop trials compared with Go trials.

Area	Talairach coordinates (mm)			Volume
	x	y	z	(mm^3)
R ventrolateral prefrontal cortex	39	3	30	2,589
R angular gyrus	33	-55	38	1,775
L claustrum	-27	21	10	749
R superior frontal gyrus	5	15	48	473
L angular gyrus	-31	-53	38	452
L cingulate gyrus	-5	-31	30	391
R superior parietal lobule	15	-65	34	170
R caudate	13	11	4	160
L caudate	-9	5	10	111
L precentral gyrus	-37	1	28	100

Note. Talairach coordinates indicate the peak voxel within each cluster (family-wise error, $p < .05$). R, right; L, left.

Table 4. Regions demonstrating greater activation for Continue trials compared with Go trials.

Area	Talairach coordinates (mm)			Volume
	x	y	z	(mm^3)
R superior parietal lobule	39	-65	44	1,371
R ventrolateral prefrontal cortex	39	-1	30	1,054
L inferior parietal lobule	-35	-53	40	909
L inferior frontal gyrus	-37	1	30	417
L superior frontal gyrus	-3	13	48	220
L insula	-37	11	10	205
R insula	39	15	4	198
L cingulate gyrus	-3	-33	30	163
R superior parietal lobule	9	-69	36	159
L middle frontal gyrus	-41	27	26	117

Note. Talairach coordinates indicate the peak voxel within each cluster (family-wise error, $p < .05$). R, right; L, left.

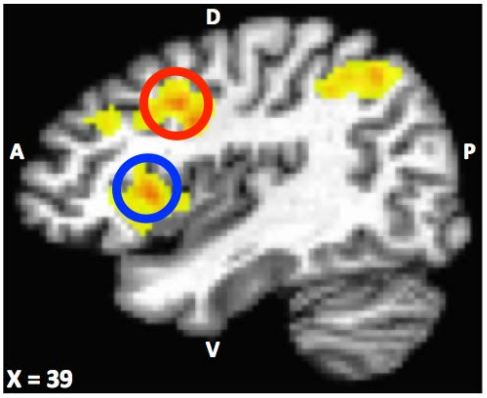

Figure 10. BOLD activation in ventral and dorsal parts of rVLPFC for testing hypothesis I and II. Red circle denotes the doral part of rVLPFC that showed elevated activity for both Stop and Continue trials (Hypothesis II). Blue circle denotes the ventral part of rVLPFC that showed elevated activity uniquely to Stop trials (Hypothesis I).

MVPA analysis testing the hypothesis III that rVLPFC is responsible for encoding task-relevant rules. Continue and Stop signals shared identical physical properties, which means that they both could either be yellow or blue and the time of SSD and CSD were identical for the same participant. The only difference between the two stimuli is the signal meaning in a particular context. If rVLPFC is responsible for encoding context-based, task-relevant rules, then patterns of activation for Stop and Continue trials, independent of the color of the signals, should be different. In Hypothesis II testing we found that increased BOLD activity in dorsal rVLPFC was observed in both Stop and Continue trials compared to Go trials, yet there was no activation magnitude difference between Stop and Continue trials. We, thus, chose dorsal rVLFPC as the ROI for MVPA analysis (details see *Method*). As predicted, we were able to classify, with above chance accuracy (one sample t test), the differential patterns of BOLD activation for the meaning of the signal (Stop versus Continue, accuracy = 70 ± 5%, $t_{(20)}$ =4.09, $p < 0.001$; light grey bar for dorsal rVLPFC in Figure 11) but not the color of the signal (blue versus yellow,

accuracy = 51 ± 4%, $t_{(20)}$ =0.15, p > 0.05; Figure 11).

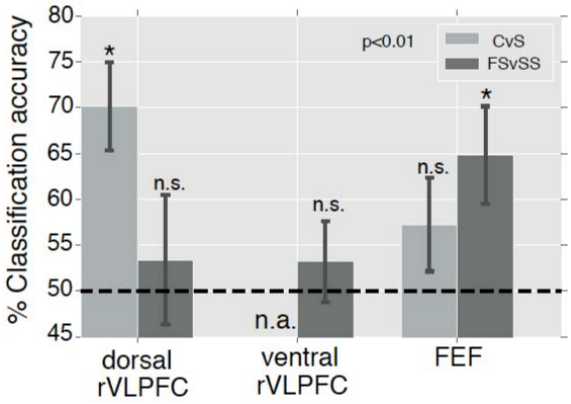

Figure 11. MVPA results showing classification accuracies for two classification types [meaning of the signal (light grey bar) and stop outcome (darker grey bar)] across three brain regions (dorsal rVLPFC, ventral rVLPFC, and bilateral FEF). MVPA classifier applied to the dorsal rVLPFC was able to classify the response patterns to the Stop signal from the response patterns to the Continue signal, but failed to classify the patterns of Failed Stop trials from Successful Stop trials with above chance (horizontal dashed line) accuracy. The classifier was also unable to successfully classify Failed versus Successful Stop trials in the ventral part of rVLPFC. On the other hand, MVPA classifier was able to classify the patterns of stop outcome but not the patterns that coded for the meaning of the signal in FEF. We did not attempt to classify Stop versus Continue in the ventral rVLPFC because this region was defined according to a difference in the magnitude of the activation for Stop trials relative to Continue trials. Error bar indicates standard error of mean.

Successful Stop vs. Failed Stop classification To investigate whether there are overlapping but dissociable neural populations engaged by SS vs. FS trials in addition to the regions showing overall different magnitudes of activation for other contrasts, we conducted ROI-based multi-variate pattern classification analysis (MVPA) using areas which showed significantly elevated activity for both SS and FS trials compared with Go trials but which showed no overall differential activity magnitude between SS and FS in the GLM analysis. This region resides in the more ventral side of rVLPFC. A similar GLM was run on each participant's data with separate regressors for each trial outcome

as described in *Methods* but with one difference: a separate GLM was applied to each run separately. MVPA was not able to classify, with above chance accuracy, the differential pattern of BOLD activation between SS and FS trials (accuracy = 53 ± 5%, $t_{(20)} = 0.71$, $p > 0.05$; darker grey bar for ventral rVLPFC in Figure 11). We further ran the classification analysis in the dorsal part of the rVLPFC to test if this region encodes different patterns of activation for FS and SS trials, but did not pass the threshold during GLM analysis. MVPA was not able to classify, with above chance accuracy, the differential pattern of BOLD activation between SS and FS trials (accuracy = 53 ± 7%, $t_{(20)} = 0.47$, $p > 0.05$; darker grey bar for dorsal rVLPFC in Figure 11). Therefore, neither GLM nor MVPA results supported the hypothesis that rVLPFC (includes both ventral and dorsal part) is responsible for directly controlling of movement inhibition.

Next, we sought to further validate the classification methods by applying the same MVPA to bilateral frontal eye field (FEF), an area known for controlling for oculomotor movement. We found that MVPA was able to successfully classify, with above chance accuracy, the stop outcome (accuracy = 65 ± 5%, $t_{(20)} = 2.71$, $p < 0.05$; darker grey bar for FEF in Figure 11), but not the meaning of the signal (accuracy = 57 ± 5%, $t_{(20)} = 1.39$, $p > 0.05$; light grey bar for FEF in Figure 11), nor the color of the signal (accuracy = 50 ± 4%, $t_{(20)} = 0.08$, $p > 0.05$; Figure 12).

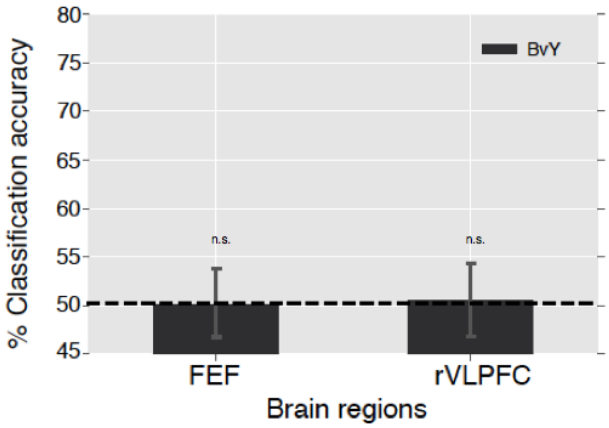

Figure 12. MVPA results failed to classify, the differential patterns of activation for the color of the signal, i.e. blue vs. yellow, in both FEF and dorsal rVLPFC.

2.4 Discussion

The current study investigated the mechanisms of the rVLPFC in controlling for context-dependent eye movement inhibition. We found that behaviorally, reaction times in Continue trials were longer than in the Go trials, and the Failed Stop trials yielded the shortest reaction times (Figure 5). Neuroimaging results showed that increased BOLD activity in dorsal rVLPFC was observed in both Stop and Continue trials compared to Go trials, but there was no activation magnitude difference between Stop and Continue trials (Figure 8, 9 and 10). On the other hand, multivariate pattern classification analysis (MVPA) was able to classify, with above chance accuracy, the meaning of the instructional stimulus for that trial (i.e., Stop signals vs. Continue signals, Figure 11), but not the color of the stimulus (i.e., yellow vs. blue, Figure 12). In contrast, ventral rVLPFC demonstrated increased BOLD activity relative to Go trials, only in Stop trials, yet there was no activation magnitude difference between Failed and Successful Stop trials (Figure 6, 7 and 10), and the MVPA classifier could not classify the patterns of the stop trial outcome (Figure 11). The MVPA classifier could, however, classify the patterns

of activity related to stop trial outcome in the FEF. Thus, contrary to some previous claims, these results suggest that the ventral rVLPFC detects signals that are stop-relevant, yet does not control motor inhibition *per se*. On the other hand, dorsal rVLPFC detects signals that are behaviorally relevant, and represents the current stimulus-response association rule. Together, the data supports hypothesis IV that sub-regions within rVLPFC contribute heterogeneous functions in movement inhibition.

Cognitive control of movement inhibition not only involves motor inhibition, but often is comprised of attending to contextually relevant sensory information, mapping the sensory information to specific goals, planning and executing appropriate actions. A limitation of much of the previous neuroimaging research is that the "stop signal" is a perceptually salient stimulus that conflates the processing associated with attentional capture of the sensory cue and response inhibition. To control for the attentional capture effect, Sharp et al., (2010) introduced Continue signal trials in addition to the conventional SST that was composed of Stop and Go trials, and found that right inferior frontal gyrus (rIFG), which is equivalent to part of the rVLPFC, was active for both Stop and Continue signals, but pre-SMA was more active for Stop trials compared to Continue trials. The authors argued that the Continue signal in their experimental design is behaviorally irrelevant, and concluded that pre-SMA is associated with response inhibition whereas rIFG is associated with attentional capture. Pre-SMA is responsible for controlling skeletomotor movement whereas FEF is responsible for controlling eye movement. Our BOLD activation results in FEF and rVLPFC provide nice complement to Sharp et al., (2010) study of movement inhibition in the skeletomotor domain.

Furthermore, our study also extended Sharp et al. (2010) by adding a third level of control, the context manipulation, and participants had to attend to both Continue and Stop signals and use the context cue to establish the meaning of the signal with the color. By adding this level of manipulation, both Continue and Stop signals became behaviorally relevant and we found not only was BOLD response in rVLPFC associated with both signals' presence, but also encoded the meaning of the signal. Thus, our finding extended previous research and suggested that rVLPFC encodes abstract information in addition to the sensory information.

Levy and Wagner (2011) performed a functional MRI meta-analysis to study the role of rVLPFC in response inhibition using SST, Go/No-Go task, Posner cueing task, and Oddball task, and found that bilateral inferior frontal junction (IFJ) was active for stopping and reflexive orienting, posterior-rVLPFC was active during the updating of action plans and mid-rVLPFC responded to decision uncertainty. In their definition of brain regions, IFJ is the most posterior and superior region of rVLPFC, where rVLPFC intersects with the middle frontal gyrus dorsally and the premotor cortex caudally (Figure 2). Posterior-rVLPFC, is bounded by the precentral sulcus and the ascending ramus of the lateral sulcus. This region also corresponds roughly to the region referred to as pars opercularis or Brodmann area (BA 44). Rostral to the ascending ramus is mid-rVLPFC, which corresponds roughly to pars triangularis or BA 45. The horizontal ramus of the lateral sulcus separates mid-rVLPFC from anterior-rVLPFC, which roughly corresponds to pars orbitalis or BA 47 (Figure 2). Notably, since the authors found consistent *bilateral* IFJ activation for stopping and reflexive orienting as opposed to right-lateralized activation for VLPFC, they singled out IFJ as a separate region from rVLPFC.

The dorsal rVLPFC in our study roughly corresponds to BA 45B and 44, whereas the ventral part of rVLPFC rough corresponds to BA 45A and 47. Furthermore, instead of grouping different studies across designs and analysis techniques, our study took a holist approach to address the complicated processes involved in context-dependent SST, which included attending to a sensory signal, interpreting its meaning, and exerting motor inhibition according to appropriate context, and was able to identify a distinct functional separation within the right ventrolateral prefrontal cortex. We found two subregions within rVLPFC that demonstrated differential response profile to the context-based SST. Whereas the BOLD activation in the dorsal part of rVLPFC is associated with detecting behaviorally relevant sensory stimuli and interpreting the meaning of the signals, the response in the ventral part of rVLPFC is associated with Stop trials only regardless of the stop outcome. Erika-Florence et al., (2014) found similar results that the magnitude in BOLD response in right inferior frontal sulcus was indifferent between successful and failed stopping. We speculate that instead of directly exerting control over motor inhibition, ventral part of rVLPFC is responsible for registering the intention to stop, or updating the action plan. Our results were not in complete agreement with Levy and Wagner's meta-analysis results for the relative special locations among rVLPFC subregions: Levy and Wagner (2011) separated IFJ from the rVLPFC, and divided rVLPFC into three subregions along the posterior-anterior axis, with the posterior-rVLPFC represents motor stopping and mid-rVLPFC represents response uncertainty. Our results, on the other hand, only identified two subregions along the dorsal-ventral axis, with dorsal rVLPFC representing for attention orientation and task rule encoding, and ventral rVLPFC representing for stopping. This difference between the two studies

could be attributed to the fact that in Levy and Wagner (2011)'s meta-analysis study, the authors included Posner Cueing and Oddball tasks that particularly manipulated response uncertainty independent of response inhibition. Moreover, the large volume of studies that were included in the analysis increased the likelihood of identifying more regions showing task-related activation. Nevertheless, both studies supported the argument that sub-regions within rVLPFC contribute heterogeneous functions in cognitive control of movement inhibition.

One possible explanation for the above chance classification accuracy for Continue and Stop signals in dorsal rVLPFC might be that the results were driven by the feedback difference that participants received during the experiment. The mean average accuracy for the Stop trials was around 50% due to task manipulation, and the average accuracy for the Continue trials was above 90%. However, if the classification results were driven by the feedback effect, then one should be able to classify Successful Stop (SS) trials vs. Failed Stop (FS) trials in this region as well because participants received positive feedback on SS and negative feedback on FS. MVPA performance on classifying stop outcome in dorsal (also in ventral) rVLPFC was at the chance level, which ruled out the "feedback" explanation. Furthermore, we used the frontal eye field (FEF) to benchmark the findings in rVLPFC. FEF is a well-studied area known for controlling saccadic eye movement initiation and inhibition. Our MVPA results suggested that FEF contains information regarding the stop outcome, but not the meaning of the signal. These results were consistent with the existing knowledge on FEF's role in oculomotor control (Schiller et al., 1987; Bruce and Goldberg, 1985; Hanes et al., 1998; Schall and Thompson, 1999). The double disassociation between rVLPFC and FEF in the types of

information that each area encodes, with FEF encoding for oculomotor-related information and rVLPFC encoding for more abstract cognitive information, further supported the idea that function and structure of prefrontal cortex as a hierarchical control system (Koechlin et al., 2003; Badre and D'Esposito, 2007).

A few issues remained standing from the current study. First, while the Continue signal serves as an appropriate control for the attention-capture effect of the Stop signal, it is not clear whether the Continue signal also affects motor inhibitory control processes. We found that although participants were able to successfully complete the saccades they had planned for upon seeing the Continue signal, the mean reaction time of those Continue trials were significantly longer than Go trials. The prolonged reaction times could possibly be the result of a delayed response, or inhibition, in reaction to the sudden onset of a signal. In the next chapter, Chapter 3, I further investigated whether the Continue signal-induced delay in motor response is the same form of response inhibition that was induced by the Stop signal. More specifically, I ask whether the process A, which is activated by the Continue signal and subsequently delays preparation of a behavioral response, and the process B, which is activated by the Stop signal and ultimately cancels preparation of a behavioral response, are the same process.

Second, we sought to further validate human fMRI findings by comparing the results from recording single neuron activity in one macaque monkey rVLPFC (area 45) and FEF while the monkey performed a context-based SST in chapter 4. Recording single neurons' activates at a millisecond scale with high temporal resolution would offer a powerful complement to the human fMRI findings.

Third, PFC is central to cognitive control, and recent theoretical and empirical results explained the function and structure of prefrontal cortex as a hierarchical control system (Koechlin et al., 2003; Badre and D'Esposito, 2007). The current study examined the neural mechanism within rVLPFC underlying context-dependent movement inhibition. It remained unknown how the functional connections among dorsal rVLPFC, ventral rVLPFC, FEF and the rest of the brain areas form distributed networks that collectively exert inhibitory control. In Chapter 5, I used a new imaging analysis technique, known as the psychological-physiological interaction (PPI) analysis to address this issue.

Chapter 3: Cognitive control of selective stopping (Experiment 2)

3.1 Introduction

Inhibitory control, or the ability to inhibit actions inappropriate for the context, is essential for meeting the shifting demands of complex environments (Logan et al., 1997). Successful inhibitory control can be achieved through both reactive and proactive control strategies, respectively involving preparation to stop *prior to* stimulus onset and stimulus-driven processing *at the time of* stimulus onset (Aron, 2011; Li et al., 2008). In chapter 2, Experiment 1, we used a variant of the conventional SST utilizing so-called "Continue" trials (modified based on Sharp et al., 2010) to address these concerns. The overall structure of the continue variant of the SST (or continue SST) is the same as the conventional SST. On the majority of trials, participants make a response (either an eye movement or a button press) following the presentation of a salient go signal. On a minority of trials, this go signal is followed after a variable delay by either a salient stop signal instructing participants to cancel the planned go response or an equally salient

Continue signal. The Continue signal instructs participants to proceed with the go response they were preparing. Although the Continue signal does not carry an imperative to alter the participant's planned response (in contrast to the Stop signal), it cannot simply be ignored because participants must first disambiguate the perceptually similar Stop and Continue signals. Therefore, it can be assumed that the Stop and Continue signals carry similar attentional and sensory processing demands, but only the Stop signal activates neural processes involved in canceling the planned go response, allowing these neural signals to be resolved from those involved in allocation of attention or conflict monitoring.

However, while the Continue signal serves as an appropriate control for the attention-capture effect of the Stop signal, it is not clear whether the Continue signal also affects motor inhibitory control processes. Responses on Go and Continue trials are unlikely to be identical in practice because processing the identity of the surprising signal (either Continue or Stop) takes time, and participants are likely to pause or delay the generation of their planned response in order to avoid making an error during this period of ambiguity, resulting in longer reactions times (RTs) on those trials. Critically, if this is true, RTs on Continue trials should be bimodally distributed because, as in Stop trials, on some trials when the Continue signal is presented, preparation of the go response has already reached a point of no return at which it cannot be delayed or altered and therefore the go response would be emitted as normal (Schilleret al., 1987). These Continue trials would have very fast reaction times, similar to Failed Stop trials. Other Continue trials, in which the participant did not make a saccade until after the ambiguity was resolved regarding the identity of the Continue signal, would be slower.

This bimodal distribution of Continue-trial RTs was found by Sharp et al., (2010) in a previous study, with some Continue-trial RTs being significantly slower than Go-trial RTs (Slow-Continue trials), while others were identical to Go-trial RTs (Fast-Continue trials). However, on a large proportion of trials (>95%), participants subsequently made correct go responses, suggesting that the go response was merely delayed, rather than canceled as in Stop trials. These data indicated that, as in Stop trials, responses on Fast Continue trials result from completion of the go process and are simply sampled from the fast portion of the go trials RT distribution. By contrast, responses on Slow Continue trials are delayed because of the action of some internal process.

In the current study, we examined whether the process, when activated by the Continue signal, subsequently delays preparation of a behavioral response, is the same as the process, when activated by the Stop signal, ultimately cancels preparation of a behavioral response. We hypothesized that the mechanism that delays responding on Continue signal trials as observed in Sharp et al. (2010) is similar, if not the same, as the process that ultimately cancels preparation of a go response and, therefore, would have the same latency as the one measured by SSRT. To test this hypothesis, we used a novel analytic method called the modified integration method developed to estimate SSRT using continuous RT distributions rather than discrete trial outcomes (Mayse et al., 2014). Because participants make a response on most (>95%) continue signal trials, it is impossible to use the standard integration method, or other commonly used methods, for estimating the latency of inhibition because these methods rely on quantification of the proportion of Stop trials with a response, which would not be appropriate for Continue trials. By using the modified integration method, we were able to estimate the latency of

inhibition on Continue signal trials even though participants ultimately make a response on the vast majority of these trials. We found that not only were Continue-Trial RTs bimodal as predicted, but SSRTs and the Continue-Trial equivalent, continue signal reaction times (CSRTs), were statistically indistinguishable, suggesting that the mechanism by which Continue-Trial RTs were delayed has the same latency as the mechanism by which the go process is canceled on stop signal trials.

To further evaluate whether these processes are identical we leveraged a phenomenon called post-stop-signal improvement of inhibition. Succinctly, when participants perform two stop trials consecutively, stopping performance is improved on the second trial (trial n) compared to the first trial (trial n-1) as measured by both faster SSRT and a lower proportion of failed stop trials (Bissett and Logan, 2012). If this effect is caused by stopping itself, and if the continue signal activates the stop process, then we should observe post-continue-signal improvement of inhibition that is similar to post-stop-signal improvement of inhibition. To test this, we computed the change in SSRT on stop signal trials following either a stop or continue signal trial and CSRT on continue trials following either a stop or continue trial. If the continue signal trial RT delay is achieved by activation of the stop process, then we should observe both faster CSRT and faster SSRT following continue trials. If instead, the delay during slow continue trials is achieved by activation of a different mechanism for delaying a response or by partial or incomplete activation of the stop process that is insufficient to cause post-stop improvement of inhibition, then we should find speeding of SSRT but not CSRT following a stop signal trial. Overall, our results provide evidence for a multi-component stopping process in which a rapid process delays the preparation of a response in order

for a slower process to either cancel the planned Go response on Stop trials or resume it on Continue trials. We found post-stop-signal improvement of both SSRT and CSRT, but no post-continue-signal improvement in either, suggesting that activation of the processes delaying the Go response on Stop and Continue trials is insufficient to drive subsequent adjustments in SSRT and CSRT. Additionally, participants slowed their Go RTs following both Failed Stop and Successful Stop, but not Fast- or Slow-Continue trials. Critically, these effects could not be attributed to differences in trial feedback or as a result of the initial delay captured by SSRT and CSRT; therefore, we conclude that these effects result from post-error slowing in the case of Failed-Stop trials and from activation of a second, slower stopping mechanism for suppressing the Go response present on Successful-Stop but not Slow Continue trials.

3.2 Method

Participants. Fifty-eight participants [19 M, 39 F, mean age of 22 (range, 18-25 years); the age for one participant was inadvertently not recorded] were recruited from the Johns Hopkins community. All were screened for normal or corrected-to-normal visual acuity and color vision. Participants were compensated $15 for a single 1.5-hour session. Written, informed consent was obtained from all participants, and all of the experimental procedures were approved by the Johns Hopkins University Institutional Review Board. The data inclusion criteria were set *a priori,* such that only data from participants in which the average performance accuracy was no less than 40% for Stop trials and 80% for Continue trials were included. Four participants' performance data did not meet these criteria, and were excluded from further analysis. The current report is based on the data from the remaining fifty-four participants.

Apparatus and stimuli. A Mac Mini (Apple Inc., Cupertino, California, USA) equipped with MATLAB software (http://www.mathworks.com/) and PsychToolbox-3 extensions (http://psychtoolbox.org/) was used to present the stimuli on an Asus LED HD monitor (60 Hz refresh rate). The participants viewed the monitor from a distance of ~56 cm in a dimly lit room. Eye positions were sampled and recorded with an infrared corneal reflection system, EyeLink 1000 (SR Research Ltd, Mississauga, Ontario, Canada) at a sampling rate of 500 Hz. Saccadic eye movements were detected online using the EyeLink built-in algorithm. A valid saccade was further admitted to the behavioral analysis if it started from the central fixation window (3° x 3°, visual degrees) and ended in the peripheral target window (3° x 3°). Stimuli and task sequence are illustrated in Figure 13. Stimuli included a central fixation point, a target, a stop signal, and a continue signal. The fixation point and the target were both black dots. Stop and continue signals were either blue or yellow dots, respectively, or vice versa, counterbalanced across participants. All stimuli were 1° x 1° in visual degree, and were presented against a gray background. The target stimuli were presented at an eccentricity of 10° horizontally from the fixation point, either to the left or to the right.

Procedure.

All trials started with the participants acquiring a central fixation spot on a screen for a variable delay period (200-400ms, 50-ms steps). Next, the central fixation spot disappeared and, simultaneously, a visual target appeared signaling the participants to generate a saccade to the target as quickly as possible. On Go trials, the target appeared alone and a trial was considered correct if the participants generated a single saccade to the target within the 500ms maximum response time window and maintained their gaze

at the target for an additional 200ms. In Stop trials and Continue trials, a central stimulus (blue or yellow dot) was presented after a variable delay (stop signal delay, SSD; ranging from 50ms to 250ms) following the target onset. On Stop trials, the trial was correct if participants maintained fixation for 400ms after the stop signal was presented, indicating that they had canceled the preparation of their planned saccade. On Continue trials, the trial was correct if the participants successfully generated a saccade to the target, despite the presentation of a continue signal. Four fixed SSDs (51, 84, 167, and 284ms) were used, such that at the shortest SSD, participants generally inhibited the movement in >75% of the Stop trials and at the longest delay, participants inhibited the movement in <25% of the Stop trials, and most of the data points were centered around the SSD in which the participants inhibited the movement in 50% of the Stop trials. The same delays were used for continue trials, and are referred to as continue signal delays (CSDs). SSD/CSD were determined empirically in pilot studies to result in approximately 50% failed inhibition/slow continue trials and were the same for all participants. Notably, the method used here to estimate SSRT is relatively robust to deviations from 50% failed inhibition/slow continue trials (Mayse et al., 2014).

In the current study, we sought to examine the effects of immediate trial history on measures of response control. To this end, we examined specific sequences of three types of trials, Go trials (G, 52%), Stop trials (S, 24%), and Continue trials (C, 24%). Each trial sequence began with a Go trial and was followed by a combination of Stop and Continue trials (G-S-S, G-S-C, G-C-C, and G-C-S). To ensure appropriate statistical power for estimating CSRT and SSRT, for each participant we randomly ordered 30 triplets of each type (120 total triplets, 360 trials) for the whole session trial sequence.

The remaining trials were completely randomly ordered in accordance with the overall trial proportions. This preparation ensured that we had approximately 30 of each triplet sequence and was unbeknown to the participant. The direction of the eye response for each trial (left or right) was independently randomly determined.

The experiment began with participants viewing an interactive demo instruction shown on the test screen. Participants were instructed to respond quickly and accurately to the target, to do their best to withhold their response when a stop signal occurred, and to continue their responses while ignoring the continue signal when it occurred. The color of the stop and continue signals were counterbalanced across participants (high-contrast, equal-luminance blue and yellow). Since there was no behavioral difference between when the stop/continue signal was yellow/blue versus blue/yellow, we collapsed across both colors for the same trial type in the data analyses. Participants were told not to slow their responses in anticipation of the Stop/Continue signal to discourage use of proactive slowing mechanisms and to ensure the completion of the saccade during the 500ms response window. After viewing the interactive demo instructions and practicing, participants completed the main task, which included 6 blocks, each with 160 trials, for a total of 960 trials. At the end of each trial, participants were given auditory feedback in the form of a high-pitch tone for a correct response, and low-pitch tone for an error response. Between blocks, participants were verbally debriefed to ensure that they understood the overall task instructions and the correct color-response mapping (Figure 13).

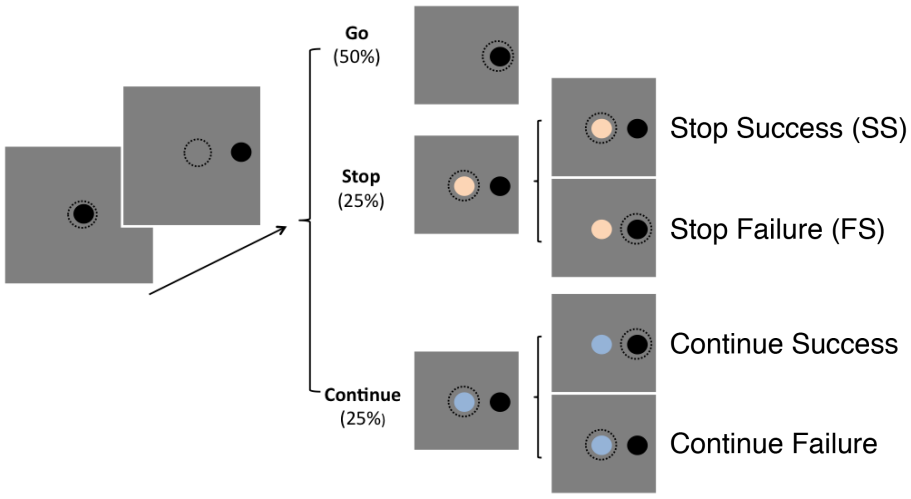

Figure 13. Stop signal task variant. All trials started with a central fixation spot on the screen for a variable delay period (200-400ms, 50-ms steps). Next, the central fixation spot disappeared and, simultaneously, a visual target appeared signaling participants to saccade to the target as quickly as possible. On Go trials (50% of all trials), the target appeared alone and a trial was considered correct if the participants generated a single saccade to the target within the 500ms maximum response time window and maintained their gaze at the target for an additional 200ms. In Stop trials (25%) and Continue trials (25%), a central stimulus (blue or yellow dot) was presented after a variable delay following the target onset (stop signal delay, SSD; continue signal delay, CSD; 4 fixed SSDs/CSDs ranged from 50ms to 250ms).

Data Analysis and Estimation of SSRT/CSRT

All data were analyzed using custom-written MATLAB scripts. RTs were calculated as the time between an event (e.g., Go signal onset) and the initiation of a saccade and are expressed as mean ± 1 s.e.m. Inhibition functions were constructed by fitting a logistic regression to the relationship between the stop or continue signal delay and the proportion of failed stop and fast continue trials, respectively.

To estimate SSRT we used the modified integration method. This method has been described in detail previously in chapter 2. To evaluate the effect of sequential

Stop/Continue trials on SSRT and CSRT, we calculated SSRT and CSRT using the same procedures with one important alteration. Because participants adjust RTs following stop and possibly continue trials, it is inappropriate to compare stop- or continue-aligned RT distributions to the full session go RT distribution. Simply, the go RT distribution is non-stationary as a function of the preceding trial type. Therefore, for each triplet we sampled from a subsample of the full Go trial RT distribution as follows. On trial *n-1* (the continue trial in a G-**C**-S triplet, for instance), we sampled n_C Go trials from the distribution of all Go trials preceded by a Go trial (G-G trials). On trial n, (G-C-**S**), we sampled n_S Go trials from the distribution of all Go trials preceded by a Continue trial (C-G trials). For G-S-S or G-S-C triplets, the yoked go distribution was constructed from all Go trials preceded by a stop trial (G-S). This procedure is necessary because participants cannot know on a given trial whether a stop or continue signal will be presented, or there will be no signal; therefore, proactive RT adjustments observed following Stop trials or errors reflect a change in the general state of an individual that must be taken into account when trying to estimate the appropriate go distribution for comparison.

Finally, we evaluated whether proactive RT adjustments were present in our study by calculating the change in Go trial RT as a function of the preceding trial. This procedure was identical to that used above to find the appropriate go RT distribution. Essentially, to examine proactive RT adjustments we calculated RT on Go trials preceding and following a specific trial. For instance, to find the effect of a Stop trial on RT, we compared RT on the first and second Go trial in a G-S-G triplet. If RT is slower on the second Go trial as compared to the first, then we can conclude that participants slow their RTs following a Stop trial.

3.3 Results

The SST-variant task shared similar behavioral features as a conventional SST

We first examined participants' performance in both go and stop tasks. The mean saccadic reaction time (RT) in Go trials was 249.17 ± 4.8 ms (mean ± s.e.m., n = 54). The inhibition function plots the probability of participants generating a saccade to the target (Failed Stop trials) as a function of stop-signal delay (SSD). Analysis of inhibition functions showed the proportion of Failed Stop trials increased as a function of SSD (Figure 14B). Note that here the proportion of Failed Stop trials is calculated as the number of Failed Stop trials divided by the number of all Stop trials. The mean RT for Failed Stop trials was 229.11 ± 4.8 ms, significantly faster than the mean RT for Go trials ($t_{(106)} = 3.07$, $p = 0.0027$, Figure 14A). These features are consistent with key properties of stop failure error predicted by the independent race model between the go and stop processes (Logan and Cowan, 1984; Logan et al., 1984).

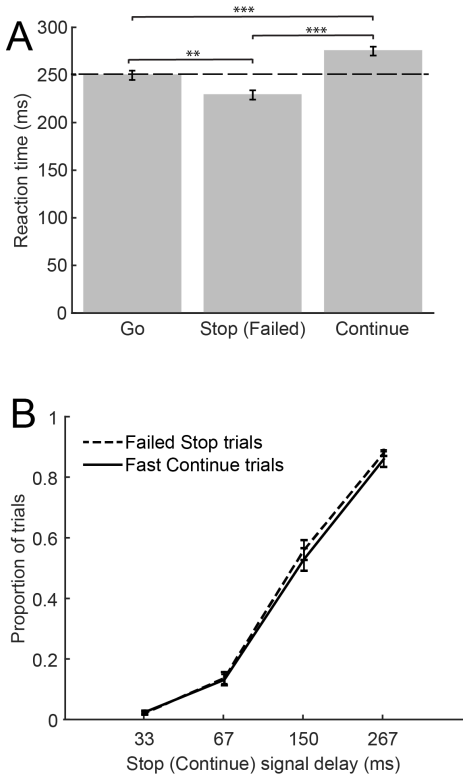

Figure 14 A) Mean reaction times for Go, Failed Stop, and Continue trials. Reaction times in Failed Stop trials (middle) are significantly faster than in Go trials (left) and Continue trials (right), and reaction times in Continue trials are significantly slower than in Go trials and Stop trials. **B) Inhibition/continue functions for stop/continue trials.** Dashed line shows the proportion of Stop Trials in which participants failed to stop as a function of the Stop signal delay. Solid black line depicts the proportion of Continue trials that were classified as fast continue trials as a function of the Continue signal delay. Fast continue trials were defined as those trials with an RT faster than the continue signal reaction time, CSRT.

Bi-modal distribution of RTs in Continue trials

Next, we examined participants' performance on Continue trials. Since participants were instructed to ignore the Continue signal and "continue" to generate the saccade that they had been preparing for, an ideal participant might be assumed to show no performance difference between Continue and Go trials. In contrast to this assumption (see Introduction and Sharp et al., 2010), the mean RT for Continue trials was 275.18 ± 4.7 ms, significantly slower than the mean RT for Go trials ($t_{(106)} = 3.82$, $p = 2.24 \times 10^{-4}$,

Figure 14A). Closer examination of RT distributions showed that, unlike Go trial RTs, Continue trial RTs were bimodally distributed (Figure 15B). The first and fast mode of Continue trial RTs closely overlapped with the fast portion of the Go trial RT distribution, as is observed for Stop trials (Figure 14B). This Fast Continue trial RT was abruptly truncated about 80–150ms after the onset of the Continue signal, which reflected a pause in behavioral response (Figure 15B). The pause was followed by the second and slower mode of Continue trial RT, which reflected a resumed behavioral response whose RT distribution eventually overlapped with the slow portion of the Go trial RT distribution (Figure 15B). We hypothesized that the fast mode of Continue RT corresponded to trials in which participants started saccade generation immediately after the Go signal onset, *before* the Continue signal onset, and therefore these Continue trial RTs (Fast Continue RTs) were highly similar to fast Go trial RTs. We further hypothesized that the slow mode of Continue RT corresponded to trials in which participants paused their saccade preparation in order to process the Continue signal, and therefore saccade generation was delayed, and these Continue trial RTs (Slow Continue RT) were highly similar to slow Go trial RTs. According to these hypotheses, Fast Continue trials appear to be analogous to Failed Stop trials, and had the continue signal been replaced by a stop signal, participants would have failed to withhold saccades and received an error feedback. Conversely, slower RTs in Continue trials appear to be the result of response inhibition.

Continue trials shared similar behavioral features as Stop trials

To test whether participants' responses in Fast Continue trials and Failed Stop trials were similar, we investigated whether the proportion of Continue trials that were classified as fast changed as a function of CSD (as calculated from the continue function,

analogous to the inhibition function). We first demarcated Continue trials as Fast and Slow Continue trials by calculating a continue signal reaction time (CSRT), applying the same method of calculating SSRT (the modified integration method, see Methods and Mayse et al 2014). Continue trials with RTs faster than 99.9% CI of the yoked Go trial RT distribution were considered Fast Continue trials, and trials with RT slower than this cutoff were considered Slow Continue trials (Figure 15B). We found that median CSRT and SSRT were statistically indistinguishable (CSRT = 93.5 ± 1.8 ms, SSRT = 91.7 ± 1.5 ms, $t_{(102)} = -0.79$, $p = 0.43$). Furthermore, the proportion of Fast Continue trials was small at the short CSD, and increased as the CSD increased, which closely resembled the inhibition function (Figure 14B), supporting the idea that participants responded similarly in both Fast Continue trials and Failed Stop trials.

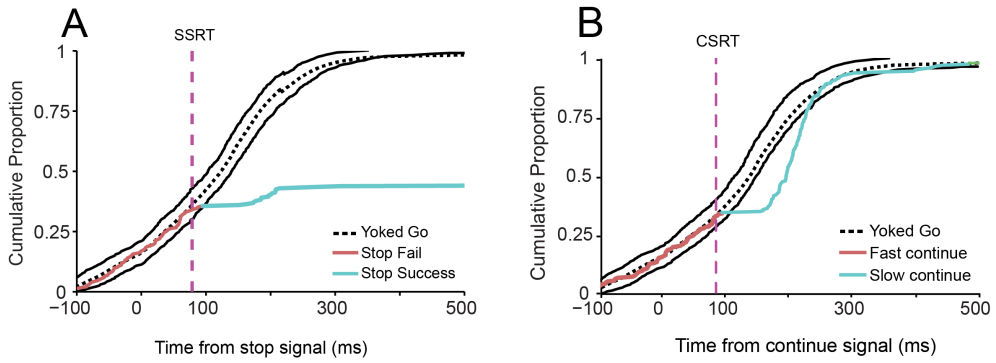

Figure 15. Cumulative distribution functions of reaction times using the new modified integration method. A. Stop trial reaction time distributions relative to Stop signal onset from Stop trials (colored) and yoked (re-aligned) Go trials (mean, dotted black; 99.9% CI, solid black). The intersection of Stop trials and the upper 99.9% CI bound (solid black) defined an optimal Stop signal reaction time cutoff (magenta vertical dashed line) that best separated Failed Stop (red line) and Successful Stop (blue line) trials. **B.** Continue trial reaction time distributions relative to Continue signal onset from Continue trials (colored) and yoked Go trials (mean, dotted black; 99.9% CI, solid black). The intersection of Continue trials and the upper 99.9% CI bound (solid black) defined an optimal Continue signal reaction time cutoff (magenta vertical dashed line) that best separated Fast Continue (red line) and Slow Continue (blue line) trials.

Stop and Continue trials do not share similar inhibitory mechanisms

To test whether the inhibitory mechanism that is engaged on Stop trials is also involved in Continue trials, we examined the effects of consecutive stop or continue trials on subsequent SSRTs and CSRTs. Bissett and Logan (2012) found that SSRTs were faster on Stop trials that immediately followed a stop trial, and argued that this form of post-stop-trial improvement in subsequent stopping was the result of an activation of a proponent motor inhibition by the first stop trial. According to this argument, if Continue trials and Stop trials engage the same inhibitory mechanism, then stopping should improve inhibition on subsequent continue trials, and vice versa. In other words, SSRT should be faster following either a Stop trial or a Continue trial, relative to the session-wide baseline SSRT, and similarly CSRT should be faster following either a Stop trial or a Continue trial, relative to the session-wide baseline CSRT. Replicating Bissett and Logan (2012), we found that the mean SSRT for the second stop trial in the Stop-Stop pair (84.1 ± 4.6 ms), was faster than the median session-wide baseline SSRT (91.7 ± 1.5 ms), while the median SSRTs on Stop trials following a Continue trial (92.5 ± 3.2 ms) was, not different from the baseline ($t_{(49)} = -2.11$, $p = 0.04$, and $t_{(53)} = 1.04$, $p > 0.3$, respectively; Figure 17). Median CSRT for Continue trials following a Stop trial (86.7± 5.2 ms), was somewhat faster than the median baseline CSRT (93.5 ± 1.8 ms), although this decrease was not statistically significant ($t_{(34)} = -1.48$, $p = 0.15$). Furthermore, CSRT for the second Continue trials in the Continue-Continue pair (93.4 ± 2.9 ms), was not numerically different from the baseline CSRT ($t_{(29)} = -0.54$, $p = 0.6$; Figure 16). Taken together, these results showed that while CSRT and SSRT likely shared a common initial inhibitory mechanism that pauses the generation of a saccade (because SSRTs and

CSRTs are numerically indistinguishable), there is a component of stopping present on Stop trials but not Continue trials that contributes to post-stop improvement in stopping.

To reconcile these results, we propose that stopping is a (at least) two-stage process. The initial stage involves pausing the generation of a motor response in order to allow for evaluation of evidence needed for selective control of behavior. The latency of this stage is captured by SSRT and CSRT and is similarly present on both Stop and Continue trials. After this initial stage (which itself could possibly be a composite of multiple substages), a second inhibitory mechanism completes the cancelation of the behavioral response on Stop trials, while on Continue trials the response is reinstated. Once the planned response is paused, additional processing takes place in order to resume the response on Continue trials, and this time to resume the response is captured by the time between CSRT and the fastest post-CSRT continue response, termed as Resuming RT (mean Resuming RT = 36.8 ± 2.9 ms). This two-stage model of stopping and continuing suggests that the post-stopping speeding of SSRT and CSRT observed here is the result of the second stage of stopping, when the paused response plan is cancelled, and that the first stage of stopping common to both Stop and Continue trials is insufficient to cause better inhibition on the subsequent trial.

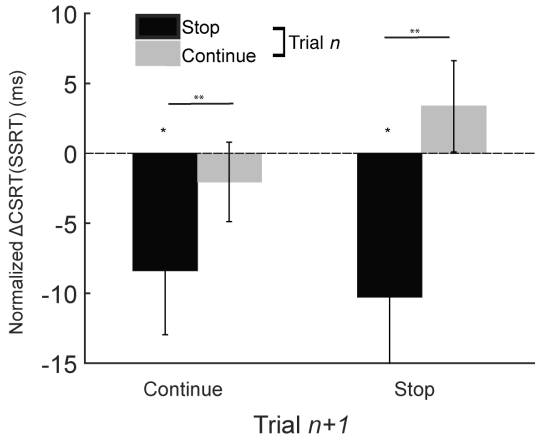

Figure 16. Continue signal reaction time (CSRT) and Stop signal reaction time (SSRT) were both faster following a Stop trial, but not a Continue trial. Black bars represent trials following Stop trials, while grey bars represent trials following Continue trials (for example, the left most blue bar is a Continue trial that follows a Stop trial).

Proactive control of Go RTs following Stop, but not Continue trials

If this second stage of stopping is both selectively activated on Stop trials (i.e., activated only when responses must be fully suppressed) and also contributes to subsequent proactive adjustments, then we might predict differential modulation of primary task RTs following Stop and Continue trials. To investigate the change in Go RTs following Stop and Continue trials, we first identified all triplets of trial sequence where the first and last trial in the triplet was a Go trial, and then calculated the RT difference between the first and second Go trials based on the interleaving trial type (G_1-G_2-G_3, G_1-S-G_2 and G_1-C-G_2 trial triplets). Consistent with what others have found, Go RT decreased across multiple, successive Go trials (median Go_1 = 191.52 ms, Go_2 = 184.23 ms, and Go_3 = 180.96 ms; $F(2, 61) = 36.32$, $p < 0.001$; Figure 17). Interestingly, we found that the median of post-Stop Go trial (i.e., G_1-S-G_2) RTs was slower than the overall session-wide median Go trial RT (G_1-S-G_2 trials; $Go_{overall}$ = 188ms, $Go_{postStop}$ = 201.9ms; $t_{(53)} = 7.99$, $p = 1.17 \times 10^{-10}$), but median post-Continue Go trial RT was

indistinguishable from the overall median Go trial RT (G_1-C-G_2 trials; $Go_{postContinue}$ = 189.8ms; $t_{(53)} = 1.97$, $p > 0.05$, Figure 17). However, this analysis does not account for the fact that on both Failed Stop and Fast Continue trials the initial delay mechanism proposed above may not be activated because the Go response reaches threshold before the initial delay mechanism has any effect. Therefore, we hypothesized that if this initial delay mechanism affects RT on the subsequent trial, we should observe similar post-trial RT slowing following Successful Stop and Slow Continue trials, and no RT slowing following Fast Continue trials (Failed Stop trials include error feedback, potentially complicating attribution of any RT change to activation of a specific mechanism for stopping). Note that no error feedback was provided on continue trials regardless of the latency of the response unless participants made a saccade in the wrong direction, removing the contribution of error feedback for RT adjustments. To examine this, Stop and Continue trials were further separated into Failed Stop (G-FS-G), Successful Stop (G-SS-G), Fast Continue (G-FC-G), and Slow Continue (G-SC-G) trials. We found that Go RTs slowed down relative to the session-wide median Go RT (188ms) after both Successful and Failed Stop trials (Go_{postSS} = 205.6ms, $t_{(49)} = 7.09$, $p = 4.89 \times 10^{-9}$, and Go_{postFS} = 207.4ms, $t_{(49)} = 6.80$, $p = 1.24 \times 10^{-8}$, respectively; Figure 18). There was no change in median Go RT from the first to the second Go trial following either Fast (G_1= 179.8 and G_2 = 184.1ms, $t_{(52)} = -1.14$, $p = 0.3$) or Slow Continue (G_1= 196.8 and G_2 = 202.7 ms, $t_{(53)} = 0.84$, $p = 0.4$) trials. However, Go RTs were slower than the session-wide median Go RT after Slow Continue but not Fast Continue trials (Go_{postSC} = 196.8ms, $t_{(53)} = 5.38$, $p = 1.73 \times 10^{-6}$, and Go_{postFC} = 184.1ms, $t_{(52)} = -1.98$, $p > 0.05$, respectively; Figure 18). See discussion for a possible explanation of the seeming difference between

these two analyses. These data support the independent race model that suggests that participants will fail to stop when they are prepared to make a rapid response and will successfully stop when they are prepared to make a slow response. Participants received positive feedback in Fast Continue trials; however, had the continue signal been replaced by a stop signal, they would have failed to stop and received an error feedback. These observations suggest that post-stop slowing of Go RTs were driven by two different mechanisms: error-feedback (in the case of Failed Stop trials) and activation of the second stage in the inhibitory process (in the case of Successful Stop). Because participants receive no error feedback and the second stage of stopping is not activated on Continue trials regardless of outcome, participants do not subsequently proactively adjust their RTs.

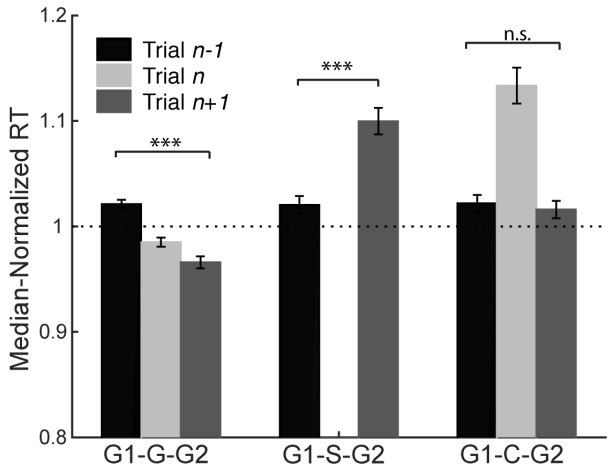

Figure 17. Go trial RTs, normalized by the median of all RTs, sorted according to preceding trial types. Trials were grouped into triplets of Go-*n*-Go and sorted by the type of trial in the intervening, *n,* position. Left: Go-Go-Go triplets. Middle: Go-Stop-Go triplets. Right: Go-Continue-Go triplets. Go reaction became faster when proceeded by more Go trials (G1-G2-G3). Compared to the reaction time in the first Go trial (black), the second Go trial (dark grey) reaction time was slower when preceded by a Stop trial (G1-S-G2), whereas there was no reaction time change in the second Go trial from the first Go trial when preceded by a Continue trial (light grey, G1-C-G2). Note that

Successful Stop trials (middle bars) have no valid RT, so the median Stop trial RT is truncated for visualization purposes.

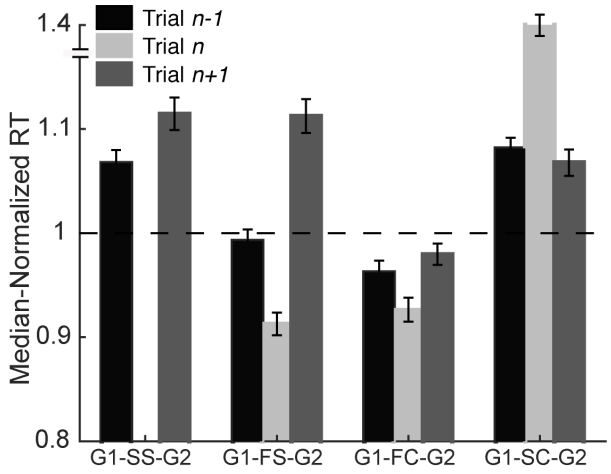

Figure 18. Mean RTs, normalized by the median of all RTs, according to preceding trial types separated by behavioral outcome. Trials were grouped into triplets of Go-*n*-Go and sorted by the intervening trial *n*, then further sorted by the outcome of that trial. The triplets from left to right are: Go-Successful Stop-Go (G1-SS-G2), Go-Failed Stop-Go (G1-FS-G2), Go-Fast Continue-Go (G1-FC-G2), Go-Slow Continue-Go (G1-SC-G2). Compared to the reaction time in the first Go trials (black), the second Go trial (dark grey) reaction time was slower when proceeded by either a Successful Stop trial (G1-SS-G2) or a Failed Stop trial (light grey, G1-FS-G2). There was no reaction time change in the second Go trial from the first Go trial when preceded by either a Fast Continue trial (light grey, G1-FC-G2) or a Slow Continue trial (light grey, G1-SC-G2). Note for trials in which the participant failed to stop or was fast to continue, G1 was faster than the median RT, whereas on trials in which the participant successfully stopped or was slow to continue, G1 was slower than the median RT.

3.4 Discussion

In the current study we investigated whether the mechanism that delays the generation of a behavioral response following the presentation of a Continue signal is the same mechanism present on Stop trials. We found, in agreement with previous studies, that RTs on Continue trials were bimodally distributed and slower than primary task (Go) RTs (Figure 14 A and Figure 15; Sharp et al., 2010). Leveraging a novel analytic method for estimating the latency of response inhibition using continuous RT distributions (the

modified integration method, Mayse et al., 2014), we found that this latency – called SSRT on Stop trials and CSRT on Continue trials – was identical for stopping and continuing. This finding suggests that the preparation of a response was delayed on Stop and Continue trials by a common mechanism; yet, these trials differed greatly in the ultimate behavior (make or suppress a saccade), whether positive or negative feedback was received, and subsequent behavioral adjustments. We found post-stop speeding of both SSRT and CSRT (though the latter did not reach statistical significance) following Stop but not Continue trials (Figure 16). Similarly, we found that participants slowed Go RTs following both Failed Stop (FS) and Successful Stop (SS) trials, but we observed no such slowing following either Fast Continue (FC) or Slow Continue (SC) trials (Figures 17 and 18). FC trials are similar to FS trials in that neither trial involves an initial delay of the response. These trial types are different, however, in that Failed Stop trials result in negative feedback while Fast Continue trials result in positive feedback. Both SS and SC trials demonstrated an initial response delay, and both result in positive feedback. Together, these data suggest that stopping is at least a two-stage process achieved first by a rapid delay of response preparation followed subsequently by either resumption (Continue) or suppression (Stop) of the planned behavioral response. The results also indicate that the first stage of stopping is not sufficient to affect subsequent behavior. Either successful completion of both stages, resulting in cancelation of the response, or negative feedback in failed stop trials resulted in greater engagement of inhibitory processes in the subsequent trial. Merely delaying the planned behavior, however, does not change subsequent behavior.

Leveraging a new method of bootstrapping to quantify CSRT and SSRT

The current study leverages a novel method for comparing two continuous data distributions, the modified integration method (for a detailed methodological explanation of this method, see Mayse et al., 2014). In this method, continuous data – in our study, RT distributions on Stop and Continue trials – are aligned to a common point (the Stop or Continue signal) and compared to a yoked comparison distribution (i.e. Go trial RTs). This comparison distribution is considered yoked to the Stop or Continue signals because it represents the estimated distribution of RTs relative to the Stop or Continue signal that would have been observed had such a signal never been presented (Figure 15A). Because participants make a saccade on the vast majority of Continue trials, conventional methods relying on discrete trial outcomes (i.e., indicating success or failure of stopping based on whether a saccade occurred on a Stop trial) to estimate CSRT is impossible for Continue trials. However, the modified integration method does not rely on discrete outcomes, allowing us to use the bimodal RT distributions on Continue trials to estimate CSRT. Using this method, we found that SSRT and CSRT were statistically and numerically indistinguishable, suggesting that these measures capture a common mechanism in inhibitory control. However, this finding presented a problem: subsequent behavior on Stop and Continue trials differs markedly, suggesting that the mechanism captured by SSRT/CSRT cannot fully explain stopping behavior. We hypothesized that the mechanism captured by SSRT/CSRT represents only the initial stage of a multi-stage stopping process (Boucher et al., 2007).

To test this, we analyzed the after effects of Stop and Continue trials. Previous studies have found substantial speeding of SSRT (Bissett and Logan, 2012) following Stop trials. We hypothesized that if these effects are mediated by the initial stopping

mechanism, we should observe improvement in SSRT and CSRT following both Stop and Continue trials. However, we observed speeding of SSRT and CSRT following Stop but not Continue trials, suggesting that activation of the initial stop mechanism present on both trial types is not sufficient to drive subsequent improvement in the speed of stopping. These data suggest that either the presence of the Stop signal itself, activation of the Stop rule, or suppression of the planned Go response engaged only on Stop but not Continue trials is necessary for post-stop improvement in stopping. While we cannot rule out the first possibility, it is worth noting that the Stop and Continue signals are both highly salient, visually similar stimuli presented in the same spatial location. Furthermore, previous studies have found that post-stop improvements in stopping are modality-specific but within a modality are highly generalizable, suggesting that it is unlikely that post-stop improvement in stopping is mediated simply by presentation of the stop signal itself (Bissett and Logan, 2012). We propose that these effects are mediated instead by either activation of the Stop rule, engagement of mechanisms for completing the selective suppression of the planned Go response after the initial delay, or both.

Similarly to post-stop improvement in SSRT, many studies have found post-stop slowing of primary task RTs (Cai et al., 2011; Emeric et al., 2007; Staub et al., 2014). To investigate whether this post-stop slowing is due to the initial delay in the response or processes that happen after this stage, we compared proactive adjustments following Continue and Stop trials with different outcomes, i.e. FC, SC, FS, and SS trials, and found that while participants slowed down following either failed or successful Stop trials,we observed no change in RT following any Continue trial. These findings are striking because participants are initially in the same overall behavioral state on FC/FS

(G_1 RTs faster than session-wide median, Figure 18) and SC/SS (G_1 RTs slower than session-wide median, Figure 18) trials, but the influence of these trials on subsequent behavior is markedly different. Additionally, proactive adjustments of Go RTs can be driven both by error monitoring mechanisms (i.e., present following FS but not SS trials) and by engagement of mechanisms that successfully cancel the planned response (Hendrick et al., 2010; Ide and Li, 2011; Li et al., 2008; Verbruggen and Logan, 2009). It then seems likely that post-FS slowing of RT is mediated by error feedback, because neither the initial or late stages of stopping are activated on these trials. By contrast, post-SS slowing of RT is likely mediated by the later stages of stopping. It cannot be the case that activation of the early stage of stopping (captured by SSRT/CSRT) is sufficient to drive subsequent RT slowing because we did not observe such slowing following SC trials. Finally, we did not observe post-Continue speeding of RT even though we observe speeding on successive Go trials (Figure 5, G_1-G_2-G_3). This finding is interesting because a saccade is generated on both trial types, but RT adjustments are present only on Go trials: participants neither slow down nor speed up following either FC or SC trials. These data suggest that, even though a saccade is generated on most Continue trials, this is not sufficient to drive subsequent speeding of RT as is observed following Go trials. Similarly, one could view these results as indicating that the mere presence of the Continue signal, regardless of whether the initial delay process is engaged, does not cause subsequent slowing of RT, but it is sufficient to counteract the subsequent speeding of RT observed during repeated Go trials.

Stopping, as a multi-stage process, involves both global and local inhibitory control

If stopping is a multi-stage process, then it seems likely that SSRT captures only the initial stage of this process. This interpretation is not inconsistent with the existing Horse Race model, which states that SSRT (or CSRT) captures the earliest time at which a response is captured and suppressed by the Stop process (Boucher et al., 2007; Logan et al., 1984). It is possible that this early, rapid stage of stopping captured by SSRT and CSRT is mediated by the basal ganglia (BG). The BG has long been implicated in the control of movement and especially response inhibition (Aron et al., 2007; Aron et al., 2007; Aron and Poldrack, 2006; Rieger et al., 2003; Schmidt et al., 2013). Recently, a study recording single unit activity in the rodent subthalamic nucleus (STN), a region thought especially important for response inhibition, found that neurons there are rapidly activated by both the Stop and the Go signal (Schmidt et al., 2013). Critically, the latency of this STN response did not correlate with SSRT but was strongly correlated with RT on Go trials, suggesting that the STN provides a brief, global motor pause whenever a surprising and salient stimulus appears in order to allow time for more selective modification of behavior (Schmidt et al., 2013). A similar mechanism may account for similar response inhibition latencies on Stop and Continue trials here, with a more selective mechanism engaging to fully suppress the planned response on Stop trials or to reengage/resume the planned response on Continue trials (Boucher et al., 2007).

One interesting future experiment to test this hypothesis could utilize EMG recordings from muscles in the neck while participants perform the Continue task utilized here. Previous studies have found activation of antagonist muscles working to counteract gaze shifts towards a peripheral target in the SST, suggesting that stopping is not merely passive suppression but active opposition of a planned response (De Jong et al., 1990; De

Jong et al., 1995; Band and van Boxtel, 1999). It is possible that similar recruitment might be observed on Continue trials. Additionally, it is worthwhile to consider the context in which the Continue variant of the SST arose. While presentation of the Stop signal instructs participants to cancel their planned response, it also is a salient, surprising stimulus appearing in an important spatial location. Comparing Stop and Continue trials, which presumably share these attentional aspects, allows for the isolation of stop-specific neuronal activity (Sharp et al., 2010). However, our current study suggests that Stop and Continue trials share a common initial delay mechanism, but differ in the engagement of later mechanisms to either cancel or resume the prepared saccade.

To tie the behavioral results in the current study with the neural imaging results in chapter 2, I speculate that it is likely that dorsal rVLPFC detects the onset of a sensory signal and encodes the meaning of that signal, being it a Continue or Stop signal, and this process requires attention and takes time which resulted in a brief pausing of ongoing go process (first stage of stopping). Furthermore if the signal requires stopping, ventral part of rVLPFC and FEF were recruited to complete stopping.

Chapter 4: Role of macaque monkey rVLPFC and FEF in context-based inhibitory movement control (Experiment 3)

4.1 Introduction

In Experiment 1 from chapter 2, we have identified two sub-regions within rVLPFC that showed differential activations during a context-dependent stop signal task. Activation in the dorsal part of the rVLPFC was associated with detecting and encoding the meaning of the signals (i.e. both Stop and Continue signals) that were behaviorally relevant, whereas the activation in the ventral part of the rVLPFC was associated with the

requirement to withhold an eye movement (i.e. Stop trial only), regardless of the stop outcome (i.e. successful stopping versus failed stopping). Furthermore, we found that the frontal eye field (FEF), an ocuolomotor area controlling for eye movement in the frontal cortex, encoded information regarding movements and the stop outcome but not the meaning of the signals or the contexts. In Experiment 2 from chapter 3, we found behavioral evidence in favor of a two-stage stopping processes, and speculated that the dorsal part of the rVLPFC is the neural basis of pausing in order to focus attention on the relevant stimulus and make a decision about the course of action (first stage), and then if the signal requires stopping, ventral part of rVLPFC and FEF were recruited to complete stopping. In this chapter, we sought to further validate human fMRI findings by comparing the results from recording single neuron activity in one macaque monkey rVLPFC (area 45) and FEF while the monkey performed a context-based SST.

4.2 Methods

General. One rhesus macaque monkey was trained to perform the tasks used in this study. All animal care and experimental procedures were approved by The Johns Hopkins University Animal Care and Use Committee. Monkeylogic software (http://www.monkeylogic.net/) (Asaad & Eskandar, 2008) was used to control task events, stimuli and rewards, and to monitor and store behavioral events. During the experimental sessions, the monkey was seated in a primate chair, with its head restrained, facing a video monitor. Eye positions were monitored and recorded with an infrared corneal reflection system, EyeLink 1000 (SR Research) at a sampling rate of 1000 Hz. Eye movements were detected offline using a computer algorithm that searched first for significantly elevated velocity (30˚/s). Saccade initiation and termination then were

defined as the beginning and end of the monotonic change in eye position lasting 15 ms before and after the high-velocity gaze shift. A valid saccade was further admitted to the behavioral analysis if it started from the central fixation window (2.5˚x 2.5˚) and ended in the peripheral target window (2.5˚x 2.5˚). Visual inspection was also applied to ensure the accuracy of saccade detection.

Behavioral tasks. The monkey was trained to perform a visually guided saccade task and a context-based stop signal task by operant conditioning with positive reinforcement. The visually guided saccade task was run after a single neuron was isolated, and was designed to locate the neuron's response field, to determine if the neuron had visual-or-movement-related activity or both. The task started with the monkey acquiring and remaining central fixation for a variable interval (300-550ms), after which a target with 10° visual eccentricity appeared at one of the six positions varying in direction (0°, 60°, 120°, 180°, and 240°), and the monkey was rewarded for generating a single saccade to the target within the 600ms maximum response time window and fixating it for 450ms.

The context-based stop signal task was run after a neuron's response field was successfully mapped out by the visually guided saccade task, and provided the main experimental data for this report. It included three trial types, Go trials (56%), Stop trials (22%), and Continue trials (22%), and all trials were pseudo-randomized (Figure 19). All trials started with the monkey fixating at a central fixation spot for 200ms, after which the fixation spot was replaced with a central context cue with either a square shape or a triangle shape. The shape of the context cue indicated the associated color of a subsequent Stop signal if the Stop were presented (in Stop trials) or a subsequent Continue signal if the Continue were presented (in Continue trials). After the presentation

of the central context cue for 350ms, the cue was replaced by a central fixation spot. The monkey was required to maintain central fixation throughout the stimuli presentation.

In Go trials, a target with 10° eccentricity appeared either inside or opposite of the isolated neuron's response field. Simultaneously, the central fixation spot disappeared, signaling the monkey to make a saccade to the target. The monkey was rewarded for generating a single saccade to the target within the 600ms maximum response time window and fixating it for 450ms.

In Stop trials, a target with 10° eccentricity appeared either inside or opposite of the isolated neuron's response field. Simultaneously, the central fixation spot disappeared, signaling the monkey to make a saccade to the target (same as in the Go trials). However, while the monkey was preparing for a saccade, a stop signal appeared at the central fixation, and the monkey was rewarded for withholding its gaze at the central spot for 700ms. The color of the Stop signal was either yellow or blue, depending on the shape of the context cue. For this monkey, a square-shaped context cue indicated that the stop signal is yellow, while a triangle-shaped cue indicated that the Stop signal is blue.

In Continue trials, a target with 10° eccentricity appeared either inside or opposite of the isolated neuron's response field. Simultaneously, the central fixation spot disappeared, signaling the monkey to make a saccade to the target. However, while the monkey was preparing for a saccade, a Continue signal appeared in the central fixation (same as in the Stop trials). The monkey was rewarded for ignoring the central Continue signal and generating a single saccade to the target and fixating it for 450ms. For this monkey, a square-shaped context cue indicated that the Continue signal is blue, while a triangle-shaped cue indicated that the Continue signal is yellow.

The Stop signal delay (SSD) ranging from 50ms to 300ms was used and was manipulated under a tracking procedure, such that at the shortest Stop signal delay, monkeys generally inhibited the movement in >75% of the Stop trials and at the longest delay, monkeys inhibited the movement in <25% of the Stop trials, and most of the data points were centered around the SSD in which the monkey inhibited the movement in 50% of the Stop trials. The Continue signal delay (CSD) had the identical timing as the SSD. The monkey generally inhibited the movement in <5% of the Continue trials, for all CSD.

The context-based stop signal task was run in a block fashion. Within each block, only one type of context cue, either a square-shaped cue or a triangle-shaped cue, was shown to the monkey. Each block contained either 50 or 100 trials, and alternated between square-cue block and triangle-cue block such that the two types of blocks were counterbalanced. The first trial of a new block was coined a “switch” trial.

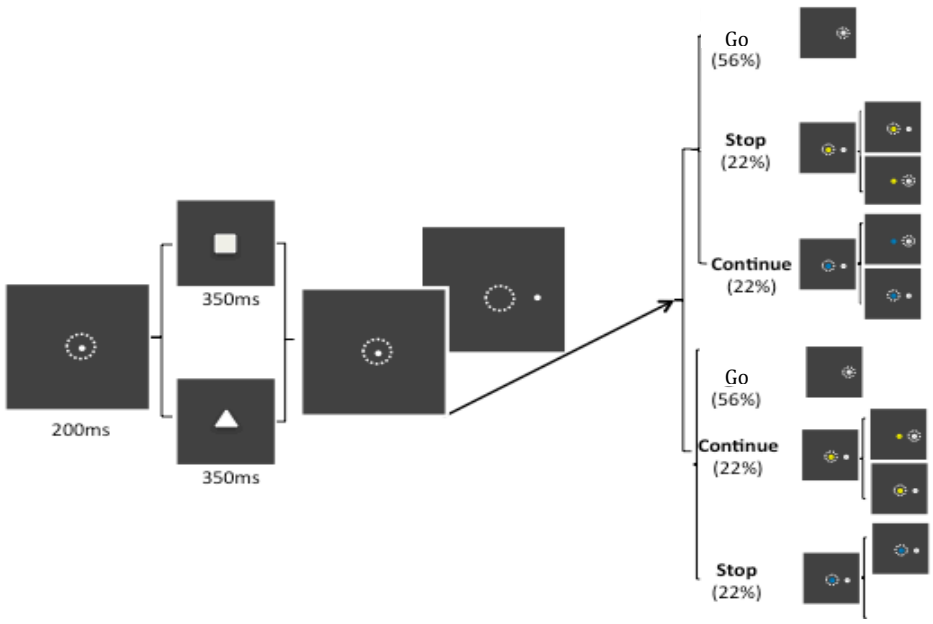

Figure 19. Experimental design for the context-based stop-signal task. The context-based stop-signal task included three trial types, Go signal trials (56%), Stop trials (22%), and Continue trials (22%). All trials started with the monkey fixating at a central fixation spot for 200ms, after which the fixation spot was replaced with a central context cue with either a square shape or a triangle shape. The shape of the contextual cue indicated the associated color of a subsequent Stop signal if the Stop signal were presented or a subsequent Continue signal if the Continue signal were presented. After the presentation of the central context cue for 350ms, the cue was replaced by a central fixation spot.

Cortical localization. We used the magnetic resonance images (MRIs) obtained for the monkey (3.0 T) to determine the location of the area45 and FEF. Anatomically, area45 is located in the midline, 12mm anterior to the inferior spur of the arcuate sulcus, extending to the principle sulcus. FEF is located anterior to the prearcuate sulcus, more posterial and medial relative to area 45.

Single-unit recording. After training, we surgically placed a hexagonal chamber centered over area45 and FEF on the right hemisphere of the animal. Single units were recorded using tungsten microelectrodes (2–4 MΩ) that were under the control of a microdrive. An electrode was inserted through a guide tube positioned and lowered to just above the

surface of the Dura mater. Data were collected using the TDT system (Tucker & Davis) at a sampling rate of 1-kHz. Action potentials were amplified, filtered, and discriminated conventionally with a time-amplitude window discriminator. Spikes were isolated online if the amplitude of the action potential was sufficiently above background to reliably trigger the time-amplitude window discriminator, the waveform of the action potential was invariant throughout experimental recording, and the isolation could be sustained for sufficient period of recording. The identification and isolation of individual spikes was reevaluated and corrected offline using three-dimensional PCA and visual inspection of selected waveforms (Offline Sort Program, Plexon .Inc) to ensure only single units were included in consequent data analysis.

Spike density functions. To represent neural activity as a continuous function, we calculated spike density functions by convolving the peri-stimulus time histogram with a growth-decay exponential function that resembled a postsynaptic potential (Hanes et al., 1998). Each spike therefore exerts influence only forward in time. The equation describes rate (R) as a function of time (t): $R(t) = (1 - \exp(-t/\tau_g))*\exp(-t/\tau_d)$, where τ_g is the time constant for the growth phase of the potential and τ_d is the time constant for the decay phase. Based on physiological data from excitatory synapses, we used 1 ms for the value of τ_g and 20 ms for the value of τ_d (Sayer et al., 1990).

Behavioral data analysis. We termed five trial types to characterize the possible behavioral results: Go trials, in which the monkey successfully made a saccade to the periphery target; Successful Stop trials, in which the monkey successfully withheld its gaze at the central fixation; Failed Stop trials, in which the monkey failed to withheld central fixation and generated a saccade to the target instead; Continue trials, in which the

monkey successfully ignored the continue signal, and generated a saccade to the target; and Error Continue trials, in which the monkey failed to generate a saccade to the target and withheld its gaze at central fixation instead.

The relevant behavioral data for describing the inhibitory process are: (1) the inhibition function, and (2) the reaction time distribution for the eye movements in Go trials. The inhibition function plots the proportion of Stop trials in which the monkey generates an eye movement as a function of the delay between target onset and Stop onset (the Stop delay). The probability of erroneous initiation of the movement increases as SSD increases. Performance on the Stop trials can be modeled as a race between a stochastic process that generates the eye movement (GO process) and a stochastic process that inhibits the eye movement (STOP process) (Logan & Cowan, 1984; Logan et al., 1984). The two processes race independently toward their respective thresholds. If the STOP process finishes before the GO process, the eye movement is not generated (Successful Stop trials). However, if the GO process finishes before the STOP process, the eye movement is generated (Failed Stop trials). This race model provides an estimate of the stop signal reaction time (SSRT), which is the time needed to cancel the planned eye movement. SSRT was estimated using two methods detailed previously (Hanes & Schall, 1995; Hanes et al., 1998). First, the method of integration, which assumes the SSRT is constant, was used. The mean of the SSRT was calculated individually for each SSD. Second, a method based on the mean of the inhibition function was used. One SSRT estimate was calculated based on the raw behavioral data (i.e., the frequency of Failed Stop trials for each SSD). An overall estimate of SSRT was obtained by averaging over the two different estimates.

Identification of neuronal activity sufficient to control saccade initiation or inhibition. For a neuron to sufficiently control a saccade initiation or inhibition, two criteria must be fulfilled. First, the neuron must discharge differently when a saccade is initiated versus when a saccade is withheld. Second, this activity differentiation must occur within the SSRT for it to control the saccade initiation/inhibition in time. If the activity differentiates after the SSRT, it is too late to influence the saccade initiation/inhibition. Both criteria are fulfilled by movement-related neurons in the FEF and superior colliculus (SC); these neurons increase their firing rate when a saccade is initiated, and decrease their firing rate when a saccade is withheld. In contrast to movement-related neurons, fixation-related neurons in FEF decrease their firing rate when a saccade is initiated, and increase their firing rate when a saccade is withheld (Brown et al. 2008; Hanes et al. 1998; Pare´and Hanes 2003).

The activity when a movement is cancelled can be compared with the activity when a movement is produced, but would have been cancelled if the stop signal had been presented. This comparison consists of Successful Stop trials and Go trials with reaction times greater than the stop signal reaction time added to the stop signal delay (latency-matched trials). The rationale is that the saccades, generated with slow reaction times (i.e. reaction times exceeding the SSRT + SSD) in Go trials, are those slow saccades that could have afforded enough time for the STOP process to finish before the GO process, and on which the planned movement therefore would have been cancelled had there been a stop signal presented.

We compared the spike rate in Successful Stop trials and latency-matched Go trials for movements inside and outside of the response fields as a function of time from

target presentation. This was done to provide a complementary estimate of whether and when neural activity distinguished saccade inhibition from saccade initiation. To perform this time-course analysis, we subtracted the average spike density function Successful Stop trials from the average spike density function during latency-matched Go trials. This subtraction was performed for cells with visually evoked activity and for cells with movement-related activity. Because of their opposite sign of modulation, for cells with fixation-related activity, we subtracted the average spike density function for latency-matched Go trials from the average spike density function during cancelled Stop trials. The resulting spike density functions will be referred to as differential spike density functions. The time at which significant differential activity began during Successful Stop and latency-matched Go trials was defined as the instant when the differential spike density function exceeded by 2 SD the mean difference in activity during the 500-ms interval before target presentation, provided the difference reached 3SD and remained >2 SD threshold for 50ms. The time interval between the defined onset of differential activity and the SSRT then was determined. If the time when the differential activity arose was earlier than or equal to the SSRT, we regarded this as positive evidence for a cancellation signal.

4.3 Results

Data from single neuron recordings showed that neurons in the frontal eye field (FEF) carry neuronal signals that are sufficient in controlling movement inhibition and execution (Figures 20 A and B). These FEF movement-related neurons increased their firing rate when a saccade was generated (Go trials) and decreased their firing rate when a saccade was successfully inhibited (Successful Stop trials). Critically, the signal

differentiation occurred before the stop signal reaction time (Figure 20A). In contrast, FEF fixation neurons decreased their firing rates for Go trials, and increased their firing rates for Successful Stop trials. The signal differentiation time occurred well before the SSRT, sufficient to effectively exert inhibitory control (Figure 20B). However, FEF neurons did not encode context-dependent information. Furthermore, in Experiment 1 in chapter 2, we found that MVPA was able to successfully classify, with above chance accuracy, the stop outcome but not the meaning of the signal, nor the color of the signal in FEF (Figure 12). The human imaging results further corroborated the findings in primate electrophysiology and suggested that FEF is associated with encoding information related to oculomotor control, but not abstract information for higher-level cognitive control.

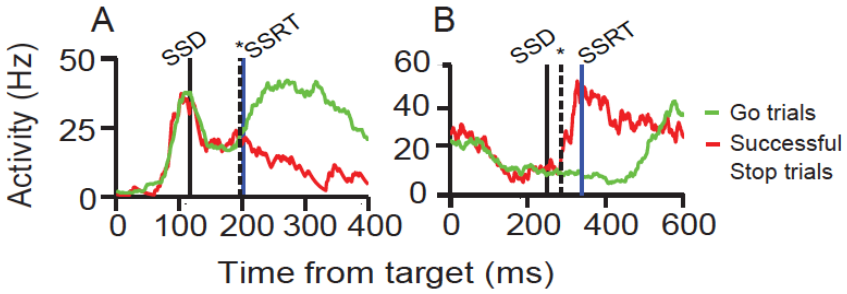

Figure 20. Examples of two FEF neurons. A) A movement-related neuron increased its firing rate ~100 ms after the target onset for Go trials (green line) and decreased its firing rate for Successful Stop trials (red line). Critically, the signal differentiation time (indicated by the dashed black line) occurred before SSRT (blue solid line). Solid black line indicated a stop signal delay (SSD). B) A fixation neuron decreased its firing rate for Go trials, and increased its firing rate for Successful Stop trials. The signal differentiation time occurred well before the SSRT.

On the other hand, very few rVLPFC (area 45) neurons encoded movement

execution or inhibition, and among those that showed movement-related activities, the signal differentiation time for Go trials versus Successful Stop trials occurred after the SSRT, which suggested that rVLPFC movement-related neurons were unable to exert inhibitory control in time (Figure 21).

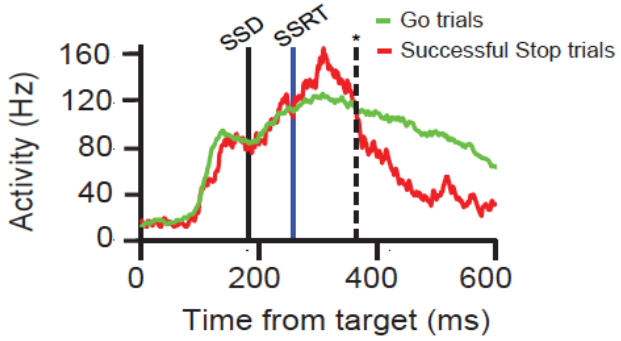

Figure 21. Examples of a movement-related neuron in area 45. A movement-related neuron increased its firing rate ~120 ms after the target onset for Go trials (green line) and decreased its firing rate for Successful Stop trials (red line). However, the signal differentiation time (indicated by the dashed black line) occurred after SSRT (blue solid line). Solid black line indicated a stop signal delay (SSD).

Nevertheless, neurons in area 45 showed context-dependent modulation. In our data from recordings of single neuron activity while one primate performing a comparable context-dependent SST, we found that some neurons in area 45, a putative primate homologue of a portion of human VLFPC (Petrides and Pandya 2009), increased firing rate on switch trials, where a new context replaced the old context (Figure 22A). These neurons increased their firing rate after the onset of a new context cue on switch trials (black line in Figure 22A), but not for trials immediately after switch trials (red line) and in the middle of a block (blue line). We also found a second group of neurons in area 45 that increased firing rate gradually following a context switch (Figure 22B).

These neurons increased their firing rate for switch trials (black line in Figure 21B), and continue to increase their firing rate for the trials immediately following switch trials (red line), as well as the trials in the middle of a block (blue line).

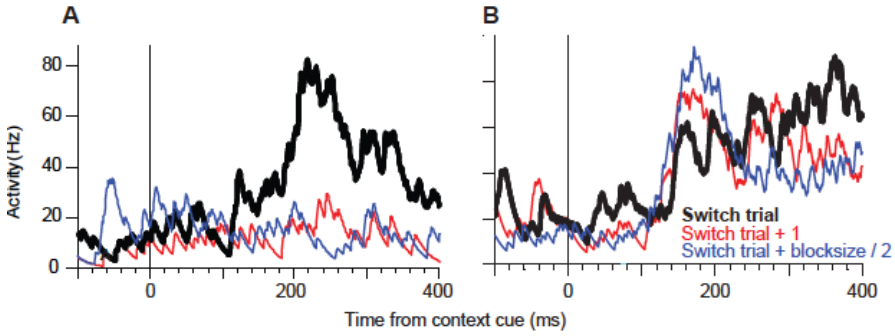

Figure 22. Spike density functions of two exemplar "switch" neurons. A) Activity of an area 45 neuron increased on "switch" trials (black line) compare to the trial immediately after switch trials (red line) and in the middle of a block (blue line). B) Activity of an area 45 neurons gradually increased its firing rate for switch trials (black line), and continue to increase its firing rate for the trials immediately following switch trials (red line), as well as the trials in the middle of a block (blue line).

In addition to finding neurons that encoded for context switching, we also found neurons that encode for specific contexts by preferentially increasing firing rate to a particular context. Figure 23 red line shows an example of a context-specific neuron that increased its firing rate to context A, in which a square context cue appeared at the beginning of a trial, 100 ms after the onset of the context cue. In contrast, the firing rate of the same neuron remained around the baseline for context B (blue line), in which a triangle context cue appeared at the beginning of a trial. The firing rate between the two contexts remained different even after the offset of the context cue, and only became indifferent at the time of the target onset.

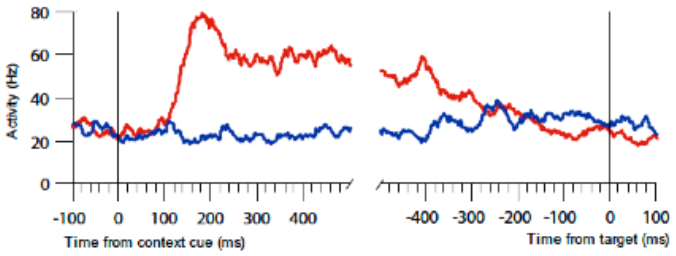

Figure 23. Spike density functions of a "context-specific" neuron in area 45. A neuron increased its firing rate to context A 100 ms after the onset of the context cue (red line). In contrast, the firing rate of the same neuron remained around the baseline for context B (blue line). The firing rate between the two contexts remained different even after the offset of the context cue, and only became indifferent at the time of the target onset.

In other cases, the firing rate for the two contexts remained different long after the offset of the context cue, and even after the onset of the target, suggesting a strong preference for one context over the other (Figure 24).

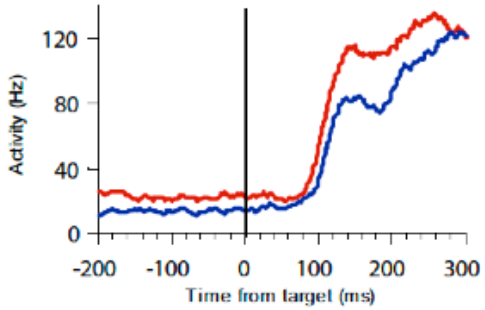

Figure 24. Spike density functions of a "context-specific" neuron in area 45 after the target onset. The firing rate of a neuron to context A (red line) remained higher than context B (blue line) ever after the target onset.

4.4 Discussion

Our data from recordings of single neuron activity while one primate performing a comparable context-dependent SST suggested that FEF neurons encode for movement-related activities, but not the meaning of the signal. On the other hand, neurons in area 45, a primate homologue of human rVLFPC, encoded context information by either

selectively increasing their firing rate to a particular context (Figure 23 and 24), or by increasing their firing rate at the time of context switching (Figure 22).

Hanes et al. (1998) found that movement-related neurons in FEF increased their firing rate when a saccade was made, while decreased their firing rate when a saccade was successfully inhibited. Furthermore, fixation neurons exhibited the opposite firing pattern: decreased firing rate during saccade execution and increased firing rate during saccadic inhibition. Critically, the neuronal signal separation occurred before stop signal reaction time, suggesting effective and timely motor control. Another human imaging study (Curtis et al., 2005) that used eye movements during a SST also found that FEF showed greater BOLD activation on Go trials, where participants made visually guided saccades, compared to catch trials where participants maintained central fixation. Furthermore, greater BOLD activations were observed during Stop trials, regardless of the stop outcome, compared with Go trials. The authors argued that the greater BOLD activation during Stop trials were likely due to co-activation of separate populations of movement-related and fixation neurons in FEF. Our data were consistent with Hanes et al. (1998), and also support the interpretation of the fMRI data in Curtis et al., (2005).

The current electrophysiological data corroborated the fMRI data in the human imaging study (Chapter 2). In Experiment 1, we found that the frontal eye field (FEF), an ocuolomotor area controlling for eye movement in the frontal cortex, encoded information regarding movements but not the meaning of the signals or the contexts. On the other hand, increased BOLD activity in dorsal rVLPFC in both Stop and Continue trials compared to Go trials, which suggested that the dorsal rVLPFC is associated with attending to sensory information that is behaviorally relevant. Furthermore, Stop and

Continue signals were associated with different *patterns* of BOLD activation within the same area, which indicated that dorsal rVLPFC also encodes task-specific rules. In contrast, ventral rVLPFC demonstrated increased BOLD activity relative to Go trials, only in Stop trials, yet there was no activation magnitude difference between Failed and Successful Stop trials, which suggested that the ventral rVLPFC detects signals that are stop-relevant, yet does not control motor inhibition *per se*.

It is also worth noting that in contrary to the human fMRI result, we did not find neurons in rVLPFC that responded preferentially only to the Stop signal but not to the Continue signal from the single cell recording data. One explanation for the apparent difference is that we only recorded neurons in monkey area 45, a small subregion within the rVLPFC, while the primate homologue of human ventral rVLFPC is area 47 (Levy and Wagner, 2011).

Nevertheless, both fMRI and electrophysiology data demonstrated differential response properties for FEF and rVLPFC (including dorsal rVLPFC and ventral rVLPFC). A question remains unresolved; that is, how do dorsal rVLPFC, ventral rVLPFC and FEF collectively instantiate context-dependent inhibitory control? In the next chapter, chapter 5, I used psychophysiological interactions (PPIs) based functional connectivity analysis to examine the functional connections among ventral rVLPFC, dorsal rVLPFC and bilateral FEFs during different task conditions that require either stopping or not stopping a planned eye movement (i.e. Go, Stop, and Continue trials), and the modulatory effect each of these regions have on the rest of the brain during these different task conditions.

Chapter 5: Additional analyses of Experiment 1: functional network view on the mechanism of rVLFPC in context dependent inhibitory control

5.1 Introduction

Chapter 4 emphasized the difference between FEF and rVLPFC regarding motor control as revealed by differences in single cell activity. Chapter 2, on the other hand, considered primarily the differential roles of the two subregions within the rVLPFC. It is unknown how these two areas relate to each other or to other parts of the brain (including FEF) during voluntary control of movement inhibition. The current chapter aimed to use additional analyses using the same fMRI data from Experiment 1, and examine the neural mechanism in context dependent inhibitory control from a functional network persepctive.

A psychophysiological interactions (PPIs) based analysis tests the hypothesis that activity in one brain region can be explained by an interaction between the presence of a cognitive process (psychological effect, the experimental task manipulation) and activity in another part of the brain (physiological effect; McLaren et al, 2012; Cisler et al, 2013). In the current study, we applied a PPI analysis to test the task-dependent functional connectivity (FC) among ventral rVLPFC, dorsal rVLPFC on FEF during Go, Stop, and Continue trials, and further explore the possible influence these regions may also have on other parts of the brain that were not defined *a priori*. Specifically, I speculated that dorsal rVLPFC and ventral rVLPFC were connected differentially to FEF and to other parts of the brain that are not defined *a priori*, and furthermore, these distributed functional networks may give rise to the cognitive control hierachy. The study offered insight on functional integration between separate brain regions in cognitive control of movement inhibition.

5.3 Methods

The same fMRI data set from twenty-one participants that was collected for Experiment 1 in chapter 2 was used for the current study. Data preprocessing and three ROIs (ventral rVLPFC, dorsal rVLPFC and bilateral FEF) were the same as described in the method section of chapter 2.

Psychophysiological interactions (PPIs) based functional connectivity analysis

A generalized form of context-dependent psychophysiological interactions (gPPI) method (McLaren et al, 2012; Cisler et al, 2013) was used with implementations in AFNI. The three seed regions were the ventral rVLPFC, dorsal rVLPFC and bilateral FEF, which were defined at the group-level analysis and transformed back to individual space using 3dNwarpApply in AFNI. For each seed, changes in BOLD signal were modeled to test the effect of modulation in other parts of the brain by the seed region during Go, Stop, and Continue trials. For each run, the average time series of the voxels in a seed region was extracted, and a deconvolution process was run on the time series to remove the signal component that had previously been modeled with a canonical hemodynamic response function (HRF). The remaining residual signals were considered the neuronal responses at the seed region and were convolved with the condition timing profile for each task, i.e. Go, Stop, and Continue trials, respectively, to generate three PPI-regressors per run. Next, the three PPI-regressors were concatenated across all six runs respectively. In addition to the three PPI-regressors, three regressors of trial types (Go, Stop, and Continue), the seed region itself, and six head-motion parameters were included in the model. All 13 regressors were convolved with the canonical HRF using a double gamma function. The general linear model (GLM) was estimated for each participant separately

using AFNI's 3dDeconvlve function, and a Talairach transformation was applied for each participant to combine the resulting statistical maps across the 21 participants for group-level analysis. All contrasts created at the participant-level were entered into a group-level random-effect analysis using a one-sample t test against a contrast value of zero at each voxel. The statistical maps were thresholded using a voxel-level threshold of $p < 0.01$, corrected for multiple comparisons at a cluster-level of $p < 0.05$ (family-wise error correction), based on a Monte Carlo simulation with 1,000 iterations run via the AFNI software package, using a smoothing kernel of 4 mm on the task-related mask.

5.4 Results

Results from Experiment 1(chapter 2) suggested that ventral and dorsal parts of rVLPFC might be two separate functional regions instead of one. The PPI group-level analysis further corroborated this finding showing that a set of cortical and subcortical regions, which demonstrated increased connectivity with the ventral part of right VLPFC as a seed region interacting with Stop trials comparing to the baseline activation, was different from another set of regions which demonstrated increased connectivity with the dorsal part of right VLPFC as a seed region for the same contrast comparison. Specifically, using the dorsal part of rVLPFC as a seed region modulating Stop-related activity, increased activation was observed in caudate and middle temporal gyrus (MTG; Figure 25A; see Table 5 for a complete list of areas). In contrast, using ventral part of rVLPFC as a seed region modulating Stop-related activity, increased connectivity was observed with bilateral frontal eye field (FEF), left superior parietal lobule (SPL) and left putamen (Figure 25B, Table 5).

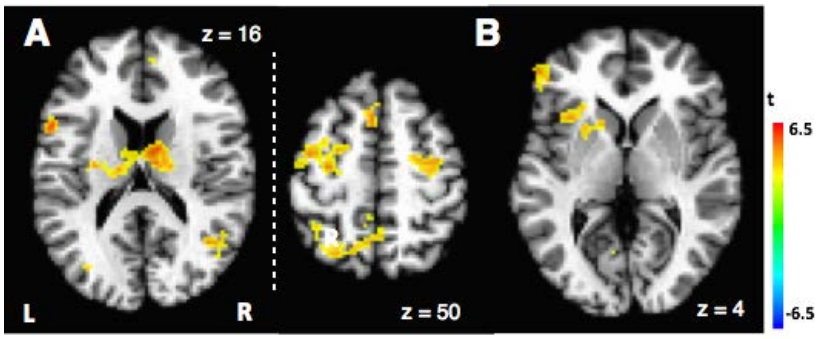

Figure 25. Areas showing greater connectivity with dorsal rVLPFC as the seed region (A) and ventral rVLPFC as the seed region (B) during Stop trials, compared with baseline.

In addition, activation in the ventral part of rVLPFC significantly modulated Go-related activity in inferior parietal lobule (IPL), superior parietal lobe (SPL), and superior colliculus (SC) (Figure 26A; see Table 6 for a complete list of areas). Activation in the ventral part of rVLPFC also was observed to modulate Continue-related activity in FEF, IPL, and SPL (Figure 26B, see Table 7 for a complete list of areas). No significant modulation was observed when using the dorsal part of right VLPFC as the seed region for the Go- or Continue-related activity.

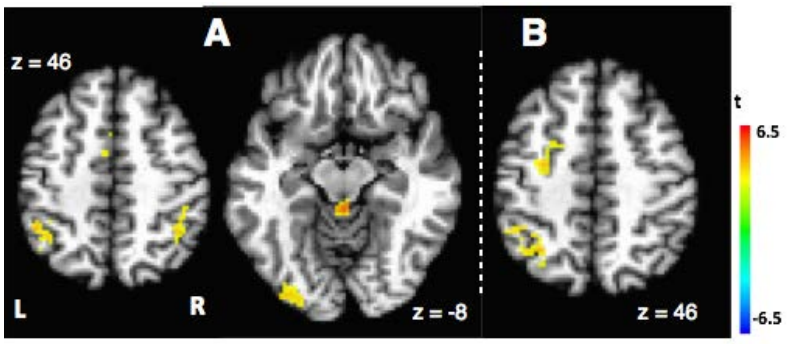

Figure 26. Areas showing greater connectivity with ventral rVLPFC as the seed region during Go trials (A) and Continue trials (B), compared with baseline.

Table 5. Regions demonstrating greater connectivity with the seed region, during Stop trials, compared with baseline.

Area	Talairach coordinates (mm)			Volume (mm^3)
	x	y	z	
Seed: ventral rVLPFC				
L superior parietal lobule	-7	-49	46	1,001
L frontal eye field	-27	-7	48	565
L superior frontal gyrus	-3	15	50	278
L insula	-31	15	4	170
L putamen	-15	11	4	159
R frontal eye field	31	11	48	146
R cingulate gyrus	1	-41	30	135
R superior temporal gyrus	45	-57	14	92
L superior temporal gyrus	-53	-47	12	91
Seed: dorsal rVLPFC				
L Caudate	-19	-13	20	375
R Caudate	15	-11	20	348
L precentral gyrus	-51	9	10	346
R medial frontal gyrus	7	45	34	313
L superior temporal gyrus	-47	-23	5	222
L ventrolateral al prefrontal cortex/ inferior frontal gyrus	-45	37	4	171
R middle temporal gyrus	41	-57	16	169
L insula	-33	19	4	165
L superior frontal gyrus	-23	49	28	123
L middle occipital gyrus	-29	-73	14	81
Seed: bilateral FEF				
L middle occipital gyrus	-27	-89	6	433
L cingulate gyrus	-3	15	28	138
R middle frontal gyrus	37	19	40	119
R insula	37	13	4	116
R thalamus	9	-7	20	84

Note. Talairach coordinates indicate the peak voxel within each cluster (family-wise error, $p < .05$). R, right; L, left.

Table 6. Regions demonstrating greater connectivity with the seed region, during Go trials, compared with baseline.

Area	Talairach coordinates (mm)			Volume (mm^3)
	x	y	z	
Seed: ventral rVLPFC				
L inferior parietal lobule	43	-55	46	349
L middle frontal gyrus	-33	41	18	197
R superior parietal lobule	7	-49	62	118
R inferior parietal lobule	39	-55	46	113
L middle occipital gyrus	-29	-81	-8	108
R cingulate gyrus	3	1	48	87
R superior colliculus	1	-37	-10	84
Seed: bilateral FEF				
R insula	53	1	10	644
R superior colliculus	1	-33	-8	453
L insula	-33	5	18	262
L middle frontal gyrus	-39	43	24	175
L precentral gyrus	-51	-3	6	139
R inferior parietal lobule	51	-45	40	99
R precuneus	27	-71	36	80

Note. Talairach coordinates indicate the peak voxel within each cluster (family-wise error, $p < .05$). R, right; L, left.

Furthermore, using bilateral FEF as a seed region, modulation of activation was observed in IPL, bilateral anterior insula (IA), ventral rVLPFC and superior colliculus (SC) for Go-related activity (Figure 27, Table 6), and in left middle occipital gyrus , right IA, right thalamus for modulating Stop-related activity (Figure 28, Table 5).

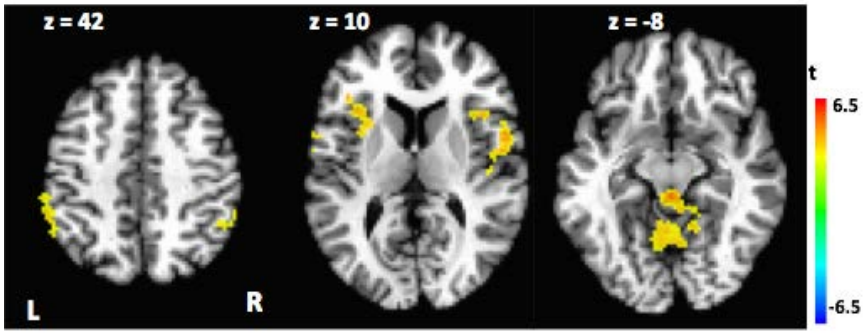

Figure 27. Areas showing greater connectivity with bilateral FEF as the seed region during Go trials, compared with baseline.

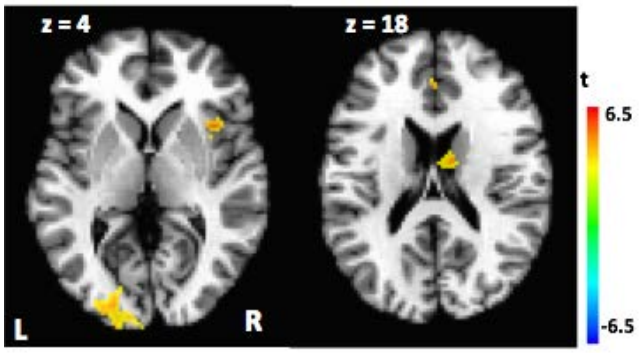

Figure 28. Areas showing greater connectivity with bilateral FEF as the seed region during Stop trials, compared with baseline.

Table 7. Regions demonstrating greater connectivity with the seed region, during Continue trials, compared with baseline.

Area	Talairach coordinates (mm)			Volume (mm^3)
	x	y	z	
Seed: ventral rVLPFC				
L superior parietal lobule	-39	-57	48	331
L frontal eye field	-25	-9	50	144
L precentral gyrus	-33	3	28	106
L inferior parietal lobule	-49	-45	38	84
Seed: bilateral FEF				
R precuneus	5	-65	38	133

Note. Talairach coordinates indicate the peak voxel within each cluster (family-wise error, $p < .05$). R, right; L, left.

5.5 Discussion

The current study used psychophysiological interactions (PPIs) based functional connectivity analysis to examine the functional connections among ventral rVLPFC, dorsal rVLPFC and bilateral FEFs during different task conditions that required stopping of a planned response or execution of that response (i.e. Go, Stop, and Continue trials), and the modulatory effect each of these regions have on the rest of the brain during these different motor response conditions. We found that dorsal rVLPFC modulated areas of

the brain that are known to be related to attention control during Stop trials, whereas ventral rVLPFC modulated areas of the brain, including FEF, that are known to be involved more directly in motor control during Stop trials, supporting our previous findings in Experiment 1 that dorsal and ventral rVLPFC are two separate subregions within rLVPFC and further demonstrating that these subregions are differentially functionally connected to separate brain regions during inhibitory control. Furthermore, FEF modulated movement-related subcortical areas such as superior colliculus and thalamus. Figure 29 shows hypothetical connections of ventral rVLPFC, dorsal rVLPFC, and bi-lateral FEF with other parts of the brain areas during Stop, Go, and Continue tasks.

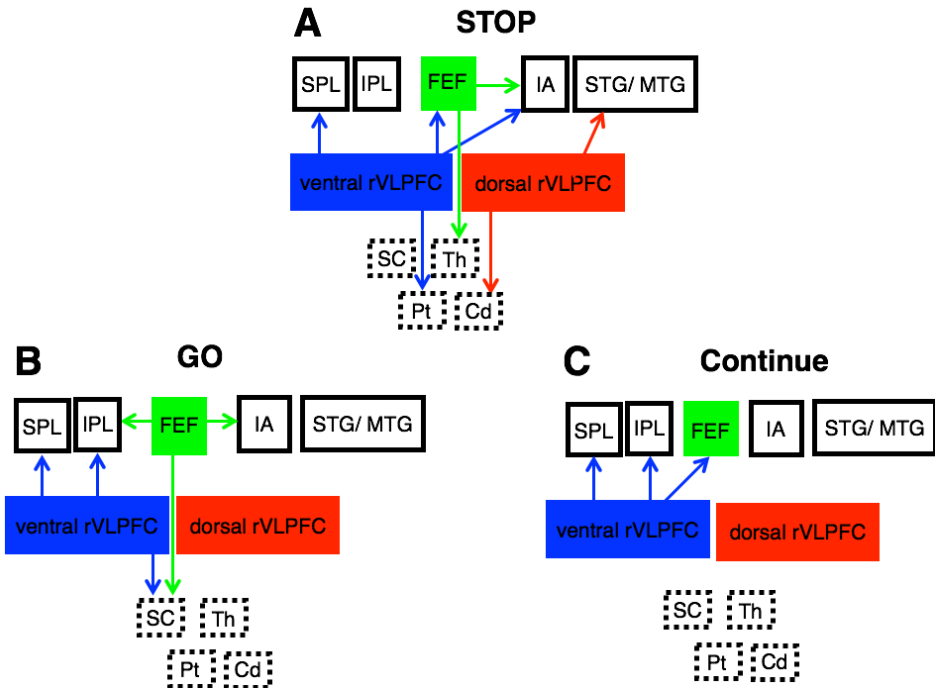

Figure 29. Hypothetical functional connections among ventral rVLPFC, dorsal rVLPFC, bilateral FEF and the rest of the brain during Stop task (A),Go task (B), and Continue task (C). Solid borders indicate cortical brain regions whereas dashed borders indicate subcortical regions. IPL: inferior parietal lobe, SPL: superior parietal

lobe, FEF: frontal eye fields, IA: insula, STG: superior temporal gyrus, MTG: middle temporal gyrus, rVLPFC: right ventrolateral prefrontal cortex, SC: superior colliculus, Th: thalamus, Pt: putamen, Cd: caudate. Note: arrows do not indicate directionality, and the tail of the arrow indicates the seed region.

Corbetta and Shulman (2002) argued that there are two different attentional networks with one that involves preparing and applying goal-directed, top-down control of stimulus- and response-selection, and the other that involves detecting behaviorally relevant stimuli with high saliency and especially when they appear unexpectedly. The authors termed this later network the "circuit-breaking" network. The "top-down" control network includes part of the intraparietal sulcus (IPS) and superior frontal cortex, including the frontal eye field (FEF); the "circuit-breaking" network is mostly lateralized to the right hemisphere, which includes temporoparietal junction (TPJ) and the ventral frontal cortex (VFC), together forming the right ventrao frontoparietal network (Corbetta and Shulman, 2002). Our PPI results showed that FEF and superior parietal lobe (SPL) were recruited through the mutual connection with rVLPFC during Go and Stop tasks to exert top-down, goal-direct control of eye movements—either to initiate or inhibit an saccade. In addition, dorsal rVLPFC was engaged along with superior temporal gyrus (STG) and middle temporal gyrus (MTG) during Stop task, presumably because the Stop signal was behaviorally relevant, with a high visual saliency and appeared unexpectedly. In this sense, the dorsal rVLPFC, STG and MTG served as a ventral attnetional circuit-breaker to interrupt the goal-directed attentional control during stopping[4].

[4] We could not directly compare the anatomical locations of MTG/STG in our study to TPJ in Corbetta and Shulman (2002), nor could we directly compare the anatomical locations of SPL/IPL in our study with IPS in Corbetta and Shulman (2002) because we used the Talairach template whereas Corbetta and Shulman (2002) used a customized template that took the average of all participants in their study Corbetta et al., 2002.

Aron (2006) argued that rVLPFC controls for stopping by directly projecting to subthalamic nucleus (STN) through the hyperdirect pathway (Figure 1). However, Erika-Florence et al. (2014) found that rVLPFC subregions were not functionally unique in their sensitivities to inhibitory control, but instead formed distributed networks that were active when infrequent stimuli appeared, regardless whether inhibitory control was needed, or whenever novel stimuli appeared that led to new response adjustment as opposed to predictable or routine responses. The authors thus concluded that there is no specific module in the prefrontal cortex that is dedicated to inhibitory control, but rather, response inhibition is an emergent property of a distributed network in the brain that instantiates cognitive control (Erika-Florence et al., 2014).

There is evidence in our study that further supports Erika-Florence et al. (2014)'s interpretation of the role of rVLPFC in inhibitory control. We did not find direct connection between either of the subregions of rVLPFC to STN during either Stop or Go trials. Instead, ventral rVLPFC is functionally connected with putamen while the dorsal rVLPFC is functionally connected with caudate during Stop, suggesting a potential cognitive versus motor functional dissociation. Second, ventral rVLPFC is connected with superior colliculus (SC) during Go trials, suggesting a role in reflexive, expected motor execution, not just in inhibitory motor control. Furthermore, ventral rVLPFC modulated FEF activity not only during the Stop task but also during the Continue task. In light of what Erika-Florence (2014) has proposed, it is very likely that both ventral and dorsal rVLPFC are parts of a distributed network that broadly underlies cognitive control,

---

However, based on the diffusion tensor imaging (DTI) results from Kamali et al., (2014) it is reasonable to assume that TPJ is highly related to both MTG and STG, and IPS is highly related to SPL/IPL.

which includes both Stop, Go, and Continue in our experimental design. However, our study did not allow us to directly test the idea whether response inhibition requires an inhibitory module that is unique and separated from the rest of the cognitive control net work, or is an emergent property of cognitive control that shares the same neural basis as other forms of cognitive control (e.g. motor planning or updating motor actions). In our design, we used Continue trials to control for the attentional capture effect due to the abrupt onset of a Stop signal. In both Continue and Go trials, however, the end response was the same, making the saccade to the *same* direction that a participant had already been planning for, only in the Continue trial case, the preparation was briefly interrupted by the onset of a salient Continue signal. A future study could be done where a second control would be introduced, in which, instead of instructing a participant to continue to make a saccade to the *same* direction as was in the current Continue trials, instructing a participant to make a saccade to the *opposite* direction. This would allow us to examine the question that whether there are specific inhibitory modules in the frontal cortex, or response inhibition is an emergent property of a broad aspect of cognitive control that also includes motor task switching and updating action plans.

How does information flow through different functional networks during cognitive control? It is plausible to hypothesize that the dorsal rVLPFC exerts top-down inhibitory control by detecting context relevant signals, deciphering their meaning, and then sending the relevant information to areas such as ventral rVLPFC, FEF and SC, where appropriate actions are to be carried out. However, in our current PPI analysis, we did not find evidence that ventral rVLPFC and dorsal rVLPFC form either a direct or an indirect functional connection that would allow information to flow directly between

each other. One explanation would be that PPI analysis is non-directional and only examines the functional connection, but not effective interaction (which is directional), between brain areas (McLaren et al, 2012; Cisler et al, 2013). To determine a causal relationship between dorsal and ventral rVLPFC, as well as each region with the rest of the brain, dynamic causal modeling (DCM) would be a more appropriate analysis for future consideration (Friston et al., 2003). In addition to DCM, future studies that use techniques with higher temporal precision such as EEG, or single cell recordings would allow us to examine the temporal dynamics of information flow between these two rVLPFC subregions in the cognitive control of movement inhibition.

Chapter 6: General discussions

The current thesis examined the behavioral characteristics and the neural basis of context-dependent, selective inhibitory control. Specifically, we found that the preparation of a response was delayed on both Stop and Continue trials by a similar mechanism; yet, these trials differed greatly in the ultimate behavior (make or suppress a saccade), whether positive or negative feedback was received, and subsequent behavioral adjustments. Furthermore, we found two functionally distinct subregions within the rVLPFC: increased BOLD activity in dorsal rVLPFC was observed in both Stop and Continue trials compared to Go trials, and MVPA analysis successfully decoded the meaning of the sensory signal in dorsal rVLPFC. In contrast, ventral rVLPFC demonstrated increased BOLD activity relative to Go trials, only in Stop trials, yet there was no activation magnitude difference between Failed and Successful Stop trials. Our findings suggested that dorsal rVLPFC detects signals that are behaviorally relevant and represents the current stimulus-response association, and the ventral rVLPFC detects

signals that are stop-relevant, yet does not control motor inhibition *per se*. We further investigated how dorsal and ventral rVLPFC form distributed networks to collectively control for contextual stopping, and found that dorsal rVLPFC modulated areas of the brain that are known to be part of the "attention-breaker" network during Stop task, whereas ventral rVLPFC modulated areas of the brain, including FEF, that are known to be part of the top-down goal directed attentional network as well as for controlling eye movements during Stop task. Together these results suggest that sub-regions within rVLPFC contribute heterogeneous functions and form distributed networks in cognitive control of movement inhibition.

Taken together, we found that context-dependent inhibition of a planned behavior is not governed by a single brain system as had been previously proposed, but instead depends on two behaviorally and neutrally distinct processes. One process involves delaying the behavior while enhancing attention to the relevant information in the environment, in order to decide the appropriate course of action. The second process seems to be more directly involved in canceling or changing the planned behavior. Furthermore, the second process has a greater effect on future behavior. Understanding the biological and computational processes it takes for the brain to control for complicated situations such as context-dependent movement inhibition will shed light on the advancement of artificial intelligence (e.g. the development of self-driving car). On the other hand, understanding the contribution of rVLPFC on inhibitory control is also highly significant from a clinical point of view, because it might lead to improvements in assessing or even treating disorders such as ADHD, Parkinson's diseases, and OCD.

References

Andrés, P., Guerrini, C., Phillips, L.H., Perfect, T.J., (2008). Differential effects of aging on executive and automatic inhibition. *Dev. Neuropsychol*. 33, 101–123.

Aron, Adam R., Fletcher, Paul C., Bullmore, Ed T., Sahakian, Barbara J., and Robbins, Trevor W. (2003). Stop-signal inhibition disrupted by damage to right inferior frontal gyrus in humans. *Nature Neuroscience, 6*(2), 115-116.

Aron, A.R., Poldrack, R.A., (2006). Cortical and subcortical contributions to Stop signal response inhibition: role of the subthalamic nucleus. *J. Neurosci. Off. J. Soc. Neurosci*. 26, 2424–2433.

Aron, A.R., Behrens, T.E., Smith, S., Frank, M.J., Poldrack, R.A., (2007). Triangulating a cognitive control network using diffusion-weighted magnetic resonance imaging (MRI) and functional MRI. *J. Neurosci. Off. J. Soc. Neurosci*. 27, 3743–3752.

Aron, A.R., Durston, S., Eagle, D.M., Logan, G.D., Stinear, C.M., Stuphorn, V., (2007). Converging Evidence for a Fronto-Basal-Ganglia Network for Inhibitory Control of Action and Cognition. *J. Neurosci*. 27, 11860–11864.

Aron, A.R., (2011). From reactive to proactive and selective control: developing a richer model for stopping inappropriate responses. *s* 69, e55–68.

Asaad, W. F., Rainer, G. and Miller, E. K. (1998). Neural activity in the primate prefrontal cortex during associative learning. *Neuron*, *21*(6), 1399–407.

Asaad, W. F., & Eskandar, E. N. (2008). A flexible software tool for temporally-precise behavioral control in Matlab. *Journal of neuroscience methods*, *174*(2), 245-58.

Bunge, Silvia A., and Jonathan D. Wallis. *Neuroscience of Rule-guided Behavior*. Oxford: Oxford UP, (2008). Print.

Badre, D., and D'Esposito, M. (2007). Functional magnetic resonance imaging evidence for a hierarchical organization of the prefrontal cortex. *Journal of cognitive neuroscience*, *19*(12), 2082–99.

Badre, D. and A.D. Wagner. (2007). Left ventrolateral prefrontal cortex and the cognitive control of memory. *Neuropsychologia* **45**:2883–2901.

Badre, D., and D'Esposito, M. (2009). Is the rostro-caudal axis of the frontal lobe hierarchical? *Nature reviews. Neuroscience*, *10*(9), 659–69.

Band, G.P.H., van der Molen, M.W., Logan, G.D., (2003). Horse-race model simulations of the stop-signal procedure. *Acta Psychol. (Amst.)* 112, 105-142.

Bissett, P.G., Logan, G.D., (2012). Post-stop-signal adjustments: Inhibition improves subsequent inhibition. *J. Exp. Psychol. Learn. Mem. Cogn*. 38(4): 955-66.

Boucher, L., Palmeri, T.J., Logan, G.D., Schall, J.D., (2007a). Inhibitory control in mind and brain: an interactive race model of countermanding saccades. *Psychol. Rev.* 114, 376–397.

Boucher, L., Stuphorn, V., Logan, G.D., Schall, J.D., Palmeri, T.J., (2007b). Stopping eye and hand movements: are the processes independent? *Percept. Psychophys*. 69, 785–801.

Brown, J.W., Hanes, D.P., Schall, J.D., Stuphorn, V., (2008). Relation of frontal eye field activity to saccade initiation during a countermanding task. *Exp. Brain Res. Exp. Hirnforsch. Expérimentation Cérébrale* 190, 135–151.

Bruce, C. J., Goldberg, M. E., and Goldberg, E. (1985). Primate frontal eye fields. I. Single neurons discharging before saccades. *Journal of neurophysiology*, *53(3)*, 603–635.

Bryden, D.W., Burton, A.C., Kashtelyan, V., Barnett, B.R., Roesch, M.R., (2012). Response inhibition signals and miscoding of direction in dorsomedial striatum. *Front. Integr. Neurosci*. 6, 69.

Cai, W., Oldenkamp, C.L., Aron, A.R., (2011). A proactive mechanism for selective suppression of response tendencies. *J. Neurosci. Off. J. Soc. Neurosci.* 31, 5965–5969.

Chambers, C. D., Garavan, H. and Bellgrove, M. a. (2009). Insights into the neural basis of response inhibition from cognitive and clinical neuroscience. *Neuroscience and biobehavioral reviews*, *33*(5), 631–46.

Chang CC, Lin CJ. LIBSVM: A Library for Support Vector Machines (Online). http://www.csie.ntu.edu.tw/_cjlin/libsvm [2001].

Chatham, C. H., Claus, E. D, Banich, M. T., Curran, T,. Kim, A., and Munakata, Y. (2012) Cognitive control reflects context monitoring, not motoric stopping, in response inhibition. *PLoS One*. 7(2). e31546.

Chikazoe, J., K. Jimura et al. (2009). Preparation to inhibit a response complements response inhibition during performance of a stop-signal task. *J Neurosci* 29(50): 15870-7.

Connolly, J. D., Goodale, M. a, Goltz, H. C., Munoz, D. P., & Jason, D. (2005). fMRI Activation in the Human Frontal Eye Field Is Correlated With Saccadic Reaction Time. *Brain*, 605– 611.

Corbetta, M. and Shulman, G. L. (2002). Control of goal-directed and stimulus-driven attention in the brain. *Nature reviews. Neuroscience*, *3*(3), 201–15.

Corbetta, M., Kincade, J.M., and Shulman, G.L. (2002) Neural systems for visual orienting and their relationship to spatial working memory. *Journal of Cognitive Neuroscience*: 14, 508-523.

Courtney, S.M. Ungerleider, L.G., Keil,K, Haxby, J.V. (1996). Object and Spatial Visual Working Memory Activate Separate Neural Systems in Human Cortex. *Cereb. Ctx,* 6: 39-49.

Courtney, S.M., Petit, L., Ungerleider, L.G., Maisog, J.M., Haxby, J.V. (1998). An Area Specialized for Spatial Working Memory in Human Frontal Cortex. *Science,* 279:1347-51.

Cox, R. W. (1996). AFNI: Software analysis and visualization of functional magnetic resonance neuroimages. *Computers and Biomedical Research*, 29, 162-173.

Coxon, J.P., Impe, A.V., Wenderoth, N., Swinnen, S.P., (2012). Aging and Inhibitory Control of Action: Cortico-Subthalamic Connection Strength Predicts Stopping Performance. *J. Neurosci.* 32, 8401–8412.

Curtis, C. E., Cole, M. W., Rao, V. Y., and D'Esposito, M. (2005). Canceling planned action: an FMRI study of countermanding saccades. *Cerebral cortex (New York, N.Y. : 1991)*, *15*(9), 1281-9.

Desimone, R. and J. Duncan. (1995). Neural mechanisms of selective visual attention. *Annu. Rev. Neurosci.* **18**: 193–222.

De Jong, Ritske, Coles, Michael G. H., Logan, Gordon D, Gratton, Gabriele. (1990). In search of the point of no return: The control of response processes. Journal of Experimental Psychology: *Human Perception and Performance*, 16(1), 164-182.

De Jong, Ritske, Coles, Michael G. H., Logan, Gordon D. (1995). Strategies and mechanisms in nonselective and selective inhibitory motor control. *Journal of Experimental Psychology: Human Perception and Performance*, 21(3), 498-511.

Dias R, Robbins TW, Roberts AC. (1996b). Primate analogue of the Wisconsin Card Sorting Test: effects of excitotoxic lesions of the prefrontal cortex in the marmoset. *Behav. Neurosci*. 110:872–86.

Dias R, Robbins TW, Roberts AC. (1997). Dissociable forms of inhibitory control within prefrontal cortex with an analog of the Wisconsin Card Sort Test: restriction to novel situations and independence from "on-line" processing. *J. Neurosci* 17:9285–97.

Dosenbach, N. U. F., Fair, D. a, Cohen, A. L., Schlaggar, B. L., and Petersen, S. E. (2008). A dual-networks architecture of top-down control. *Trends in cognitive sciences*, *12*(3), 99–105.

Eagle, D. M., Bari, A. and Robbins, T. W. (2008). The neuropsychopharmacology of action inhibition: cross-species translation of the stop-signal and go/no-go tasks. *Psychopharmacology*, *199*(3), 439–56.

Emeric, E.E., Brown, J.W., Boucher, L., Carpenter, R.H.S., Hanes, D.P., Harris, R., Logan, G.D., Mashru, R.N., Paré, M., Pouget, P., Stuphorn, V., Taylor, T.L., Schall, J.D., (2007). Influence of history on saccade countermanding performance in humans and macaque monkeys. *Vision Res*. 47, 35–49.

Erika-Florence, M., Leech, R., & Hampshire, a. (2014). A functional network perspective on response inhibition and attentional control. *Nat Commun*, *5*, 4073.

Evdokimidis, N. Smyrnis, T.S. Constantinidis, N.C. Stefanis, D. Avramopoulos, C. Paximadis, Theleritis C, Efstratiadis C, Kastrinakis G, Stefanis CN. (2002). The antisaccade task in a sample of 2006 young men–I. Normal population characteristics *Experimental Brain Research*, 147, 45–52.

Everling, S., Paré, M., Dorris, M.C., Munoz, D.P., (1998). Comparison of the discharge characteristics of brain stem omnipause neurons and superior colliculus fixation neurons in monkey: implications for control of fixation and saccade behavior. *J. Neurophysiol.* 79, 511–528.

Friston, K. J., Harrison, L., & Penny, W. (2003). Dynamic causal modelling. *NeuroImage*, *19*(4), 1273–1302.

Fuster, J. M. (2001). The prefrontal cortex—An update : Time is of the essence. *Neuron, 30*, 319-333.

Felleman, D. J., and Van Essen, D. C. (1991). Distributed hierarchical processing in the primate cerebral cortex. *Cerebral cortex (New York, N.Y. : 1991)*, *1*(1), 1–47.

Gauggel, S., Rieger, M., Feghoff, T.-A., (2004). Inhibition of ongoing responses in patients with Parkinson's disease. J. Neurol. Neurosurg. Psychiatry 75, 539–544.

Gerbella, M., Belmalih, A., Borra, E., Rozzi, S., and Luppino, G. (2010). Cortical connections of the macaque caudal ventrolateral prefrontal areas 45A and 45B. *Cerebral cortex (New York, N.Y. : 1991)*, *20*(1), 141-68.

Gold, B.T. *et al* . 2006. Dissociation of automatic and strategic lexical-semantics: functional magnetic resonance imaging evidence for differing roles of multiple frontotemporal regions. *J. Neurosci.* 26: 6523–6532.

Goldberg, M. E., & Bushnell, M. C. (1981). Behavioral enhancement of visual responses in monkey cerebral-cortex .II. Modulation in frontal eye fields specifically related to saccades. *Journal of Neurophysiology, 46*(4), 773-787.

Hampshire, A., Chamberlain, S. R., Monti, M. M., Duncan, J. and Owen, A. M. (2010). The role of the right inferior frontal gyrus: inhibition and attentional control. *NeuroImage*, *50*(3), 1313–9.

Hanes, D.P., Patterson, W.F., Schall, J.D., (1998). Role of frontal eye fields in countermanding saccades: visual, movement, and fixation activity. *J. Neurophysiol*. 79, 817–834.

Hanes, D.P., Schall, J.D., (1996). Neural control of voluntary movement initiation. *Science* 274, 427.

Hanke, M., Halchenko, Y. O., Sederberg, P. B., Hanson, S. J., Haxby, J. V. and Pollmann, S. (2009). PyMVPA: A Python toolbox for multivariate pattern analysis of fMRI data. *Neuroinformatics*, 7, 37-53.

Haynes JD, Sakai K, Rees G, Gilbert S, Frith C, Passingham RE. (2007). Reading hidden intentions in the human brain. *Curr Biol* 17: 323–328.

Haynes, W.I.A., Haber, S.N., (2013). The organization of prefrontal-subthalamic inputs in primates provides an anatomical substrate for both functional specificity and integration: implications for Basal Ganglia models and deep brain stimulation. *J. Neurosci. Off. J. Soc. Neurosci*. 33, 4804–4814.

Hendrick, O.M., Ide, J.S., Luo, X., Li, C.R., (2010). Dissociable processes of cognitive control during error and non-error conflicts: a study of the stop signal task. *PloS One* 5, e13155.

Ide, J.S., Li, C.R., (2011). A cerebellar thalamic cortical circuit for error-related cognitive control. *NeuroImage*, 54, 455–464.

Ito S, Stuphorn V, Brown JW, Schall JD. (2003). Performance monitoring by the anterior cingulate cortex during saccade countermanding. *Science*, 302(5642):120-2.

Jenkinson, M., Beckmann, C. F., Behrens, T. E., Woolrich, M. W., and Smith, S. M. (2012) FSL. *NeuroImage*, 15, 782-790.

Kamali, a., Sair, H. I., Radmanesh, a., & Hasan, K. M. (2014). Decoding the superior parietal lobule connections of the superior longitudinal fasciculus/arcuate fasciculus in the human brain. *Neuroscience*, *277*, 577–583.

Koechlin, E., Ody, C., and Kouneiher, F. (2003). The architecture of cognitive control in the human prefrontal cortex. *Science, 302*(5648), 1181-1185.

Kriegeskorte N, Goebel R, Bandettini P. (2006) Information-based functional brain mapping. *Proc Natl Acad Sci* 103: 3863–3868.

Lappin, J.S., Eriksen, C.W., (1966). Use of a delayed signal to stop a visual reaction-time response. *J. Exp. Psychol*. 72, 805–811.

Levy, B. J., and Wagner, A. D. (2011). Cognitive control and right ventrolateral prefrontal cortex: reflexive reorienting, motor inhibition, and action updating. *Annals of the New York Academy of Sciences*, *1224*(1), 40–62.

Lipszyc, Jonathan and Schachar, Russell. (2010). Inhibitory control and psychopathology: A meta-analysis of studies using the stop signal task. *Journal of the International Neuropsychological Society*, 16(06), 1064-1076.

Li, C.R., Huang, C., Constable, R.T., Sinha, R., (2006). Imaging response inhibition in a stop-signal task: neural correlates independent of signal monitoring and post-response processing. *J. Neurosci. Off. J. Soc. Neurosci*. 26, 186–192.

Li, C.R., Huang, C., Yan, P., Paliwal, P., Constable, R.T., Sinha, R., (2008). Neural correlates of post-error slowing during a stop signal task: a functional magnetic resonance imaging study. *J. Cogn. Neurosci*. 20, 1021–1029.

Logan, G.D., Cowan, W.B., (1984). On the ability to inhibit thought and action: A theory of an act of control. *Psychol. Rev*. 91, 295–327.

Logan, G.D., Cowan, W.B., Davis, K.A., (1984). On the ability to inhibit simple and choice reaction time responses: a model and a method. *J. Exp. Psychol.* 10, 276–291.

Logan, G.D., Schachar, R.J., Tannock, R., (1997). Impulsivity and Inhibitory Control. *Psychol. Sci*. 8, 60–64.

Mayse, J.D., Nelson, G.M., Park, P., Gallagher, M., Lin, S.-C., (2014). Proactive and reactive inhibitory control in rats. *Front. Neurosci*. 8,104.

McAlonan, G.M., Cheung, V., Chua, S.E., Oosterlaan, J., Hung, S., Tang, C., Lee, C., Kwong, S., Ho, T., Cheung, C., Suckling, J., Leung, P.W.L., (2009). Age-related grey matter volume correlates of response inhibition and shifting in attention-deficit hyperactivity disorder. *Br. J. Psychiatry J. Ment. Sci.* 194, 123–129.

McLaren, D. G., Ries, M. L., Xu, G., & Johnson, S. C. (2012). A Generalized Form of Context-Dependent Psychophysiological Interactions (gPPI): A Comparison to Standard Approaches. NeuroImage, 1–41.

Miller, E. K., Cohen, J. D. (2001). An integrative theory of prefrontal cortex function. *Annual Review of Neuroscience, 24*, 167-202.

Milner, B. (1963). Some effects of different brain lesions on card sorting: The role of the frontal lobes. *Archives of Neurology*, *9*, 90– 100.

Mirabella, G., Iaconelli, S., Romanelli, P., Modugno, N., Lena, F., Manfredi, M.,

Cantore, G., (2011). Deep Brain Stimulation of Subthalamic Nuclei Affects Arm Response Inhibition In Parkinson's Patients. *Cereb. Cortex,* doi:10.1093/cercor/bhr187

Munakata, Y., Herd, S. a., Chatham, C. H., Depue, B. E., Banich, M. T. and O'Reilly, R. C. (2011). A unified framework for inhibitory control. *Trends in Cognitive Sciences*, *15*(10), 453–459.

Nambu, H. Tokuno, I. Hamada, H. Kita, M. Imanishi, T. Akazawa, Y. Ikeuchi, N. Hasegawa (2000), Excitatory cortical inputs to pallidal neurons via the subthalamic nucleus in the monkey. *Journal of Neurophysiology*, 84, 289–300.

Nambu, H. Tokuno, M. Takada, (2002). Functional significance of the cortico-subthalamo-pallidal 'hyperdirect' pathway. *Neuroscience Research*, 43, 111–117.

Norman, K. A., Polyn, S. M., Detre, G. J. & Haxby, J. V. (2006). Beyond mind-reading: multi-voxel pattern analysis of fMRI data. *Trends in Cognitive Science*, *10*, 424–430.

Nichols, T. E. & Holmes, A. P. (2002). Nonparametric permutation tests for functional neuroimaging: a primer with examples.*Human Brain Mapping*, *15*, 1–25.

Passingham, R. E. and Steven P. Wise. Ventral Prefrontal Cortex: Generating Goals Based on Visual and Auditory Contexts. The Neurobiology of the Prefrontal Cortex: Anatomy, Evolution, and the Origin of Insight. Oxford: Oxford Univ., (2012). Print.

Paré, M., Hanes, D.P., (2003). Controlled movement processing: superior colliculus activity associated with countermanded saccades. *J. Neurosci. Off. J. Soc. Neurosci.* 23, 6480–6489.

P.E. Hallett (1978) Primary and secondary saccades to goals defined by instructions. *Vision Research*, 18 (1978), 1279–1296.

Petrides, M., and Pandya, D. N. (2009). Distinct parietal and temporal pathway to the homologues of Broca's area in the monkey. *PLoS biology*, *7*(8), e1000170.

Poldrack, R.A. *et al* . (1999). Functional specialization for semantic and phonological processing in the left inferior prefrontal cortex.*Neuroimage* 10: 15–35.

Rieger, M., Gauggel, S., Burmeister, K., (2003). Inhibition of ongoing responses following frontal, nonfrontal, and basal ganglia lesions. Neuropsychology 17, 272–282.

Rubia, Katya, Russell, Tamara, Overmeyer, Stephan, Brammer, Michael J., Bullmore, Edward T., Sharma, Tonmoy, . . . Taylor, Eric. (2001). Mapping Motor Inhibition: Conjunctive Brain Activations across Different Versions of Go/No-Go and Stop Tasks. *NeuroImage, 13*(2), 250-261.

Sakagami, M., Tsutsui Ki, Lauwereyns, J., Koizumi, M., Kobayashi, S., and Hikosaka, O. (2001). A code for behavioral inhibition on the basis of color, but not motion, in ventrolateral prefrontal cortex of macaque monkey. *The Journal of neuroscience : the official journal of the Society for Neuroscience*, *21*(13), 4801–8.

Sakagami, M., Pan, X., and Uttl, B. (2006). Behavioral inhibition and prefrontal cortex in decision-making. *Neural networks : the official journal of the International Neural Network Society*, *19*(8), 1255-65.

Schall, J. D., and Thompson, K. G. (1999). Neural selection and control of visually guided eye movements. *Annual review of neuroscience*, *22*, 241–59.

Schiller, P. H., Sandell, J. H., and Maunsell, J. H. (1987). The Effect of Frontal Eye Field and Superior Colliculus Lesions on Saccadic Latencies in the Rhesus Monkey. *Journal of Neurophysiology*, 57(4), 1033–1049.

Schmidt, R., Leventhal, D.K., Mallet, N., Chen, F., Berke, J.D., (2013). Canceling actions involves a race between basal ganglia pathways. *Nat. Neurosci*. 16, 1118–1124.

Serences, J. T., Schwarzbach, J., Courtney, S. M., Golay, X., and Yantis, S. (2004). Control of object-based attention in human cortex. *Cerebral Cortex*,14, 1346-1357.

Serences, J.T., Shomstein, S., Leber, A., Golay, X., Egeth, H., and Yantis, S. (2005). Coordination of voluntary and stimulus-driven attentional control in human cortex. *Psychological Science, 16*, 114-122.

Sharp, D.J., Bonnelle, V., De Boissezon, X., Beckmann, C.F., James, S.G., Patel, M.C., Mehta, M.A., (2010). Distinct frontal systems for response inhibition, attentional capture, and error processing. *Proc. Natl. Acad. Sci. U. S. A*. 107, 6106–6111.

Smith, R., (1992). Inhibition: history and meaning in the sciences of mind and brain. University of California Press, Berkeley.

Sparks, D.L., (1978). Functional properties of neurons in the monkey superior colliculus: coupling of neuronal activity and saccade onset. *Brain Res*. 156, 1–16.

Stanton, G. B., Bruce, C. J., and Goldberg, M. E. (1993). Topography of projections to the frontal lobe from the macaque frontal eye fields. *The Journal of comparative neurology*, *330*(2), 286–301.

Staub, B., Doignon-Camus, N., Bacon, E., Bonnefond, A., (2014). Age-related differences in the recruitment of proactive and reactive control in a situation of sustained attention. *Biol. Psychol.* 103C, 38–47.

Stroop, J.R. (1935) Studies of interference in serial verbal reactions. *Journal of Experimental Psychology*, 28, 643–662.

Stuphorn, V., (2014). Neural mechanisms of response inhibition. *Curr. Opin. Behav. Sci.,* 1, 64-71.

Suzuki, H., and Azuma, M. (1983). Topographic Studies on Visual Neurons in the Dorsolateral Prefrontal Cortex of the Monkey. *Experimental brain research*, 53(1), 47–58.

Swann, N., N. Tandon et al. (2009). Intracranial EEG reveals a time- and frequency-specific role for the right inferior frontal gyrus and primary motor cortex in stopping initiated responses. *J Neurosci*, 29(40): 12675-85.

Takahara, D., Inoue, K.-I., Hirata, Y., Miyachi, S., Nambu, A., Takada, M., and Hoshi, E. (2012). Multisynaptic projections from the ventrolateral prefrontal cortex to the dorsal premotor cortex in macaques - anatomical substrate for conditional visuomotor behavior. *The European journal of neuroscience*, *36*(10), 3365–3375.

Talairach and Tournoux, 1988 J. Talairach, P. Tournoux Co-planar stereotaxic atlas of the human brain Thieme Medical Publishers, New York (1988)

Tomáš Paus, (1996) Location and function of the human frontal eye-field: A selective review, *Neuropsychologia*, 34(6),475-483.

Verbruggen, F. and Logan, G. D. (2008). Response inhibition in the stop-signal paradigm. *Trends in cognitive sciences*, *12*(11), 418–24.

Verbruggen, F., Logan, G.D., (2009). Proactive adjustments of response strategies in the stop-signal paradigm. *J. Exp. Psychol. Hum. Percept. Perform*. 35, 835–854.

Verbruggen, F., Aron, A. R., Stevens, M. A., and Chambers, C. D. (2010). Theta burst stimulation dissociates attention and action updating in human inferior frontal cortex. *PNAS*. 107 (31), 13966-13971.

Wallis JD, Anderson KC, Miller EK (2001) Single neurons in the prefrontal cortex encode abstract rules. *Nature 411*: 953-956.

Yamagata, T., Nakayama, Y., Tanji, J., and Hoshi, E. (2012). Distinct Information Representation and Processing for Goal-Directed Behavior in the Dorsolateral and Ventrolateral Prefrontal Cortex and the Dorsal Premotor Cortex. *Journal of Neuroscience*, *32*(37), 12934–12949.

Yantis, S. and Jonides, J. (1990). Abrupt visual onsets and selective attention: Voluntary vs. automatic allocation. *Journal of Experimental Psychology: Human Perception and Performance, 16,* 121-134.

Yantis, S. (1993). Stimulus-driven attentional capture and attentional control settings. *Journal of Experimental Psychology: Human Perception and Performance, 19*, 676-681.

Zandbelt, B.B., Vink, M., (2010). On the Role of the Striatum in Response Inhibition. *PLoS ONE* 5, e13848.

Curriculum Vitae

Kitty Zhe Xu

The Johns Hopkins University

3400 N Charles Street
Baltimore, MD 21218

Phone (650) 862 4025
Email kitty.zhexu@gmail.com

EDUCATION

Ph.D. in Psychological and Brain Sciences 05/16
Johns Hopkins University, Baltimore, MD (Expected)
Research Advisor: Dr. Susan Courtney and Dr. Steven Yantis
Thesis: The neural basis of cognitive control of movement inhibition

M.A. in Psychological and Brain Sciences 05/13
Johns Hopkins University, Baltimore, MD
Research Advisor: Dr. Steven Yantis and Dr. Veit Stuphorn

B.S. in Biology, Summa Cum Laude, Phi Beta Kappa 05/09
The City College of New York, New York, NY
Research Advisor: Dr. Jay Edelman

WORKING EXPERIENCE

Summer data scientist intern 05-08/15
Thomson Reuters/MarkMonitor, San Francisco, CA

Research assistant 08/09- 05/11
Stanford University, Stanford, CA
Research Advisor: Dr. Tirin Moore

Summer research intern 05- 08/08
University of Rochester, Rochester, NY
Research Advisor: Dr. Gary Paige

AWARDS AND HONORS

PBS Collaborative Research Grant	05/14
Dean's List, the City College of New York	05/06-05/09
CCNY fellowship	05/07-05/09
Summa Cum Laude with Honors	05/09
Phi Beta Kappa Society	05/09
Palm Beach County Alumni Chapter Scholarship	05/09
Ephraim & Libby Banks Memorial Scholarship	05/08

PUBLICATION

Xu, K.Z., Sali, A.W., Anderson, B., Emeric, E.E., Yantis, S., Stuphorn, V., Courtney, S. M. (in preparation). The neural basis of context-dependent movement inhibition: a parallel human fMRI and primate electrophysiology study.

Xu, K.Z., Mayse, J. D., Courtney, S. (in preparation) Evidence for two types of inhibitory control in a variant of the stop signal task.

Zirnsak, M., Steinmetz**,** N. A., Noudoost. B**, Xu, K. Z**., Moore, T. Visual space is compressed in prefrontal cortex before eye movements. *Nature* 507: 504–507.

Edelman, J., **Xu, K. Z**. (2009). The inhibition of voluntary saccadic eye movement commands by abrupt visual onsets. *J Neurophysiol* 101: 1222 - 1234.

CONFERENCE PRESENTATIONS

Posters:

Xu, K. Z., Sali, A.W., Anderson, B.A., Yantis, S., Courtney, S., (October, 2015). *fMRI activation of dorsal andventral right inferior frontal cortex in a context-dependent stop signal task indicates different roles in motor control.* Society for Neuroscience, Chicago.

Xu, K. Z., Stuphorn, V., Yantis, S., Courtney, S., (November, 2014). *Humans and a non-human primate show similar behavior in a novel context-dependednt stop signal task.* Society for Neuroscience, Washington D.C..

Xu, K. Z., Emeric, E., Stuphorn, V., (November, 2013) *Neuronal activity related to context-dependent selective inhibitory control in the primate ventrolateral prefrontal cortex.* Society for Neuroscience, San Diego.

Zirnsak, M., Noudoost. B**,** Steinmetz**,** N. A, **Xu, K. Z**., Moore, T. (October, 2012). *An overrepresentation of target space in the frontal eye field during saccadic eye movements.* Society for Neuroscience, San Diego.

Fishman, Z. H., **Xu, K. Z.**, Edelman, J. A. (November, 2010). *A spatial dissociation between stimulus location and movement endpoint for express-like saccadic eye movements,* Society for Neuroscience, San Diego.

Xu, K. Z, Edelman, J. A. (November, 2008). *Temporal and spatial effects of abruptly appearing visual stimuli on the execution of voluntary saccadic eye movements*, Society for Neuroscience, Washington D.C..

Xu, K. Z, Dobreva, M.S., O'Neill, W. E., Paige, G. D. (August, 2008). *Influence of auditory and visual distraction on spatial localization in young and elderly adults.* University of Rochester, Summer Scholars Program, Rochester, NY.

Xu, K. Z, Edelman, J. A. (May, 2008). *Disruption of voluntary eye movement commands by abruptly appearing visual stimuli.* Vision Science Society, Naples, FL.

Talks:
Zirnsak, M, **Xu, K. Z.,** Noudoost, B, Moore, T. (May, 2011) Mapping of presaccadic receptive field profiles in the macaque frontal eye field. Vision Science Society, Naples, FL.

TEACHING EXPERIENCE

Johns Hopkins University, Baltimore, MD

Instructor: Research Methods in Psychological Sciences (Fall 2013)

Teaching Assistant: Neuroscience of Decision Making (Spring 2012 and 2013),

Animal Cognition (Fall 2012)

The City College of New York, New York, NY

Teaching Assistant: Introductory Biology, Animal Physiology

UNIVERSITY AND ACADEMIC SERVICE

Departmental representative of **the Graduate Representative Organization, Johns Hopkins University,** Baltimore, **MD** 08/12- 08/15

Career Chair of the Graduate Representative Organization, Johns Hopkins University, Baltimore, MD 08/15- 05/16

PROFESSIONAL MEMBERSHIPS

Society for Neuroscience
Phi Beta Kappa Society

TECHNICAL SKILLS

MATLAB, R, Python, SPSS, AFNI, PyMVPA, git, shell/bash command line scripting, Adobe Photoshop and Illustrator; experience with Apache Spark